

**INVESTIGATION OF ULTRASONIC AND
MICROBIAL REMOVALS OF
C.I. REACTIVE ORANGE 107 TEXTILE DYESTUFF
IN SINGLE AND IN SERIAL SYSTEMS**

**C.I. REACTIVE ORANGE 107 TEKSTİL
BOYARMADDESİNİN ULTRASONİK VE
MİKROBİYAL GİDERİMİNİN
TEKLİ VE ARDIŞIK SİSTEMLERDE İNCELENMESİ**

ÖZLEM TUNÇ

Submitted to
HACETTEPE UNIVERSITY
THE INSTITUTE FOR GRADUATE STUDIES
IN SCIENCE AND ENGINEERING
in partial fulfilment of the requirements for the degree of
DOCTOR OF PHILOSOPHY
in
CHEMICAL ENGINEERING

Temmuz 2008

To the Directory of the Institute for Graduate Studies in Science and Engineering,

This study has been accepted as a thesis for the degree of **DOCTOR OF PHILOSOPHY in CHEMICAL ENGINEERING** by our Examining Committee.

Head: Prof.Dr. Gönül DÖNMEZ

Advisor: Prof.Dr. Zümriye AKSU

Member (Co-Advisor): Prof.Dr. Astrid REHOREK

Member: Prof.Dr. Menemşe GÜMÜŞDERELİOĞLU

Member: Prof.Dr. Süleyman Ali TUNCEL

This is to certify that the Board of Directors of the Institute for Graduate Studies in Science and Engineering has approved this thesis on .../.../2008

Prof.Dr. Erdem YAZGAN
Director
The Institute for Graduate Studies
in Science and Engineering

Dedicated to my beloved family and my dear...

C.I. REACTIVE ORANGE 107 TEKSTİL BOYARMADDESİNİN ULTRASONİK VE MİKROBİYAL GİDERİMİNİN TEKLİ VE ARDIŞIK SİSTEMLERDE İNCELENMESİ

Özlem TUNÇ

ÖZ

Tekstil endüstrisi atıksuları içerdikleri çok çeşitli kimyasallardan ve özellikle de boyarmaddelerden dolayı arıtılması zor olan sulardır. Boyarmaddelerin sentetik kökenli olması ve karmaşık aromatik yapılar içermesi, boyaların kararlı yapıda olmasını sağlamakta ve biyolojik ayrışabilirliklerini zorlaştırmaktadır. Yapılan çalışmalar dünyada en fazla tüketilen boyarmaddelerin başında gelen reaktif boyarmaddelerin %90'ının aktif çamur proseslerinden değişmeden çıktığını; bir kısmının anaerobik arıtım proseslerinde parçalanabildiğini fakat parçalanma ürünlerinin toksik olduğunu göstermiştir. Boyarmaddelerin gideriminde kullanılan ozonlama, kimyasal indirgeme-oksidasyon, koagülasyon-flokülasyon, adsorpsiyon gibi yöntemler etkin olmalarına karşın yüksek maliyet, zararlı yan ürünlerin oluşumu ve fazla enerji gereksinimi gibi dezavantajlara sahiptir. Son zamanlarda ise ultrasonik yöntemlerle ve boyarmaddeleri hücre dışı ürettikleri spesifik olmayan enzimlerle parçalayabilen beyaz çürükçül funguslarla reaktif boyaların giderim çalışmaları önem kazanmaya başlamıştır.

Bu tez çalışmasında, kot kumaşların boyanmasında kullanılan ve tekstil atıksularında sıklıkla rastlanılan Reactive Orange 107 mono-azo reaktif boyarmaddesinin hidrolize formunun ultrasonik ve mikrobiyal yöntemlerle giderimi tekli ve ardışık sistemlerde incelenmiş, boyarmaddenin orijinal ve hidroliz formları ile degradasyon bileşiklerinin yapısal analizlerinden yararlanılarak giderim mekanizmaları önerilmiştir.

Ultrasonik yöntemle renk giderim çalışmaları üç farklı frekans (378, 850 ve 992 kHz), iki farklı sıcaklık (20, 30 °C) ve üç farklı başlangıç boyarmadde derişimi (50, 100, 200 mg/l) değerinde gerçekleştirilmiş ve en yüksek giderimin 850 kHz frekans ve 50 mg/l derişim değerinde sağlandığı gözlenmiş, sıcaklığın ise önemli bir etkisi görülmemiştir.

Mikrobiyal degradasyon çalışmaları beyaz çürükçül fungus *Trametes versicolor*'la gerçekleştirilmiş, sonuçlar anaerobik-aerobik bakteri çamuru ile elde edilenlerle karşılaştırılmıştır. Fungal giderimde glukoz tek başına ve bir atık olan melasla birlikte karbon kaynağı olarak kullanılmıştır. Boya giderimine ortam pH'ının etkisi incelendiğinde, pH 5.0'de en yüksek giderim gözlenmiştir. Bu pH değerinde, 2.5 ila 30 g/l arasında sabit tutulan her bir glukoz derişiminde, 25-300 mg/l aralığında değiştirilen başlangıç boyarmadde derişiminin fungusun üremesine ve boyarmadde giderimine etkileri araştırıldığında ise, glukoz derişiminin 20 g/l'ye, boyarmadde derişiminin ise 100 mg/l'ye kadar artmasıyla boyarmadde gideriminin arttığı görülmüştür. Ortama melas katıldığında ise fungal kütlenin önemli ölçüde arttığı, boyarmadde giderimindeki artışın ise daha az olduğu saptanmıştır.

Çalışmaların son kısmında mikrobiyal ve ultrasonik sistemler seri halde kullanılarak boya giderim hız ve veriminin yükseltilmesi hedeflenmiştir. Bulunan sonuçlar bu amaca ulaşıldığını göstermiştir.

Anahtar Kelimeler: Atıksu, tekstil, reaktif boyarmadde, Reactive Orange 107, degradasyon, ultrasonik yöntem, fungus, *Trametes versicolor*, melas

Danışman: Prof. Dr. Zümriye AKSU, Hacettepe Üniversitesi, Kimya Mühendisliği Bölümü

Eş Danışman: Prof. Dr. Astrid REHOREK, University of Applied Sciences Cologne, Chemical Engineering and Plant Design

INVESTIGATION OF ULTRASONIC AND MICROBIAL REMOVALS OF C.I. REACTIVE ORANGE 107 TEXTILE DYESTUFF IN SINGLE AND IN SERIAL SYSTEMS

Özlem Tunc

ABSTRACT

Wastewaters from the textile industries are one of the most difficult ones to treat because they contain various chemicals and especially dyestuffs. Dyes usually have a synthetic origin and complex aromatic molecular structures, which make them more stable and more difficult to be biodegraded. It was reported that approximately 90% of reactive dyes, which are extensively used in the worldwide textile industry, entering activated sludge process pass through with no change; some parts can be degraded under anaerobic biological treatment but reduction products are toxic. Although the methods used for the removal of dyestuffs like ozonation, chemical reduction-oxidation, coagulation-flocculation, adsorption, are effective, most of them have some drawbacks such as high cost, formation of hazardous by-products, and intensive energy requirement. In recent years, the use of ultrasonic methods and white-rot fungi, which are able to produce nonspecific oxidative enzymes and have the ability to convert textile dyes to simple compounds by using these enzymes, has become important for the removal of reactive dyes.

In this thesis study, the removal of hydrolyzed form of C.I. Reactive Orange 107, a mono-azo reactive dye, used for dyeing jeans in textile industries and found in textile wastewaters in large amounts, was investigated by using ultrasonic and microbial methods both alone and in series systems, and degradation mechanisms were proposed by evaluation the structural analysis of original and hydrolyzed forms of dye and degradation compounds.

Ultrasonic dye removal studies were performed at three different frequencies (378, 850 ve 992 kHz), at two different temperatures (20, 30 °C) and at three different initial dye concentrations (50, 100, 200 mg/l). The highest dye removal was obtained at 850 kHz frequency and at 50 mg/l initial dye concentration and it was observed that temperature has no significant effect on dye removal.

Microbial degradation studies were investigated by using *Trametes versicolor*, a white rot fungus and the results were compared with the findings obtained by anaerobic-aerobic bacterial sludge. In fungal degradation, glucose was used as the single and binary carbon source together with the molasses waste. When the effect of medium pH on the fungal dye removal was examined, maximum dye removal was obtained at pH 5.0. At this pH value, the effect of initial dyestuff concentration changing between 25-300 mg/l on the fungal growth and dye removal at a constant glucose concentration varied for each experimental set from 2.5 to 30 g/l, was studied and it was found that dye removal increased with both glucose concentration up to 20 g/l and dye concentration up to 100 mg/l . When molasses was added to growth medium, it was observed that fungal biomass increased considerably, but dye removal increased slightly.

In the final part of studies, it was aimed to achieve higher dye removal rates and efficiencies by using microbial and ultrasonic systems in series. The results obtained showed that use of binary system is much more favourable than that of single system.

Keywords: Wastewater, textile, reactive dyestuff, Reactive Orange 107, degradation, ultrasonic method, fungus, *Trametes versicolor*, molasses.

Advisor: Prof. Dr. Zümriye AKSU, Hacettepe University, Department of Chemical Engineering

Co-Advisor: Prof. Dr. Astrid REHOREK, University of Applied Sciences Cologne, Chemical Engineering and Plant Design

ACKNOWLEDGEMENTS

First of all, I would like to thank my supervisor Prof.Dr. Zumriye Aksu not only for sharing with me her experience and knowledge, but also for her encouragement and friendship. She was so patient during the writing period of my thesis that I will never forget it.

My special thanks to Prof.Dr. Astrid Rehorek, my co-advisor, for her continued guidance and advice throughout my studies and her encouragement and friendship.

I would like to express my deepest thanks to all people in Hacettepe University, Chemical Engineering Department. My unlimited thanks everyone that I felt with me during my PhD thesis for their conversations, help and friendship. Please forgive me, I could not mentioned here the names. Thanks all of you my dearest friends.

I would like to thank also all people in Cologne (Alexander, Rainer, Johannes, Johanna, Marion, Csilla, Verena, Ari) for their collaboration during my studies in Cologne. Of course my deep deep thanks to Betül. She was always with me in Cologne and now in Ankara.

My unspeakable gratefulness to my family; my dad Efendi, my mom Fatma, my sisters Özgür and Özen, my brother Burhan and his wife Pinar, my aunt Suna and uncle Ismail and of course my dear dear Ömer for their endless patience, love and pep. I love you, thank you very much.

Finally, I would like to thank my new coworkers in DSI for their friendship and moral support.

TABLE OF CONTENTS

	<u>Page</u>
ÖZ	i
ABSTRACT	ii
ACKNOWLEDGEMENTS.....	iii
TABLE OF CONTENTS	iv
LIST OF FIGURES.....	vii
LIST OF TABLES	xi
SYMBOLS AND NOMENCLATURE	xiii
1. INTRODUCTION	1
2. LITERATURE SURVEY.....	4
2.1. History of Dyestuff	4
2.2. Textile Dyestuffs	5
2.3. Classification of Dyestuff.....	6
2.3.1. Reactive Dyes.....	6
2.3.1.1. Structure of reactive dyes	8
2.3.1.2. Azo reactive dyes.....	8
2.4. Textile wastewaters	10
2.5. Treatment Methods for Textile Wastewaters	12
2.5.1. Physical Methods.....	12
2.5.1.1. Adsorption.....	12
2.5.1.2. Membrane Filtration	14
2.5.1.3. Ion Exchange.....	14
2.5.2. Chemical methods	15
2.5.2.1. Coagulation/Flocculation.....	15
2.5.2.2. Treatment with NaOCl (Sodium hypochlorite).....	15
2.5.2.3. Electrochemical Destruction.....	16
2.5.2.4. Oxidative Processes	16

H ₂ O ₂ -peroxidase treatment	17
H ₂ O ₂ - Fe (II) salts (Fenton's reagent) treatment	17
H ₂ O ₂ -ozone treatment:	18
Ultrasound.....	19
2.5.3. Biological Methods.....	24
2.5.3.1. Anaerobic biodegradation	24
2.5.3.2. Aerobic biodegradation	26
2.5.3.3. Fungal Biodegradation.....	26
<i>Trametes versicolor</i>	27
3. MATERIALS AND METHODS.....	28
3.1. The dye used in the experimental studies.....	28
3.2. The microorganisms used in the experimental studies	28
3.3. Experimental Setups.....	30
3.3.1. Ultrasound treatment system	30
3.3.2. Microbial treatment systems	30
3.3.2.1. Fungal biodegradation system	30
3.3.2.2. Anaerobic-aerobic biodegradation system.....	31
3.4. Analytical Methods.....	32
4. RESULTS AND DISCUSSION	34
4.1. The Structural Analysis of Original Form of RO107	34
4.2. The Structural Analysis of Hydrolyzed RO107	37
4.3. Ultrasonic Decolourization Studies of Hydrolyzed RO107	41
4.3.1. Effect of frequency on ultrasonic degradation of hydrolyzed dye.....	41
4.3.2. Effect of temperature on ultrasonic degradation of hydrolyzed RO107.	42
4.3.3. Determination of the sonication mechanism in the degradation of hydrolyzed RO107	43
4.3.4. Effect of initial hydrolyzed dye concentration on ultrasonic degradation	44
4.4. Microbial Biodegradation Studies of Hydrolyzed RO107	54

4.4.1. Biodegradation of RO107 hydrolyzed dye by using bacterial sludge	54
4.4.1.1. Anaerobic (AN) biodegradation of hydrolyzed RO107	55
4.4.1.2. Aerobic (AE) degradation of anaerobic (AN) effluent	60
4.4.2. Fungal Biodegradation of hydrolyzed RO107	65
4.4.2.1. Effect of pH on fungal growth and dye decolourization	65
4.4.2.2. Effect of initial glucose concentration on fungal growth in the absence of dye	66
4.4.2.3. Effect of dual substrate (glucose+molasses sucrose) concentration on fungal growth in the absence of dye	68
4.4.2.4. Effects of initial glucose and dye concentrations on fungal growth and dye decolourization in the presence of dye	69
4.4.2.5. Effects of dual substrate (glucose+molasses sucrose) and dye concentrations on fungal growth and dye decolourization in the presence of dye	78
4.5. Using of Ultrasound and Microbial Systems in Series	79
4.5.1. Combined anaerobic (AN) + ultrasound (US) degradation system	79
4.5.2. The combined aerobic (AE) + ultrasound (US) degradation system	81
4.5.3. The combined fungal (F) + ultrasound (US) degradation system	82
4.5.4. The combined ultrasound (US) + fungal (F) biodegradation	84
5. CONCLUSIONS	86
6. SONUÇLARIN TARTIŞILMASI	91
REFERENCES	96
APPENDIX	104
App 1. The LC-MS/MS system used during experimental studies	104
App 2. The evaluation of DAD data and calculation of relative concentration	107
App 3. Dye calibration curve for fungal degradation	110
App 4. Determination of glucose concentration and glucose calibration curve	111
App 5. The enhanced product ion spectrums and fragmentation patterns of components of hydrolyzed dye	113
CURRICULUM VITAE	115

LIST OF FIGURES

	<u>Page</u>
Figure 2.1 The general structure of a reactive dye molecule (Kirk-Othmer, 2001).	8
Figure 2.2 The general structure of an azo reactive dye (Kirk-Othmer, 2001).	9
Figure 2.3 The general structure of C.I. Reactive Orange 107 (RO107).	10
Figure 2.4 Classification of sound frequency ranges of ultrasound.	19
Figure 2.5 Formation of cavitation in liquids irradiated with ultrasound (Suslick, 1994).	21
Figure 2.6 The scheme for reductive cleavage of the azo bond.	25
Figure 3.1 The view of two stage anaerobic-aerobic bioreactor.	32
Figure 4.1 Total wavelength chromatogram and DAD chromatogram of commercial azo reactive dye RO107.	35
Figure 4.2 Enhanced Product Ion (EPI) spectrum and fragmentation pattern of RO107 original form (RO107_O).	36
Figure 4.3 Enhanced Product Ion (EPI) spectrum and fragmentation pattern of hydrolyzed RO107 with one acetyl group (RO107_H+NA).	36
Figure 4.4 Enhanced Product Ion (EPI) spectrum and fragmentation pattern of original dye components of PBSA and NA-ABSA.	37
Figure 4.5 Hydrolysis of dye during dyeing process.	37
Figure 4.6 The hydrolysis way of RO107 original dye.	38
Figure 4.7 Total wavelength chromatogram and DAD chromatogram of hydrolyzed RO107.	39
Figure 4.8 Enhanced Product Ion (EPI) spectrum and fragmentation pattern of RO107 hydrolyzed form without acetyl group (RO107_H-NA).	39
Figure 4.9 The variation of relative decolourization% of RO107_H-NA, m/z: 399, the main compound of hydrolyzed RO107, with frequency (C ₀ : 50 mg/l, T: 20 °C).	41
Figure 4.10 The effect of temperature on relative concentration of RO107_H-NA; m/z: 399, the main compound of hydrolyzed RO107, (C ₀ : 50 mg/l, f: 850 kHz).	42
Figure 4.11 The effect of the addition of t-BuOH on the degradation of RO107_H-NA, main compound of hydrolyzed RO107 (C ₀ : 50 mg/l, f: 850 kHz, T: 20 °C).	44

Figure 4.12 DAD chromatograms of hydrolyzed RO107 at 50 mg/l initial dye concentration.	45
Figure 4.13 The comparison of TWC of DAD spectral data for hydrolyzed RO107 before and after 24 h sonication time (C_0 :50 mg/l, f:850 kHz).....	45
Figure 4.14 DAD chromatograms of hydrolyzed RO107 at 100 mg/l initial dye concentration.	46
Figure 4.15 DAD chromatograms of hydrolyzed RO107at 200 mg/l initial dye concentration.	47
Figure 4.16 The comparison of TWC of DAD spectral data for hydrolyzed RO107 before and after 47 h sonication time (C_0 :100 mg/l, f:850 kHz).....	48
Figure 4.17 The comparison of TWC of DAD spectral data for hydrolyzed RO107 before and after 58 h sonication time (C_0 :200 mg/l, f:850 kHz).....	48
Figure 4.18 The proposed mechanism for the degradation of hydrolyzed dye during ultrasonic treatment.....	50
Figure 4.19 Effect of initial hydrolyzed RO107 concentration on relative RO107_H-NA removal percentage (f: 850 kHz, T:30 °C).....	51
Figure 4.20 Effect of initial hydrolyzed RO107 concentration on relative p-base removal percentage (f: 850 kHz, T:30 °C).....	52
Figure 4.21 Effect of initial hydrolyzed RO107 concentration on relative UNK177 removal percentage (f: 850 kHz, T:30 °C).....	52
Figure 4.22 Spectral changes during 12 h sonication of 50 mg/l hydrolyzed dye solution.....	53
Figure 4.23 Spectral changes during 47 h sonication of 100 mg/l dye solution....	53
Figure 4.24 Spectral changes during 58 h sonication of 200 mg/l dye solution....	53
Figure 4.25 Variation of chemical oxygen demand as a function of time obtained at three different initial dye concentrations.....	54
Figure 4.26 The comparison of TWC of DAD spectral data for hydrolyzed RO107 at the beginning and at the end of anaerobic treatment (1 st trial: 4 days).....	55
Figure 4.27 The mechanism of degradation of hydrolyzed RO107 in anaerobic reactor.....	56
Figure 4.28 Enhanced product ion (EPI) spectrum and fragmentation patterns of p-base and NA-ABSA intermediates.....	56
Figure 4.29 The change in relative decolourization percentage of RO107_H-NA; m/z: 399, during anaerobic biodegradation (Left:1 st trial, Right:2 nd trial).....	58

Figure 4.30	The change in decolourization percentage of p-base and NA-ABSA during anaerobic biodegradation (Left:1 st trial, Right:2 nd trial).	58
Figure 4.31	Spectral changes during anaerobic biodegradation (C ₀ :3400 mg/l 1 st trial:4 days, 2 nd trial:10 days).	59
Figure 4.32	Variation of chemical oxygen demand as a function of time obtained for anaerobic batch treatment.	59
Figure 4.33	The comparison of TWC of DAD spectral data for the dye solution before and after aerobic treatment (1 st trial: 10 days).	60
Figure 4.34	Enhanced product ion (EPI) spectrum and fragmentation patterns of DABSE+BDA.	61
Figure 4.35	The proposed mechanism for the formation of coloured compound m/z:319.	62
Figure 4.36	The change in relative concentration of p-base during aerobic biodegradation.	62
Figure 4.37	The change in relative concentration of DABSE+BDA during aerobic biodegradation.	63
Figure 4.38	Spectral changes during aerobic biodegradation.	64
Figure 4.39	Variation of chemical oxygen demand as a function of time obtained for aerobic batch treatment.	64
Figure 4.40	The effect of pH on fungal growth in no dye and in dye containing growth medium (S _{G0} :10 g/l, T:30 °C, ST: 150 rpm).	65
Figure 4.41	Fungal growth and glucose consumption curves at different initial glucose concentrations in no dye containing medium.	67
Figure 4.42	Glucose consumption curves obtained at different binary combinations of glucose+molasses sucrose.	69
Figure 4.43	The effect of initial dye concentration on glucose and dye consumptions (S _{G0} :10 g/l).	71
Figure 4.44	DAD chromatograms of hydrolyzed RO107 at 50 mg/l initial dye concentration (S _{G0} : 10 g/l).	72
Figure 4.45	DAD chromatograms of hydrolyzed RO107 at 200 mg/l initial dye concentration (S _{G0} : 10 g/l).	72
Figure 4.46	The comparison of TWC of DAD spectral data for hydrolyzed RO107 before and after 21 days biodegradation period (C ₀ :50 mg/l, S _{G0} :10 g/l).	73

Figure 4.47 The comparison of TWC of DAD spectral data for hydrolyzed RO107 before and after 21 days biodegradation period (C_0 :200 mg/l, (S_{G0} : 10 g/l).....	73
Figure 4.48 Two proposed mechanisms for the fungal degradation of hydrolyzed dye.	75
Figure 4.49 The change in relative RO107_H-NA removal with time obtained at two different hydrolyzed dye concentrations.	75
Figure 4.50 The change in relative p-base and BSAA removal with time obtained at two different hydrolyzed dye concentrations.	76
Figure 4.51 Spectral changes during fungal biodegradation for 50 mg/l initial dye concentration.	77
Figure 4.52 Spectral changes during fungal biodegradation for 200 mg/l initial dye concentration.	77
Figure 4.53 The effect of initial dye concentration on glucose and dye consumptions ($S_{(G+S)0}$:5+10 g/l).	79
Figure 4.54 The comparison of the change in relative concentration of RO107_H-NA with time in each AN and AN+US system (C_0 :3400 mg/l, f:850 kHz).	80
Figure 4.55 The comparison of the change in relative concentration of p-base and NA_ABSA with time in each AN and AN+US system (C_0 :3400 mg/l, f:850 kHz).....	80
Figure 4.56 The comparison of the change in relative concentration of DABSE_BDA with time in each AE and AE+US system.....	81
Figure 4.57 The comparison of the change in relative concentration of p-base with time in each AE and AE+US system.....	82
Figure 4.58 The comparison of the change in relative concentration of RO107_H-NA with time in each F and F+US system (C_0 :200 mg/l, T:30 °C).....	83
Figure 4.59 The comparison of the change in relative concentration of p-base and BSAA with time in each F and F+US system.	83
Figure 4.60 The comparison of the change in relative concentration of RO107_H-NA with time in each US and US+F system. (C_0 :200 mg/l, T:30 °C).	84
Figure 4.61 The comparison of the change in relative concentration of p-base with time in each US and US+F system. (C_0 :200 mg/l, T:30 °C).	85

LIST OF TABLES

	<u>Page</u>
Table 2.1 The regions of the electromagnetic spectrum and relationship between wavelength and colour (Santos et al., 2007).	5
Table 2.2 Classification of dyes according to their usage (Adapted from Kirk-Othmer, 2001).....	7
Table 2.3 Typical textile wastewater properties (Tezer, 2001).....	11
Table 2.4 Methods and procedures for decolourization of dye containing wastewaters (Adapted from Plum, 2005).	13
Table 3.1 Working conditions of ultrasonic systems used in the experiments (Adapted from Frömer, 2005).....	30
Table 4.1 The composition of commercial (original) azo reactive dye RO107. .	35
Table 4.2 The composition of hydrolyzed RO107.	40
Table 4.3 Some important compounds of hydrolyzed RO107 detected before and after ultrasound (US) treatment.....	49
Table 4.4 Pseudo first order degradation rate constants of RO107_H-NA, m/z:399 obtained at different initial dye concentrations.	51
Table 4.5 All the compounds detected during anaerobic treatment of hydrolyzed RO107.	57
Table 4.6 Pseudo 1 st order degradation rate constants for anaerobic degradation of RO107_H-NA.....	58
Table 4.7 All the compounds detected before and during aerobic treatment. ...	61
Table 4.8 Percentage of glucose consumption and percentage of dye removals obtained at different pH values (S_{G0} :10 g/L).....	66
Table 4.9 Glucose consumption and maximum fungal growths obtained at different initial glucose concentrations after 21 days incubation period.	67
Table 4.10 Percentage of glucose consumptions, maximum fungus concentrations and incubation periods obtained at each glucose+molasses sucrose combination.....	68
Table 4.11 Percentage of glucose consumption, percentage of dye removal and maximum fungus concentrations obtained at different initial glucose and dye concentrations.	70
Table 4.12 Some important compounds of hydrolyzed RO107 detected before and after fungal treatment.	74

Table 4.13 Pseudo first order degradation rate constants of RO107_H-NA, m/z:399 obtained at two different initial dye concentrations.....	76
Table 4.14 Percentage of glucose consumption, percentage of dye removal and maximum fungus concentrations obtained at the end of 21 days incubation.....	78
Table 5.1 The main degradation compounds with respect to the method used ...	88
Table 5.2 Comparison of the results with respect to the method used	90
Table 6.1 Kullanılan yöntemlere göre elde edilen temel degradasyon ürünleri	93
Table 6.2 Kullanılan yöntemlere göre elde edilen sonuçların karşılaştırılması.	95

SYMBOLS AND NOMENCLATURE

AN	: Anaerobic
AE	: Aerobic
APCI	: Atmospheric-pressure chemical ionization.
BSAA	: (4-Nitro benzenesulfonyl)-acetaldehyde
BOD	: Biological oxygen demand
C	: Relative bulk dye concentration (mg/l)
C ₀	: Relative initial dye concentration (mg/l)
C.I.	: Colour Index
COD	: Chemical oxygen demand
DABSA	: 2,4-Diamino-benzensulfanilic acid
DAD	: Diode array detector
DABSE+BDA	: 4-[2-(4-Diazenyl-benzensulfonyl)-ethoxy]-benzene-1,3-diamine
DH-HPA-BSA	: 2,4-Dihydroxy-5-(4-hydroxy-phenylazo)-benzenesulfonic acid
DNS	: Dinitrosalicylic acid
DimerRO107_H-NA	: Dimer-Reactive Orange 107- Hydrolyzed without acetyl group ether form
(Dimer RO107_H-NA)-SO ₃ ⁻	: Dimer-Reactive Orange 107-Hydrolyzed without acetyl group sulfonic acid
(Dimer RO107_H-NA)-2NH ₂ +OH	: 2,4-Diamino-5-[4-(2-{2-[4-(3-hydroxy-5-sulfo- phenylazo)-benzenesulfonyl]-exhoxy}-phenylazo)-benzenesulfonic acid
(Dimer RO107_H-NH ₂ +OH)-NA-OH	: 5-[4-(2-{2-[4-(2-Acetylamino-3-sulfo-phenylazo)-benzenesulfonyl ethoxy]-ethanesulfonyl)-phenylazo]-2-hydroxy- benzenesulfonic acid
EMS	: Enhanced Mass Spectrometry
EPI	: Enhanced product ion
ESI	: Electrospray ionization
f	: Frequency (kHz)
F	: Fungal
HPLC	: High performance liquid chromatography
IPC	: Ion-pair chromatographic
IC	: Ion chromatographic cation suppression
k	: Pseudo first order degradation constant (1/h)
LC-DAD	: Liquid chromatography diode array detector
LC-MS/MS	: Liquid chromatography-tandem mass spectrometry
MRM	: Multiple reactions monitoring mode
NA-ABSA	: 4-Acetylamino-2-amino-benzenesulfonic acid
NH ₄ Ac Method	: Ammonium acetate method
NA-DABSA	: 4-Acetylamino-2-5-Diamino-benzenesulfonic acid
NA-AES-PABSA	: 4-Acetylamino-2-[4-(2-amino-ethansulfonyl)-phenylamino]-benzenesulfonic acid
NA-HBSA	: 4-Acetylamino-2-hydroxy-benzenesulfonic acid
NA-HES-PABSA	: 4-Acetylamino-2-[4-(2-hydroxy-ethansulfonyl)-phenylamino]-benzenesulfonic acid
NAPB	: N-[4-(2-Hydroxy-ethansulfonyl)-phenyl]-acetamide, Vinyl para Base acetamide
η _{PeI/Pac}	: Efficiency
PB	: p-base (2-(4-Aminobenzenesulfonyl)-ethanol)

PBSA	: 2-amino-5-(2-hydroxy-ethanesulfonyl)-benzenesulfonic acid or p-Base Sulfone ester
$P_{el;max}$: Maximum electrical power (W)
$P_{ac;max}$: Maximum acoustic power (W)
PSA	: Phenol sulfonic acid
Q1	: Standard quadrupole mass spectrometer (amu)
Q3	: LIT mass spectrometer (amu)
R^2	: Regression coefficient
RO107	: Reactive Orange 107
RO107_H	: Reactive Orange 107 hydrolyzed form
RO107_H-C ₂ H ₄	: Reactive Orange 107 hydrolyzed form without ethylene
RO107_H+NA	: Reactive Orange 107 hydrolyzed form with one acetyl group
RO107_H-NA+PB	: Reactive Orange 107 hydrolyzed form without acetyl group+p-base
RO107_H-NH ₂ +PSA	: Reactive Orange 107 hydrolyzed form without amino +Phenol sulfonic acid (PSA)
RO107_H-NH ₂ +PB	: 4-Acetylamino-3-(4-{2-[2-(4-amino-benzenesulfonyl)-ethoxy]- ethanesulfonyl}-phenylazo)-benzenesulfonic acid
RO107_O	: Reactive Orange 107 original form
RO107_V	: Reactive Orange 107 vinyl form
s-Acid	: Sulfanilic acid
S_{Go}	: Initial glucose concentration
S_G	: Glucose concentration
$S_{(G+S)o}$: Initial glucose+molasses sucrose concentration
$S_{(G+S)}$: Glucose+molasses sucrose concentration
SSM	: Surface solid materials
t	: time (h, days)
T	: Temperature (°C)
TB	: Tert-butanol (t-BuOH),
TBAAc	: Tetrabutylammonium acetate
TWC	: Total wavelength chromatogram
US	: Ultrasound
UV	: Ultraviolet
V	: Reactor volume (l)
VPB+NA	: Vinyl para Base with Acetylamino Group
X	: Fungal cell concentration (g dry weight/l)

1. INTRODUCTION

Dyes take place in every part of our life and their application is growing day by day in many industries such as the food, pharmaceutical, cosmetic, leather and especially textile industries. There are more than 100,000 commercially available dyes and more than 7×10^5 tonnes of synthetic dyes are produced each year all over the world. Large amounts of wastewater, approximately 1-700 l/kg of product, are produced during dye manufacturing processes.

Among industrial wastewaters, wastewater from the textile industries is one of the most difficult one to treat because of containing various chemicals and especially dyestuffs. Dyes, usually have a synthetic origin, are complex aromatic molecular structures, more than one double bond and different functional groups which make them very stable and more difficult to be biodegraded.

Reactive dyes are an important class of textile dyestuffs and are extensively used in the worldwide textile industry. Reactive dyes are not used only to colour mainly cotton, but also wool and polyamide fibres because of their wide variety of colour shades, ease of application and brilliant colours. They contain chromophoric groups such as azo, anthraquinone, triarylmethane, etc. and reactive groups e.g. vinyl sulphone, chlorotriazine, etc. that can form covalent bonds with the fibre. Azo reactive dyes constitute the largest amount of reactive dyes. Azo reactive dyes are highly water soluble, so easily hydrolyzed. As a result, they are not used up completely during the dyeing processes and therefore discharged to the environment with the effluent coming from dyeing processes.

Reactive dyes released into the environment are stable to light and temperature and they disturb aesthetic view, affect absorbing and reflecting sunlight and also solubility of gases; thus photosynthetic activity of aquatic life. While some of textile dyes are toxic, some of them only change the colour, taste and odour of the water. Also, the removal of dyes from textile wastewaters is really so important because of most of the breakdown products of textile dyes are toxic and carcinogenic. Azo reactive dyes are generally resistant to aerobic biodegradation due to their biological recalcitrance. It was reported that approximately 90% of reactive dyes entering activated sludge sewage treatment plants pass through with no change

and no degradation. Under anaerobic bacterial reduction conditions they can form potentially carcinogenic compounds like aromatic amines. Furthermore, there might be a risk for reverse colourization when anaerobic degradation products are exposed to oxygen.

A wide range of methods have been developed for the removal of synthetic dyes from waters and wastewaters to decrease their impact on the environment. The technologies involve ozonation, chemical reduction-oxidation, coagulation-flocculation, electrochemical methods, membrane filtration and adsorption. Although these methods are effective, most of them have some drawbacks such as high cost, formation of hazardous by-products, and intensive energy requirement. For all of these reasons it is needed to investigate and to apply new alternative methods, which are environmentally friendly, economic and biocompatible. In recent years, a number of studies have been focused on some microorganisms which are able to biodegrade dyes in wastewaters. Various bacteria, yeast, fungi and algae are widely used for the removal of dyes by biosorption, bioaccumulation and biodegradation methods.

For the application of biodegradation method, the most efficient microorganism to break down coloured pollutants so far reported is white rot fungi. White rot fungi have a capability of producing extracellular, non-specific enzymes such as laccase, lignin peroxidase (LiP) and manganese peroxidase (MnP) which are able to degrade not only natural polymers, such as lignin and cellulose, but also different synthetic chemicals. This is why white rot fungi degrade textile dyes with a high efficiency. However, the disadvantage of this method is that degradation of dye takes a very long time and higher dye concentration causes growth inhibition.

Ultrasonic method, which is an advanced oxidative technique using ultrasonic waves, can be used for the decomposition of various types of chemical contaminants (dyes, aromatic compounds, chlorinated hydrocarbons etc.). In recent years, ultrasound has been actively employed for wastewater treatment. Although most of the organic compounds can be decomposed by the ultrasonic method, the decomposition rates are too still slow for practical uses. Also, it takes a longer time to achieve a higher dye removal yield, so it is not efficient to use this

method alone. In order to increase the dye removal rate and yield, biodegradation and ultrasound methods can be combined in series.

In this study, the degradation of reactive azo dye C.I. Reactive Orange 107 (Golden Yellow RNL), which is one of major components of Marine Blue dye used for dyeing jeans in textile industry, was investigated by using microbial and ultrasonic methods both alone and in series systems. Microbial degradation studies were performed with anaerobic-aerobic bacterial sludge and a white rot fungus *Trametes versicolor*. In combined ultrasound-microbial degradation system studies, microbial effluent was treated with ultrasound or ultrasound outlet was dealed with microbial cells to get higher dye removal rates and yields. The identification of original and hydrolyzed C.I. Reactive Orange 107 (RO107) dye compounds and the degradation products obtained during ultrasound or microbial treatment were done by using liquid chromatography-tandem mass spectrometry (LC-MS/MS) and the degradation mechanisms were proposed.

2. LITERATURE SURVEY

2.1. History of Dyestuff

The preparation and application of dyestuffs for painting and dyeing has been known since ancient times. The earliest written records of the use of dyestuffs were found in China dated 2600 BC. Initially all colouring matters were of natural origin obtained from plants and even animals. Woad and indigo (violet), madder (red), and weld (yellow) were typical of colouring matters extracted from plants. Colouring matters obtained from animals included Tyrian Purple from a species of whelk and the reds cochineal and kermes from insects. The first synthetic dyestuff (mauveine) was discovered and patented by the English chemist Sir William Henry Perkin (worked under a German professor, Hoffman) while attempting to synthesize quinine, the only cure for malaria in 1856. The first diazonium salt derived from picramic acid was prepared in 1858 and is still the basic chemistry behind countless commercial products. Indeed, apart from one or two notable exceptions, all the dye types used today were discovered in the nineteenth century. The introduction of the synthetic fibres, nylon, polyester, and polyacrylonitrile during the period 1930-1950, produced the next significant challenge. The discovery of reactive dyes in 1956 heralded a big breakthrough in the dyeing of cotton; intensive research into reactive dyes followed over the next two decades and is still continuing today. The oil crisis in the early 1970s, which resulted in a steep increase in the prices of raw materials for dyes, created a drive for more cost-effective dyes. The scale and growth of the dyes industry is inextricably linked to that of the textile industry. World textile production has grown steadily to an estimated 35 million tons in 1990. Because the two most important textile fibres are cotton and polyester, dye manufacturers tend to concentrate their efforts on producing dyes for these two fibres. Today, the total annual world textile production is estimated at about 800 kilo tonnes and Asia is being the largest dyestuff market (about 42%) in the world (Kirk-Othmer, 2001; Zille, 2005 and Druding, 1982)

2.2. Textile Dyestuffs

Dyes can be defined as colouring, ionising and aromatic organic compounds that show an affinity towards the substrate to which it is being applied. Dyes are aromatic compounds and they include aryl rings which have delocalised electron systems. These are responsible for the absorption of electromagnetic radiation of varying wavelengths, depending on the energy of the electron clouds (DyesPigments, 2008; StainsFile, 2005).

The electromagnetic spectrum can be divided into three different regions: ultraviolet, visible light and infrared (Table 2.1). Although visible light is considered to be between the wavelengths of 350 and 780 nm, the human eye can normally detect radiations between the wavelengths of 380 and 720 nm (Santos et al., 2007).

Table 2.1 The regions of the electromagnetic spectrum and relationship between wavelength and colour (Santos et al., 2007).

Electromagnetic region	Wavelength (nm)	Colour perception
Ultraviolet	<350	nd
Visible light	350-400	nd
	400-435	Violet
	435-480	Blue
	480-490	Greenish-blue
	490-500	Bluish-green
	500-560	Green
	560-580	Yellowish-green
	580-595	Yellow
	595-605	Orange
	605-750	Red
	750-780	nd
Infrared	>780	nd

nd is not detected by the eye.

Textile dyes are composed of two important groups, chromophore and auxochrome. The chromophore is a group of atoms, which provides the colour of the dye, and it is a radical configuration consisting of conjugated double bonds containing delocalised electrons. The most important chromophores are azo ($-\text{N}=\text{N}-$), carbonyl ($-\text{C}=\text{O}$), carbon ($>\text{C}=\text{C}<$), carbon-nitrogen ($>\text{C}=\text{NH}$ or $-\text{CH}=\text{N}-$), methine ($-\text{CH}=\text{}$), nitro ($-\text{NO}_2$ or $=\text{NO}-\text{OH}$) and sulphur ($\text{C}=\text{S}$). The auxochrome is

an electron-donating substituent that can intensify the colour of the chromophore by altering the overall energy of the electron system and provides solubility and a bonding affinity. The most important auxochromes are amine ($-\text{NH}_3$), carboxyl ($-\text{COOH}$), sulfonate ($-\text{SO}_3\text{H}$) (provides very high aqueous solubility of the dyes) and hydroxyl ($-\text{OH}$). The auxochromes can belong to the classes of reactive, acid, direct, basic, mordant, disperse, pigment, vat, anionic and ingrain, sulfur, solvent and disperse dyes (Zille, 2005; Santos et al., 2007).

2.3. Classification of Dyestuff

Dyes can be classified according to their chemical structure or by their usage or application method. The most appropriate system for the classification of dyes is by chemical structure, because it readily identifies dyes as belonging to a group that has characteristic properties, for example, azo dyes (strong and cost-effective) and anthraquinone dyes (weak and expensive). But it is more advantageous to consider the classification of dyes by usage or application because of dye nomenclature arises from this system. This classification is the principal system adopted by the Colour Index which is edited every three months since 1924 by the "Society of Dyers and Colourists (UK)" and the "American Association of Textile Chemists and Colorists (USA)". The name given is totally based upon the dye's mode of behaviour, base colour and action (Kirk-Othmer, 2001; Zille, 2005; DyesPigments, 2008 and Colour-Index, 2008). The classification of dyes according to their usage is summarized in Table 2.2. It shows the principal substrates, the methods of application and some properties for each application class.

2.3.1. Reactive Dyes

The increasing demand for colourfast and nonfading textiles leads to continuous growth in the use of reactive dyes. Reactive dyes are the most commonly used dyes in the textile industry to colour mainly cotton and also wool and polyamide fibres because of their wide variety of colour shades, high wet fastness profiles, ease of application and brilliant colours (Zille, 2005 and Yuzhu and Viraraghavan, 2001).

Table 2.2 Classification of dyes according to their usage (Adapted from Kirk-Othmer, 2001).

Class	Basic fibres to be coloured	Method of application and dye properties
Acid	nylon, wool, silk, paper, inks, and leather	Application; usually from neutral to acidic dyebaths. They are water-soluble anionic dyes and the original members of this class all had one or more sulfonic or carboxylic acid groups in their molecules. Chemically, the acid dyes consist of azo (including preformed metal complexes), anthraquinone, and triarylmethane compounds with a few azine, xanthene, ketone imine, nitro, nitroso, and quinophthalone compounds.
Azoic components and compositions	cotton, rayon, cellulose acetate, and polyester	Application; fibre impregnated with coupling component and treated with a solution of stabilized diazonium salt.
Basic	paper, polyacrylonitrile-modified nylon, polyester, and inks	Application; applied in acidic dyebaths. They are water-soluble, and yield coloured cations in solution. For this reason they are frequently referred to as cationic dyes. The principal chemical classes are diazahemicyanine, triarylmethane, cyanine, hemicyanine, thiazine, oxazine, and acridine. Some basic dyes show biological activity and are used in medicine as antiseptics.
Direct	cotton, rayon, paper, leather, and nylon	Application; applied in neutral or slightly alkaline baths containing additional electrolyte. These water-soluble anionic dyes, when dyed from aqueous solution in the presence of electrolytes, are substantive to, ie, has high affinity for, cellulosic fibres. Most of the dyes in this class are azo compounds with some stilbenes, phthalocyanines, and oxazines.
Disperse	polyester, polyamide, acetate, acrylic, and plastics	Application; fine aqueous dispersions often applied by high temperature-pressure or lower temperature carrier methods; dye may be padded on cloth and baked on or thermofixed. They are substantially water-insoluble nonionic dyes for application to hydrophobic fibres from aqueous dispersion.
Mordant	wool, leather, and anodized aluminium	Application; applied in conjunction with chelating Cr salts.
Pigments	paints, inks, plastics, and textiles	Application; printing on the fibre with resin binder or dispersion in the mass.
Reactive	cotton, wool, silk, and nylon	Application; reactive site on dye reacts with functional group on fibre to bind dye covalently under influence of heat and pH (alkaline). These dyes form a covalent bond with the fibre, usually cotton, although they are used to a small extent with wool and nylon. The principal chemical classes of reactive dyes are azo, triphendioxazine, phthalocyanine, formazan, and anthraquinon.
Sulphur	cotton and rayon	Application; aromatic substrate vatted with sodium sulfide and reoxidized to insoluble sulfur-containing products on fibre. Low cost and good washfastness properties of the dyeings make this class important from an economic standpoint.
Vat	cotton, rayon, and wool	Application; water-insoluble dyes solubilized by reducing with sodium hydrosulfite, then exhausted on fibre and reoxidized. The principal chemical classes of vat dyes are anthraquinone and indigoid.

Reactive dyes contain electrophilic functional groups which provide the formation of covalent bond between the dye and -OH, -NH or -SH groups in cotton, wool, silk and nylon fibres as a result of van der Waals forces, hydrogen bonds and hydrophobic interactions. The formation of covalent bond gives reactive dyes good stability during washing. Reactive dyes are highly sulfonated, and as such they are very water-soluble. The uptake of the dye in fibres depends on the dye nature and

its chemical constituents. In alkaline conditions, i.e. pH 9-12 and at salt concentrations from 40 to 100 g/l, and at high temperatures (30-70 °C), dyes form active reactive groups such as vinyl sulfone bonding with the fibres. However, a part of reactive groups undergo hydrolysis, i.e. a spontaneous reaction that occurs in the presence of water, and because the products do not have any affinity with the fibres, they do not form a covalent bond. Therefore, a large quantity of hydrolyzed reactive dye is discharged into the wastewater (Santos et al., 2007; Kirk-Othmer, 2001; Santos et al., 2007 and Sanghi, 2006).

2.3.1.1. Structure of reactive dyes

Reactive dyes consist basically of three components: a dye, a bridging group (B), and the reactive group (R). The schematic view of a reactive dye molecule was shown in Figure 2.1.

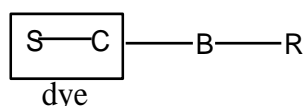


Figure 2.1 The general structure of a reactive dye molecule (Kirk-Othmer, 2001).

S: Water-soluble groups (sulfonic acid groups)

C: Chromophoric group which gives colour to the molecule

B: Bridging group which binds chromophoric group and reactive group each other

R: Reactive group which covalently binds to functional group of fibre

Reactive dyes contain chromophoric groups such as azo, anthraquinone, triarylmethane, etc. and reactive groups e.g. vinyl sulphone, chlorotriazine, trichloropyrimidine etc. that form covalent bonds with the fibre (Kirk-Othmer, 2001; Sanghi, 2006).

2.3.1.2. Azo reactive dyes

Azo reactive dyes constitute the largest class of water-soluble synthetic dyes with the greatest variety of colours and structure. There are more than 10,000 Colour Index (CI) generic names assigned to commercial colourants, approximately 4500 are in use and over 50% of these belong to the azo class. The term azo dyes is applied to those synthetic organic colourants that are characterized by the

presence of the chromophoric azo group (-N=N-). Azo reactive dyes contain at least one azo group but can contain two (disazo), three (trisazo), or, more rarely, four or more (polyazo) azo groups. The azo group is attached to two radicals of which at least one, but, more usually, both are aromatic (Kirk-Othmer, 2001; StainsFile, 2005; Hildenbrand, 1999; Rehorek et al., 2004; Wang et al., 2007; Al-Degs et al., 2000 and Manu and Chaudhari, 2002).

The structure of an azo reactive dye was represented in Figure 2.2.

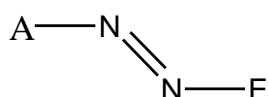


Figure 2.2 The general structure of an azo reactive dye (Kirk-Othmer, 2001).

In monoazo reactive dyes, the most important type, the A radical often contains electron-accepting groups, and the E radical contains electron-donating groups, particularly hydroxyl and amino groups. If the dyes contain only aromatic radicals such as benzene and naphthalene, they are known as carbocyclic azo dyes. If they contain one or more heterocyclic radicals, these dyes are known as heterocyclic azo reactive dyes (Kirk-Othmer, 2001).

Azo reactive dyes have been produced commercially for over 150 years and widely used in the food, pharmaceutical, cosmetic, leather and mainly in textile and dyestuff industries due to their wide variety of colour shades, high wet fastness profiles, ease of application and brilliant colours. Nearly half a million tonnes of azo dyes are produced each year all over the world, which account for almost half of all dye productions. Over 15% of the overall azo dye production is lost during manufacturing and application processes and released as effluent in hydrolyzed form. Due to their biological recalcitrance, they leave municipal wastewater plants nearly unchanged. Small amounts are precipitated or adsorbed. Little is known about their environmental fate. Because toxic and potentially carcinogenic nature of azo dyes, wastewaters from azo dye production processes and utilization industries requires a well treatment before discharge to the environment. (Hildenbrand, 1999; Kusic et al., 2006 and 2007; Zhang et al., 2005; Rehorek et al., 2004; Sayan, 2006 and Isik and Sponza, 2004).

C.I. Reactive Orange 107

Marine blue dye used for dyeing jeans is composed of three reactive dyes: Reactive Black 5, Reactive Orange 16 and Reactive Orange 107. C.I. Reactive Orange 107 (Golden Yellow RNL), one of the major components of Marine blue dye, is a vinylsulfone type mono azo reactive dye and suitable for the dyeing of all cellulosic fibres. The structure of C.I. RO107 was shown in Figure 2.3.

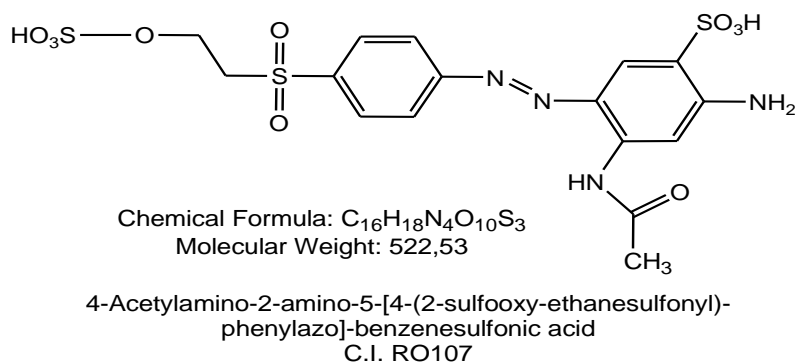


Figure 2.3 The general structure of C.I. Reactive Orange 107 (RO107).

2.4. Textile wastewaters

The textile industry and its wastewaters have been increasing proportionally with the increased demand for textile products. During dye manufacturing processes, large amounts of wastewater, approximately 1-700 L/kg of product, are produced (McMullan et al., 2001 and Kim et al., 2004)

In average 10 times more water is consumed for the preparation, dyeing, washing and rinsing stages of reactive dyeing processes than for dyeing with other dye types (acid, disperse dyes etc.) and consequently reactive dyes are found in the wastewater at higher concentrations than other dye classes and mainly in their hydrolyzed form. These wastewaters are also hard to treat because of their high biological and chemical oxygen demands and containing heavy metals, phenolic compounds, chlorides, etc. A typical textile wastewater properties contains different kinds of pollutants was shown in Table 2.3 (Tezer, 2001 and Aksu, 2005).

If these wastewaters discharge to the environment without any treatment, these dyes can remain in the environment for an extended period of time due to their

high stability to light and temperature. The presence of even very low concentrations of dyes in effluent is highly visible and undesirable. Depending on exposure time and dye concentration, dyes can have acute and/or chronic effects on exposed organisms. They also affect the absorption and reflection of sunlight through the water, oxygen solubility and threaten to the photosynthetic activity of aquatic plants and algae. This interferes with the growth of bacteria to levels sufficient to biologically degrade impurities in the water and risk the food chain. All these reasons make the elimination of reactive dyes from textile industries effluents before release into the environment really important (Slokar et al., 1998; Santos et al., 2007; McMullan et al., 2001; Nilsson et al., 2006; Allen and Koumanova, 2005 and Zhao et al., 2006).

Table 2.3 Typical textile wastewater properties (Tezer, 2001).

Parameter	1	2	3	4	5	6	7
BOD / COD	0.2	0.29	0.35	0.54	0.35	0.3	0.31
BOD (mg/l)	6000	300	650	650	350	300	250
SSM (mg/l)	8000	130	200	300	300	120	75
COD(mg/l)	300000	1040	1000	1200	1000	1000	800
Oil and Grease (mg/l)	5500	-	-	14	53	-	-
Chrome (mg/l)	0.05	4	0.014	0.04	0.05	0.42	0.27
Phenol (mg/l)	1.5	0.5	-	0.04	0.24	0.13	0.12
Sulphite (mg/l)	0.2	0.12	8	3	0.2	0.14	0.09
Colour (mg/l)	2000	1000	-	325	400	600	600
pH	8	7	10	10	8	8	11
Temperature (°C)	28	62	21	37	39	20	38
Water consumption (l/kg)	36	33	13	113	150	69	150

1-Raw wool washing, 2- Threat and fabric production, 3-Wool processing, 4-Cotton fabric processing 5-Fabric knitting finishing 6-Carpet production, 7-Threat colouring and finishing process

2.5. Treatment Methods for Textile Wastewaters

A wide range of methods have been developed for the removal of synthetic dyes from waters and wastewaters to decrease their impact on the environment (Jozwiak et al., 2007). Physical, chemical and biological methods are used as techniques for wastewater treatment. Physical methods include different precipitation methods (coagulation, flocculation, and sedimentation), adsorption (on activated carbon, biological sludge, and silica gel), filtration, reverse osmosis, etc. Chemical treatments are those, in which chemicals needed for decolourisation of wastewater are used. They include reduction, oxidation, complexometric methods, ion exchange and neutralization. Also the use of some advanced oxidation techniques (ozonation, ultrasound, H₂O₂/UV, etc.) have recently become very popular. Biological treatments differ from each other depending on the presence or absence of oxygen. In the former case the process is called aerobic (revival of biological sludge in aeration basins) and in the latter case anaerobic treatment (decay and rot in stabilizing lagoons). Another way in biological treatment is degradation by means of special fungi. Since biological treatment simulates degradation processes that occur in the environment, it is also called biodegradation. (Slokar et al., 1998) Table 2.4, the most commonly used methods for textile wastewaters treatment are summarized (Plum, 2005).

2.5.1. Physical Methods

2.5.1.1. Adsorption

Amongst the numerous techniques of dye removal, adsorption is the procedure of choice and gives good results as it can be used to remove different types of colouring materials. If the adsorption system is designed correctly it will produce a high-quality treated effluent. Adsorption process is influenced by many physio-chemical factors, such as, dye/sorbent interaction, sorbent surface area, particle size, temperature, pH, and contact time. Although activated carbon is the most commonly used sorbent, its widespread use is restricted due to high cost. In order to decrease the cost of treatment, numerous approaches have been studied for the development of cheaper and effective adsorbents. Peat, wood chips, silica gel, clay materials (bentonite, kaolinite), zeolites, siliceous materials (silica beads,

Table 2.4 Methods and procedures for decolourization of dye containing wastewaters (Adapted from Plum, 2005).

Method	Procedures	Decolourization rate	Treatment volume	Decolourization speed	Cost of investment	Properties
Activated carbon	Adsorption	++	-	-	-	Regeneration, waste disposal
Anaerobic/Aerobic	Microbiology	++	++	+	+	Waste disposal excess sludge
Electrolyze	Reduction/ Oxidation	++	-	+	-	Foam, electrode wear
Fenton's Reagent	Oxidation	++	-	+	-	Sludge disposal
Ion exchange		+	+	+	-	Ionic dyes, regeneration, concentrate disposal
Ion pair-extraction		+	-	+		Regeneration, concentrate disposal, only ionic dyes
Coagulation/ Flocculation	Solid-Liquid Separation	o	++	+/o	o	Sludge disposal, nitrification, COD elimination
Lignin Peroxidase	Enzymatic Redox reaction	-	-	-	-	Bad regeneration
Membrane Filtration*	Diffusion	++	++	+	-	Cleaning, concentrate disposal
NaOCl	Oxidation	+	+	o	o	Increasing salinity, formation of chlorinated by-products
Ozonization	Oxidation	+	+	o	-	By-products, COD elimination
Photocatalysis/ H ₂ O ₂ /TiO ₂ /ZnO	Oxidation	+	+	+	o	Little explored
Ultrasound	Radical reaction	++	-	o	-	Little explored
White rot fungi/H ₂ O ₂	Enzymatic redox reaction	+			-	Little explored

++ Very positive, + positive, o neutral/medium - negative, * Nanofiltration and reverse osmosis

alunite, perlite), agricultural wastes (sugar beet pulp, maize cob, rice husk, coconut shell), industrial waste products (waste carbon slurries, metal hydroxide sludge), biosorbents (chitosan, peat, biomass) and others (starch, cyclodextrin, cotton are used as sorbents for dye removal. The use of adsorption processes is technically easy but it has some drawbacks. Since adsorption processes are generally not selective, the other components of the wastewater can also be adsorbed by the support and the competition among the adsorbates can influence the dye binding capacity of supports in an unpredictable manner. Moreover, an adsorption process removes the synthetic dyes from wastewater by concentrating them on the surface retaining their structure practically unchanged. When the support is to be regenerated, the fate of the resulting concentrated solution of dyes presents a problem that is not satisfactorily solved. Even the mineralization of dyes

on the surface of support cannot be achieved. The regeneration of the adsorbent adds to the cost of the process, and is sometimes a very time-consuming procedure. Large-scale applications based on the adsorption process have to take into consideration the problems discussed (Slokar et al., 1998; McMullan et al., 2001; Crini, 2006; Aksu and Isoglu, 2006; Forgacs et al., 2004 and Lorimer et al., 2001)

2.5.1.2. Membrane Filtration

Membrane filtration method has the ability to clarify, concentrate and, most importantly, to separate dye continuously from effluent. This method removes all dye types, produce high-quality treated effluent. It has some special features unrivalled by other methods: resistance to temperature, an adverse chemical environment, and microbial attack. The disadvantages of this method are the concentrated residue left after separation, which poses disposal problems, the possibility of clogging, high capital cost and membrane replacement. This method of filtration is suitable for water recycling within a textile dye plant if the effluent contains low concentration of dyes, but it is unable to reduce the dissolved solid content, which makes water re-use a difficult task (McMullan et al., 2001; Lorimer et al., 2001 and Crini, 2006).

2.5.1.3. Ion Exchange

Because the opinion that ion exchangers cannot accommodate a wide range of dyes, ion exchange has not been widely used for the treatment of dye-containing effluents. For the treatment of dye containing effluent, wastewater is passed over the ion exchange resin until the available exchange sites are saturated. Advantages of this method include no loss of adsorbent on regeneration, reclamation of solvent after use and the removal of soluble dyes. A major disadvantage is cost. Organic solvents used for regeneration of the ion exchanger are expensive, and the ion exchange method is not very effective for disperse dyes (McMullan et al., 2001; Slokar et al., 1998, Crini, 2006).

2.5.2. Chemical methods

Chemicals methods include coagulation or flocculation combined with flotation and filtration, precipitation-flocculation with Fe(II)/Ca(OH)_2 , electroflotation, electrokinetic coagulation, conventional oxidation methods by oxidizing agent (ozone), irradiation or electrochemical processes. These chemical techniques are often expensive and although the dyes are removed, accumulation of concentrated sludge creates a disposal problem. There is also the possibility that a secondary pollution problem will arise because of excessive chemical use. However, other emerging techniques, known as advanced oxidation processes, which are based on the generation of very powerful oxidizing agents such as hydroxyl radicals, have been applied with success for pollutant degradation. Although these methods are efficient for the treatment of waters contaminated with pollutants, they are very costly and commercially unattractive. The high energy demand and the composition of chemical reagents are common problems. (Crini, 2006)

2.5.2.1. Coagulation/Flocculation

This is an economically feasible method of dye removal. It involves the addition of alums, ferric salts or limes, allowing excellent removal of direct dyes from wastewaters. Unfortunately, this method does not give good results with acid dyes. The optimum coagulant concentration is dependent on the static charge of the dye in solution. This process is simple, economically feasible but production of large amounts of sludge occurs, and this results in handling and disposal problems (McMullan et al., 2001; Lorimer et al., 1957 and Crini, 2006).

2.5.2.2. Treatment with NaOCl (Sodium hypochlorite)

Chemical oxidation of coloured wastewaters is possible with chlorine compounds. Electrophilic attack at the amino group by Cl initiates and accelerates the subsequent azo bond cleavage. It was reported that acid and direct dyes can be decolourised satisfactorily but it takes longer times for reactive dyes. Metal complex dyes and disperse dyes cannot be decolourised totally with NaOCl. Decolourization rate increases with increasing chlorine concentration and decreasing pH of medium. Nowadays the use of Cl for dye removal is not

preferred because of having some negative effects when released into waterways and release of carcinogenic or toxic aromatic amines (McMullan et al., 2001 and Slokar et al., 1998).

2.5.2.3. Electrochemical Destruction

This is a relatively new technique developed in the mid 1990s. The main principle of this method based on the formation of aluminium or ferric flocculated compounds by using aluminium or ferric electrodes. The flocculated compounds can be settled down by themselves or additional inorganic substances into the medium. The advantages of this method are consumption of very little or no chemicals and no formation of sludge. The breakdown metabolites are generally not hazardous and it is safe to discharge of treated wastewater into waterways. This method was reported as efficient and economical method for the removal of dyes and a high efficiency for colour removal and degradation of recalcitrant pollutants. However relatively high flow rates cause a direct decrease in dye removal. The main disadvantage is the cost of electricity used but it is comparable to the price of chemicals used in other methods (McMullan et al., 2001 and Tatli, 2003).

2.5.2.4. Oxidative Processes

Oxidation is the most commonly used chemical method for decolourization due to its simplicity of application. Hydrogen peroxide is generally used as an oxidizing agent. Hydrogen peroxide needs to be activated by some means for example Fenton's reagent, UV radiation, and etc. due to its stability in pure form. During chemical oxidation of dye-containing effluent, dyes are removed due to aromatic ring cleavage of dye molecules (McMullan et al., 2001 and Slokar et al., 1998).

There is a large number of advanced oxidation processes currently being evaluated which use ultraviolet radiation (UV) in combination with hydrogen peroxide or titanium dioxide, ultrasound or ultrasound in combination with ozonation or electrochemistry. Advanced oxidation processes have advantages of no sludge production, little or no consumption of chemicals, and efficiency for recalcitrant dyes. But they are economically unfeasible and formation of by-

products and technical constraints are the disadvantages (Crini, 2006 and Lorimer et al., 1957).

H₂O₂-peroxidase treatment

For decolourization purposes, peroxidase can also be used as hydrogen peroxide activator. The effectiveness of treatment depends on the peroxidase used, its concentration, pH and on the temperature of the medium. It was found in a study that the decolourization rate increased with increased peroxidase concentration and temperature of medium and was the greatest at pH 9.5 (Slokar et al., 1998).

H₂O₂ - Fe (II) salts (Fenton's reagent) treatment

Hydrogen peroxide can effectively decolourize dye from wastewaters in the presence of Fe(II) sulfate. Besides offering advantages in COD, colour and toxicity reduction, this process also has disadvantages. The main disadvantage of this method is the generation sludge which contains the concentrated impurities due to the flocculation of the reagent and the dye molecules. The sludge still needs ecologically questionable land-deposition. It has conventionally been incinerated to produce power, but such disposal is seen by some to be far from environmentally friendly. The performance of this method is dependent on the final flock formation and its settling quality. Optimal conditions for decolourization were found to be different for each type of dye, indicating that the development of a general oxidation method for a mixture of dyes would be very difficult. Thus, compromise must be made that is suitable for the decomposition of each dye at a reasonable oxidation rate (Jozwiak et al., 2007; Forgacs et al., 2004; McMullan et al., 2001 and Slokar et al., 1998).

H₂O₂-UV radiation treatment:

In this process, the only chemical used in the treatment is H₂O₂, which, due to its final decomposition into oxygen is not problematic. Peroxide is activated by UV light. Factors influencing H₂O₂/UV treatment are hydrogen peroxide concentration, the intensity of UV irradiation, pH, dye structure and dyebaths composition. It was reported that with increasing number of azo groups, the decolourization effectiveness decreases. This method degraded dye molecules to CO₂ and H₂O

by UV treatment in the presence of H_2O_2 . Degradation is achieved by the production of high concentrations of hydroxyl radicals. UV light is used to activate H_2O_2 and H_2O_2 is destructed into two hydroxyl radicals (1).



This method can be successfully used for the decolourization of acid, basic and reactive dyes. The major advantage of this method is no sludge production and great reducing of foul odours. But, depending on initial materials and the extent of the decolourization treatment some additional by-products, such as, halides, metals, inorganic odours, organic aldehydes and organic acids, may be produced (McMullan et al., 2001; Slokar et al., 1998 and Jozwiak et al., 2007).

H₂O₂-ozone treatment:

The use of ozone in wastewater treatment began in the early 1970s and it is a very good oxidizing agent due to its high instability. Although the original purpose of oxidation with ozone is disinfection of potable water, this method can be used for degradation of chlorinated hydrocarbons, phenols, pesticides, aromatic hydrocarbons and also synthetic dyes. Ozonation method can be effectively used for the decomposition of azo dyes in textile wastewaters. The results with H_2O_2 -ozone treatment showed that the decomposition rate is considerably higher at acidic pH. However, the influence of temperature and UV irradiation on the decomposition rate is negligible (Forgacs et al., 2004). Applied ozone dosage on the dye containing effluent depends on the total colour and residual COD. This method shows a preference for double-bonded dye molecules and leaves dye containing effluents with no colour and low COD suitable for discharge into environmental waterways. Chromophore groups in dye molecules are generally organic compounds with conjugated double bonds and cleavage of these bonds form smaller molecules and reduce the colour. These smaller molecules may be carcinogenic or toxic. Ozonation may be used as a method to prevent this and to achieve decolourization in a relatively short time. The drawback of ozonation for wastewater treatment is its short half-life, approximately 20 min. Furthermore the time can be significantly shortened if compounds like dyes are present. One of the

major disadvantages of ozonation is cost; continuous ozonation is required due to its short half-life. But applicability of ozone in its gaseous state eliminates the increase in the volume of wastewater and sludge (McMullan et al., 2001 and Slokar et al., 1998).

Ultrasound

Ultrasound is a sound wave with a frequency above the human audible range of 16 kHz. The sound frequency ranges of ultrasound were indicated in Figure 2.4 (Rehorek et al., 2004).

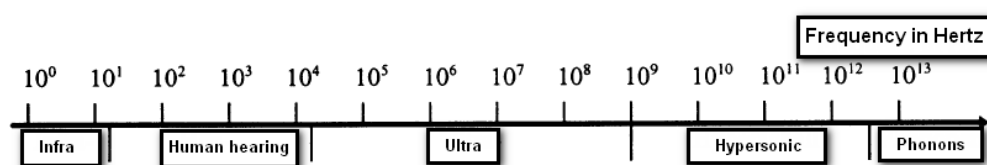


Figure 2.4 Classification of sound frequency ranges of ultrasound.

Ultrasonic waves are similar to the electromagnetic waves; they can be focused, reflected, and refracted. However, unlike light and electromagnetic waves, they cannot exist in vacuum, but require a media with elastic properties for their propagation. When ultrasonic waves pass through a liquid, particles in the elastic medium oscillate and energy is transferred through the medium in the propagation direction (Vajnhandl and Le Marechal, 2005 and Sood, 2000). Ultrasound produces its chemical effects through several different physical mechanisms and the most important nonlinear acoustic process for sonochemistry is cavitation. Cavitation is the formation, growth and implosive collapse of gas or vapour-filled microbubbles formed from acoustical waves in a body of liquid (Adewuyi, 2005). These ultrasound waves consist of expansion and compression cycles. Compression cycles exert a positive pressure on the liquid and push molecules together, while the expansion cycles exert negative pressure on the liquid, pulling the molecules away from one another. If the ultrasound is sufficiently intense, the expansion cycle can create cavities in the liquid. This will occur when the negative pressure exceeds the local tensile strength of the liquid, which varies according to the type and purity of liquid (tensile strength is the maximum stress a material can

withstand from a stretching load without tearing). Normally, cavitation is a nucleated process; that is, it occurs at pre-existing weak points in the liquid, such as gas-filled crevices in suspended particulate matter or transient microbubbles from prior cavitation events. It is difficult to produce significant negative pressures to create cavities with available ultrasonic generators for pure liquids having great tensile strength. Fortunately, most liquids are sufficiently contaminated by small particles so that cavitation can be readily initiated at moderate negative pressures. A bubble irradiated with ultrasound will absorb energy from the sound waves and grow. Cavity growth depends on the intensity of the sound. At high intensities, a small cavity may grow rapidly through inertial effects (transient cavitation). If cavity expansion is sufficiently rapid during the expansion half of a single cycle, it will not have time to recompress during the compression half of the acoustic cycle. At lower acoustic intensities cavity growth can also occur by a slower process called rectified diffusion (Figure 2.5).

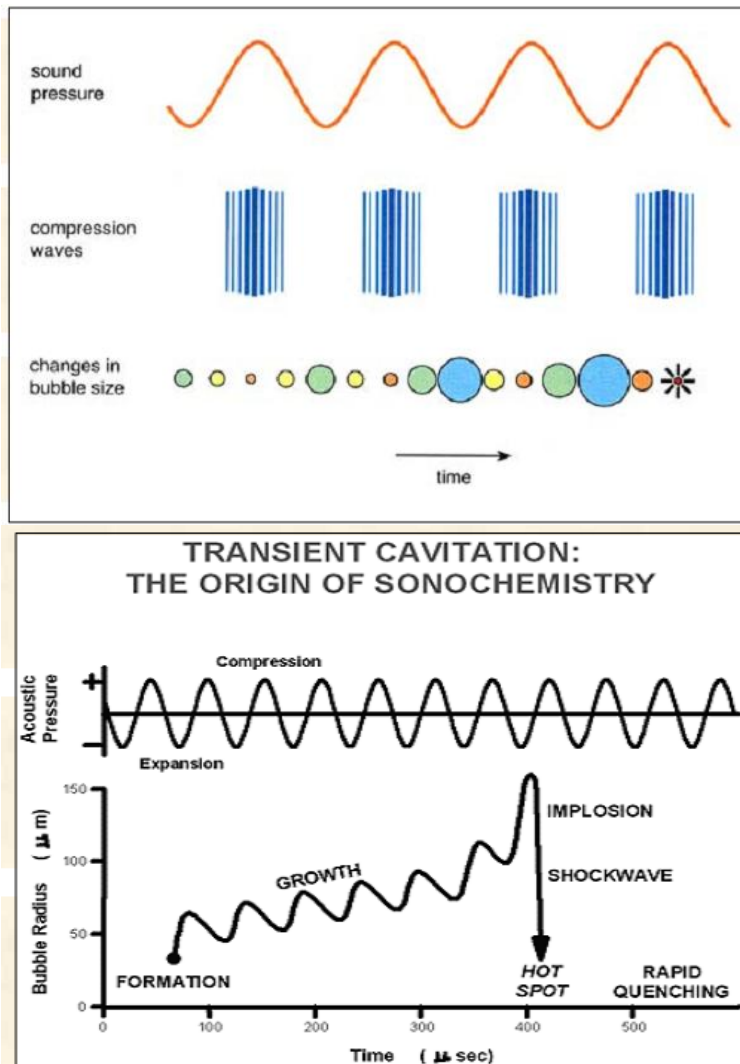


Figure 2.5 Formation of cavitation in liquids irradiated with ultrasound (Suslick, 1994).

Under these conditions a cavity will oscillate in size over many expansion and compression cycles (stable cavitation). During such oscillations the amount of gas or vapour that diffuses in or out of the cavity depends on the surface area, which is slightly larger during expansion than during compression. Cavity growth during each expansion is, therefore, slightly larger than shrinkage during the compression. Thus, over many acoustic cycles, the cavity will grow. The growing cavity can eventually reach a critical size where it can efficiently absorb energy from the ultrasonic irradiation. Called the resonant size, this critical size depends on the liquid and the frequency of sound; at 20 kHz, for example, it is roughly 170 micrometers. At this point the cavity can grow rapidly during a single cycle of

sound. Once the cavity has overgrown, either at high or low sonic intensities, it can no longer absorb energy as efficiently. Without the energy input the cavity can no longer sustain itself. The surrounding liquid rushes in, and the cavity implodes. It is the implosion of the cavity that creates an unusual environment for chemical reactions (Suslick, 1994). The important parameters affecting the cavitation and hence sonochemistry are reaction medium (viscosity, vapour pressure, pressure or generation of solid particles), reaction conditions (pressure, temperature, presence of entrained or evolved gases) and type of sonic system used (power, frequency and size and geometry of chemical reactor) (Vajnhandl and Le Marechal, 2007).

There are three regions of importance in the application of an aqueous sonochemical process. The first region is the interior of the collapsing cavitation bubbles in which extreme thermodynamic conditions were occurred due to high local temperature and pressure (5000 K, 1000 atm). In this region, a fast pyrolysis of volatile solutes takes place; water molecules also undergo thermal decomposition to produce H atoms and $\cdot\text{OH}$ radicals. The second region is the interfacial boundary between the gaseous and the liquid phases where the temperature is lower than inside the bubbles, yet still high enough to cause thermal decomposition of organic solutes.

It is believed that the reactive radicals formed from water decomposition in gas bubbles are localized in this region. The third region is the bulk of solution (usually at ambient temperature) where various reactions of organic solutes with either $\cdot\text{OH}$ radicals or H atoms, which escape from the bubbles' interface, may occur (Yasman et al., 2004 and Ge et al., 2004).

The formation of free radicals during sonolysis of aqueous solutions can be explained by the following equations;



If the solution is saturated with oxygen, additional radicals are produced in the gas phase as:



where))) refers to the ultrasound irradiation. Free hydroxyl radicals, which have a high oxidation potential, can oxidize a wide range of organic contaminants (Wang et al., 2007; Sayan, 2006; Neppolian et al., 2004; Inoue et al., 2006; Suslick et al., 1986; Goskondaa et al., 2002; Ince and Guyer, 2004; Tezcanli-Guyer and Ince, 2004 and Chitra et al., 2004).

Over the last few years, sonochemical treatments have been examined as a potential wastewater treatment method. Ultrasound can be able to convert chemical substrates like, chlorinated hydrocarbons, aromatic compounds, textile dyes, phenolic compounds and esters, into short chain organic acids, carbon dioxide and inorganic ions as final products (Vinodgopal, et al., 1998; Sayan, 2006; Neppolian et al., 2004 and Sivakumar and Rao, 2003). Among advanced oxidation methods, ultrasonic irradiation is easy to operate with no formation of harmful by-products (Ma et al., 2006; Neppolian et al., 2004; Voncina and Le Marechal, 2003; Mason, 2007 and Entezari and Sharif, 2007). Its use in industrial scale is limited because the process of producing ultrasound is very inefficient and burdened with high operating costs. If ultrasound process can be operated at milder conditions (e.g., lower temperatures and pressures), the cost may be reduced. However, the decomposition rates are still slow for practical uses. Therefore, much effort has been devoted to accelerate the decomposition rates by using combined treatment methods (Sayan, 2006 and Thompson and Doralswamy, 1999).

2.5.3. Biological Methods

Biological treatments are often the most economical alternative when compared with other physical and chemical processes. Biological methods such as microbial degradation, adsorption by (living or dead) microbial biomass and bioaccumulation by growing cells are commonly applied to the treatment of industrial effluents because many microorganisms such as bacteria, yeasts, algae and fungi are able to adsorb, accumulate and degrade different organic pollutants. Although, biological treatment processes are relatively inexpensive, the running costs are low and the end products of complete mineralization are not toxic, their application is often restricted because of treatment time, technical constraints and requires a large land area (Crini, 2006 and Forgacs et al., 2004).

Biodegradation is a biological method using living and growing microorganism which are able to degrade organic pollutants that pass through the conventional biological treatment process in unchanged form. Different kinds of microorganism (fungus, yeasts, bacterial sludge, etc.) can be used for the degradation of organic pollutants like dye, phenolic compounds, pesticides, etc. Degradation processes can be performed under anaerobic or aerobic conditions. During the degradation of azo reactive dyes by anaerobic bacteria potentially carcinogenic colourless aromatic amines are formed, which are generally not further degraded and which are accumulated under anaerobic conditions. Aerobic biodegradation of azo reactive dyes by bacteria and fungi leads to the formation of simple components of carbon dioxide and water.

2.5.3.1. Anaerobic biodegradation

Anaerobic conditions occur naturally in the lower layers of sediments in lakes and ponds, river beds and estuaries and deliberately during sewage treatment of sewage sludge (Slokar et al., 1998). Under anaerobic conditions, azo reactive dye is biodegraded to colourless, hazardous aromatic amines by the reduction of the azo bond through bacteria (Libra et al., 2004). Anaerobic reductive cleavage of the azo bond $-N=N-$ involves a transfer of four electrons (reducing equivalents), which proceeds through two stages at the azo bond. In each stage two electrons are transferred to the azo dye, which acts as a final electron acceptor (Figure 2.6)

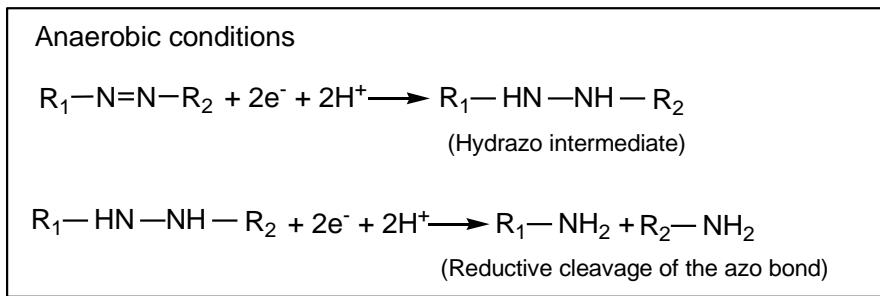


Figure 2.6 The scheme for reductive cleavage of the azo bond.

The exact mechanism of azo dye reduction, whether occurring intracellularly or extracellularly, is still a subject of investigation (Santos et al., 2007).

Anaerobic reduction of dyes can occur in three different ways:

1. The direct enzymatic reduction: This is an intracellular reduction and bacterial enzymes are responsible for the reduction of azo dyes.
2. The indirect enzymatic reduction: This is an extracellular reduction and enzymatic redox mediators act as electron shuttle at the intermediate stage. The redox mediators accelerate the reduction of azo bond and allow the reduction of azo dyes.
3. The chemical reduction: The chemical reduction succeeds in using hydrogen sulfide. Sulfate reduction bacteria use sulfate as electron acceptor in the anaerobic respiration and reduce sulfur. During this process, sulfide is oxidized to elemental sulfur and the azo bond is reduced. (McMullan et al., 2001; Plum, 2005 and Yildiz, 2006).

Anaerobic biodegradation processes are not efficient for the removal of azo reactive dyes due to the formation of toxic aromatic amines. Toxicity could be eliminated through bacterial fission of the aromatic ring structure, a process that requires oxygen. Therefore, secondary aerobic treatment should be used to detoxify dye intermediates formed. Diverse technologies have been developed for the successive anaerobic/aerobic treatment of dye wastewaters (Forgacs et al., 2004 and Chinwetkitvanich et al., 2000). However, the fragments of azo bond

cleavage can undergo auto oxidation under aerobic conditions forming again coloured products (Torres, 2003; Shaw et al., 2002; Isik and Sponza, 2006; Ekici et al., 2001; Nigam et al., 1996; Santos et al., 2007; McMullan et al., 2001; Slokar et al., 1998; Nilsson et al., 2006; Allen and Koumanova, 2005; Sponza and Isik, 2005; Çetin, 2006 and Van der Zee and Villaverde, 2005).

2.5.3.2. Aerobic biodegradation

Aerobic biodegradation is a process that often takes place in the environment, e.g. in natural ecosystems like soil or surface waters, and it is often associated with technical systems such as wastewater treatment plants (Slokar et al., 1998). Under aerobic conditions, the microbial enzymes of mono- and di-oxygenase biodegrade reactive azo dyes by ring scission of aromatic ring with the incorporation of oxygen. Azo dyes are quite recalcitrant to aerobic bacterial degradation because of nitro and sulfonic groups' substituted to aromatic structure. This fact is probably related either to the electron-withdrawing nature of the azo bond and their resistance to oxygenases attack, or because oxygen is a more effective electron acceptor, therefore it has more preference for reducing equivalents than the azo dye (Santos et al., 2007)

In recent years, many researches have indicated that white rot fungus is a promising microorganism for oxidative decolourization of reactive azo dyes and presents an interesting challenge (Sanghi, 2006; Chinwetkitvanich et al., 2000 and Eichlerova et al., 2006).

2.5.3.3. Fungal Biodegradation

White-rot fungi offer significant advantages from decomposition of recalcitrant compounds. White-rot fungi produce a wide variety of extracellular ligninolytic enzymes (laccase, lignin peroxidase, phenol oxidase, Mn-dependent peroxidase and Mn-independent peroxidase), which are substrate nonspecific. Therefore the fungus can degrade a wide variety of recalcitrant compounds including azo reactive dyes to carbondioxide and water (Libra et al., 2003; Dawen et al., 2004; D'Souza et al., 2006; Kim et al., 2004; Novotny et al., 2004; Swamy and Ramsay, 1999; Arora and Gill, 2000 and 2001; Lorenzo et al., 2002; McMullan et al., 2001

and Young and Jian, et al., 1997). Because these enzymes are extracellular, the substrate diffusion limitation into the cell, generally observed in bacteria, is not encountered. White rot fungi do not require preconditioning to particular pollutants, because enzyme secretion depends on nutrient limitation, nitrogen or carbon, rather than presence of pollutant. In addition, extracellular enzyme system enables white rot fungi to tolerate high concentration of pollutants (Kapdan et al., 2000; Nilsson et al., 2006; Sanghi, 2006 and Svobodova et al., 2007).

Trametes versicolor

The white rot fungus *Trametes versicolor* used in this thesis study belongs to *Polyporaceae sensu lato* family. *Trametes versicolor* is capable of producing three important oxidative enzymes (laccase, lignin peroxidase, Mn peroxidase) (Wesenberg et al., 2003 and Swamy and Ramsay, 1999). The optimal growth temperature is given between 28-32 °C. The fungus can grow in a medium containing glucose, malt extract, potassium dihydrogen phosphate, magnesium sulfate, ammonium dihydrogen phosphate at a pH range of 4-5. In recent years, many researches were carried out with *Trametes versicolor* for the removal of different kinds of textile dyestuffs have been encountered in the literature (Tatli, 2003; Aksu et al., 2006; Adosinda et al., 2003 and Lorenzo et al., 2002).

3. MATERIALS AND METHODS

3.1. The dye used in the experimental studies

In the present study, C.I. Reactive Orange 107 (Golden Yellow RNL) (RO107) reactive mono azo dye which was supplied from Dystar (Leverkusen, Germany) was used. Because reactive dyes are found in wastewaters as hydrolyzed form, firstly RO107 was hydrolyzed and used in hydrolyzed form for further studies. It was possible to hydrolyze the reactive anchor groups of dye gently, by process similar to those for dyeing, without changing or destroying the chromophore. For the hydrolysis of RO107, stock dye solution was prepared by dissolving approximately 155 g dye (500 mmol) in 1 l of tap water. Before the addition of dye, the tap water was first heated up to 60-80 °C, 40 g NaCl and 23 g NaOH (to get alkaline conditions) was added into the tap water and mixed continuously. When the ingredients were dissolved completely, the dye was added step by step and the solution was left at least 8 h by heating and mixing to allow complete hydrolysis. The status of hydrolysis was controlled by HPLC-analysis and after making the hydrolysis completed, the solution was cooled down to room temperature and neutralized with concentrated H₂SO₄. Test solutions used in the experiment were made by proper dilution of the stock dye solution by using deionised water.

3.2. The microorganisms used in the experimental studies

The microbial degradation of RO107 was performed by using two different microorganisms, *Trametes versicolor*, a white rot fungus, and anaerobic-aerobic sludge, a mixed bacterial culture. For fungal biodegradation studies, a pure culture of *Trametes versicolor* ATTC200801 obtained from American Type Culture Collection was used. A medium consisting of 2% (w/v) malt extract agar dissolved in distilled water was autoclaved for 20 min at 121 °C and 0.99 bar and poured into glass tubes without any pH adjustment. The tubes were let to cool down by laying out in inclined form and solid agar media were obtained. The fungal strain was then inoculated on 15-20 glass tubes (having approximately same surface area) and cultured for 6-7 days at 30 °C. The fungal cells were cultured for 6-7 days at 30 °C. The plates were preserved at 4 °C. New plates were inoculated once a

month. These glass tubes were then used for the inoculation of flasks containing aqueous growth medium with or without dye. One glass tube was used for one flask and by this way; each flask was inoculated with approximately the same amount of fungal cells (Cetin and Donmez, 2006 and Aksu et al., 2006). Two growth media (medium 1 and medium 2) containing glucose and glucose-molasses sugars as main substrates were tested for the growth of *T. versicolor* and for the dye removal by the fungus. Glucose at different concentrations was used in both growth media as the strain *T. versicolor* was capable of utilizing glucose as a carbon source. Medium 1 was composed of 10 g/l glucose, 0.1 g/l yeast extract, 0.5 g/l $\text{NH}_4\text{H}_2\text{PO}_4$, 0.5 g/l MgSO_4 , 0.2 g/l KH_2PO_4 , 1.4 g/l $\text{ZnSO}_4 \cdot 7\text{H}_2\text{O}$ and 1 g/l $\text{FeSO}_4 \cdot 7\text{H}_2\text{O}$. It was thought that an additional carbon source implies a cometabolic pathway of degradation of dye. For this reason, molasses was used as a second sugar source for medium 2 due to its high sucrose and other nutrient contents, low cost, ready availability and easy of storage. Molasses, supplied from Turkey Sugar Industry, was added to the growth medium at changing concentrations of glucose and same quantities of other chemicals given in medium 1.

The cells adapted to dye containing growth medium were used for the dye removal studies. Microbial adaptation is defined as the ability of a microbial population to adjust itself to a changing environment, in this case the presence of dye. The culture grown in low dye concentration containing medium was transferred to the next medium supplemented with a higher concentration of dye and thus, acclimatized to high concentrations. The adaptation studies were repeated two times for each dye concentration.



The other culture used for anaerobic-aerobic RO107 biodegradation studies was a mixed culture of bacteria. Anaerobic bacterial sludge was obtained from a local municipal sewage treatment plant in Germany. Aerobic activated sludge was supplied from the wastewater treatment plant of Bayer AG (Leverkusen, Germany). Each sludge was used in immobilized form. 1 cm^3 polyurethane foam cubic carriers coated with activated carbon supplied from Biosys (Leverkusen, Germany) were used for immobilization (Yildiz, 2006).

3.3. Experimental Setups

3.3.1. Ultrasound treatment system

Ultrasound experiments were carried out with two ultrasound devices called K8 and MFLG (Meinhardt Ultraschalltechnik, Leipzig, Germany) working at different frequencies. These systems were studied under conditions given in Table 3.1. The system parameters were optimized by Frömer (Frömer, 2005).

Table 3.1 Working conditions of ultrasonic systems used in the experiments (Adapted from Frömer, 2005).

Name	Data			
K8	$f = 850 \text{ kHz}$ $V_{\max} = 1,5 \text{ L}$ $P_{el;\max} = 136 \text{ W}$ $P_{ac;\max} = 60 \text{ W}$ $\eta_{Pel/Pac} = 45\%$ intensity = 4 $R^{\bullet OH\max} (\text{mmol/L} \cdot \text{min}) = 2,64$ $R^{\bullet OH60W} (\text{mmol/L} \cdot \text{min}) = 2,64$ $R^{\bullet OH30W} (\text{mmol/L} \cdot \text{min}) = 0,99$			
MFLG	<table border="0"> <tr> <td> $f = 378 \text{ kHz}$ $V_{\max} = 1,5 \text{ L}$ $P_{el;\max} = 512 \text{ W}$ $P_{ac;\max} = 62 \text{ W}$ $\eta_{Pel/Pac} = 12\%$ intensity = - $R^{\bullet OH\max} (\text{mmol/L} \cdot \text{min}) = 3,14$ $R^{\bullet OH60W} (\text{mmol/L} \cdot \text{min}) = 3,14$ $R^{\bullet OH30W} (\text{mmol/L} \cdot \text{min}) = 1,68$ </td> <td> $f = 992 \text{ kHz}$ $V_{\max} = 1,5 \text{ L}$ $P_{el;\max} = 650 \text{ W}$ $P_{ac;\max} = 44 \text{ W}$ $\eta_{Pel/Pac} = 7$ intensity = - $R^{\bullet OH\max} (\text{mmol/L} \cdot \text{min}) = 1,83$ $R^{\bullet OH60W} (\text{mmol/L} \cdot \text{min}) = -$ $R^{\bullet OH30W} (\text{mmol/L} \cdot \text{min}) = 1,15$ </td> </tr> </table>	$f = 378 \text{ kHz}$ $V_{\max} = 1,5 \text{ L}$ $P_{el;\max} = 512 \text{ W}$ $P_{ac;\max} = 62 \text{ W}$ $\eta_{Pel/Pac} = 12\%$ intensity = - $R^{\bullet OH\max} (\text{mmol/L} \cdot \text{min}) = 3,14$ $R^{\bullet OH60W} (\text{mmol/L} \cdot \text{min}) = 3,14$ $R^{\bullet OH30W} (\text{mmol/L} \cdot \text{min}) = 1,68$	$f = 992 \text{ kHz}$ $V_{\max} = 1,5 \text{ L}$ $P_{el;\max} = 650 \text{ W}$ $P_{ac;\max} = 44 \text{ W}$ $\eta_{Pel/Pac} = 7$ intensity = - $R^{\bullet OH\max} (\text{mmol/L} \cdot \text{min}) = 1,83$ $R^{\bullet OH60W} (\text{mmol/L} \cdot \text{min}) = -$ $R^{\bullet OH30W} (\text{mmol/L} \cdot \text{min}) = 1,15$	
$f = 378 \text{ kHz}$ $V_{\max} = 1,5 \text{ L}$ $P_{el;\max} = 512 \text{ W}$ $P_{ac;\max} = 62 \text{ W}$ $\eta_{Pel/Pac} = 12\%$ intensity = - $R^{\bullet OH\max} (\text{mmol/L} \cdot \text{min}) = 3,14$ $R^{\bullet OH60W} (\text{mmol/L} \cdot \text{min}) = 3,14$ $R^{\bullet OH30W} (\text{mmol/L} \cdot \text{min}) = 1,68$	$f = 992 \text{ kHz}$ $V_{\max} = 1,5 \text{ L}$ $P_{el;\max} = 650 \text{ W}$ $P_{ac;\max} = 44 \text{ W}$ $\eta_{Pel/Pac} = 7$ intensity = - $R^{\bullet OH\max} (\text{mmol/L} \cdot \text{min}) = 1,83$ $R^{\bullet OH60W} (\text{mmol/L} \cdot \text{min}) = -$ $R^{\bullet OH30W} (\text{mmol/L} \cdot \text{min}) = 1,15$			

f: frequency, V: reactor volume, $P_{el;\max}$ maximum electrical power, $P_{ac;\max}$ acoustic power, $\eta_{Pel/Pac}$: efficiency, $R^{\bullet OH}$: radical formation rate

The ultrasound system contained two parts: the device (K8 or MFLG) and a glass reactor mounted to ultrasound system. The glass reactor was surrounded by a cooling jacket to maintain the system at a certain temperature. The working volume was selected 500 ml. The experiments were performed at batch scale.

3.3.2. Microbial treatment systems

3.3.2.1. Fungal biodegradation system

Batch experiments were carried out in 250 ml Erlenmeyer flasks in a temperature and agitation rate controlled incubator shaker. Flasks were prepared in double and contained 150 ml growth media (Medium 1) with no dye or with dye at desired

concentration. All experiments were performed at 30 °C, which was optimum for fungal growth, and at 150 rpm agitation rate. To investigate the effect of initial pH on fungal growth and dye decolourization, medium 1 was prepared at a pH range of 3.0-5.5 with no dye or with 50 mg/l dye. The inoculation of fungal cells was done by acclimatized cultures and maximum fungal growth and dye removal percentages were determined at the end of 20 days incubation.

In order to examine the effect of initial dye concentration, varied between 25-300 mg/l, on the fungal growth and RO107 decolourization, glucose medium (Medium1) containing changing levels of glucose (2.5-20 g/l) was prepared at the optimum pH value. The studies were repeated with molasses containing growth medium (Medium 2) by no addition or addition of dye at changing concentrations from 25 to 300 mg/l to the medium.

To obtain the growth curves in no dye containing medium, 7 Erlenmeyer's were prepared at the same conditions (same pH, same glucose concentration). After the inoculation the growth media with fungus, the flasks were opened in turn at definite time intervals and dry weight of fungal pellets was weighted within the total incubation period of 20 days.

3.3.2.2. Anaerobic-aerobic biodegradation system

Anaerobic-aerobic treatment of RO107 was investigated by Yildiz (Yildiz, 2006). The experimental set up used by Yildiz contained two 40 L batch sequent reactors. Each of reactor filled with immobilized anaerobic and aerobic sludge had 30 L working volume. The pH of medium was held constant at 7.0 ± 0.2 in both bioreactors. The temperature of the anaerobic bioreactor was maintained at 39 ± 0.5 °C. Aerobic bioreactor was operated at ambient temperature. The schematic view of anaerobic-aerobic bioreactor system and process flow diagram can be seen in Figs. 3.1 (Yildiz, 2006 and Rehorek et al., 2004).

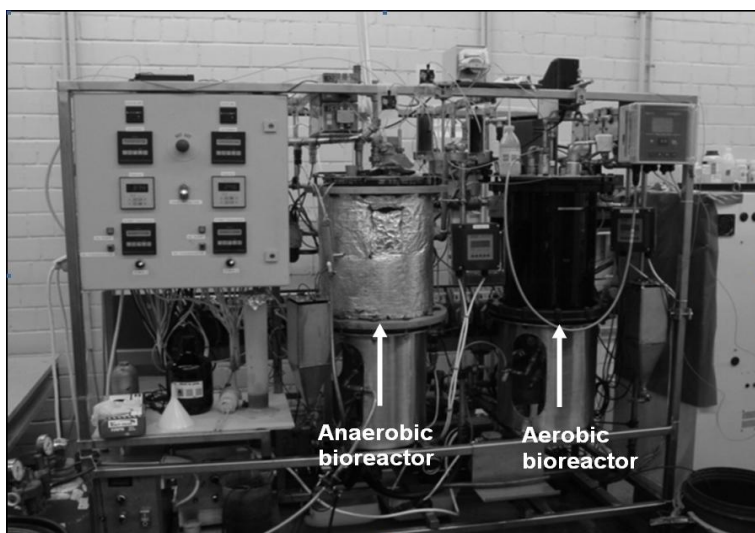


Figure 3.1 The view of two stage anaerobic-aerobic bioreactor.

In the first anaerobic reactor, RO107 dye reduction was achieved by anaerobic bacteria and the effluent containing intermediate products was fed to the aerobic reactor for further degradation to achieve complete decolourization.

3.4. Analytical Methods

4 ml of samples taken from the degradation medium at certain time intervals were analysed by using LC-MS/MS, UV-visible spectrophotometer and COD measurement.

LC/MS-MS is a multidimensional analytical system that enables separation and detection of polar, nonpolar, coloured, and colourless substances of both high and low molecular weight. In the thesis study, original and hydrolyzed forms of RO107 and degradation products were detected by using LC-MS/MS with TBAAc method and the results were evaluated with Analyst Software and the proposed structure analyses were done by using Chem Draw 7.0 Programme (Appendix 1).

During fungal degradation, the concentration of residual dye in the growth medium was determined spectrophotometrically. The absorbance of the colour was read at 425 nm by UV-Vis Spectrophotometer (Labomed Inc., USA). The cell free liquid medium was used as the blank (Appendix 2).

The total reduced sugar was measured according to Miller, 1959 (Appendix 3).

The dry weight of fungal pellet was measured by filtering the pellet through filter paper, drying at a constant temperature of 65 °C and weighing it.

For the determination of the absorption spectra of samples, a single beam spectrometer Lambda 10 (Perkin Elmer) was used in the wavelength range of 200-800 nm.

During the ultrasound degradation studies, chemical oxygen demand (COD) values were also measured. COD measurement is based on an oxidative reaction by using a strong oxidizing agent (the most often used oxidant is potassium dichromate, $K_2Cr_2O_7$) in combination with boiling sulfuric acid, H_2SO_4 , under specific conditions of temperature and for a particular period of time. To measure the COD of degradation medium, 2 ml of sample was added into the standardized test solution of COD kit (Dr.Lange Company, Dusseldorf) and held at a certain temperature (148 °C) for 2 hours for complete oxidation. And then the colour of test solution was measured with Spectra of Dr.Lange Company.

4. RESULTS AND DISCUSSION

The aim of this thesis was to investigate the degradation of hydrolyzed form of RO107, an important pollutant in textile wastewaters, by using ultrasound, fungal and sequential anaerobic-aerobic treatment methods and the ultrasound-fungal and ultrasound-anaerobic-aerobic systems in series to obtain higher degradation rates and removal yields. Other important objective of this thesis was to detect the original and hydrolyzed forms of RO107 and degradation products by using LC-MS/MS analysis and to characterize the structures formed during degradation by Analyst Software and Chem Draw 7.0 programme.

Ultrasonic decolourization studies were performed by changing the frequency, temperature and initial dye concentration.

For fungal decolourization studies, the effect of pH on fungal growth and dye removal was firstly examined and the optimum pH was determined. The effects of carbon substrate types (glucose, glucose-molasses sucrose) on fungal growth and dye removal were investigated under optimum growth conditions. A summary of sequential anaerobic-aerobic degradation results of the dye investigated by Yildiz (Yildiz, 2006) was put into the thesis to compare the ultrasonic, fungal and bacterial systems and findings.

The results obtained by combined ultrasonic and microbial systems were also discussed.

4.1. The Structural Analysis of Original Form of RO107

When commercial dye C.I. Reactive Orange 107 (RO107) is dissolved in water, different kinds of structures are formed besides original form of dye (RO107_O) mainly including vinyl form of dye (RO107_V, m/z:423). The results of the structural analysis of RO107 by using LC-MS/MS were given in Figure 4.1 on a basis of the total wavelength and diode-array detector chromatograms.

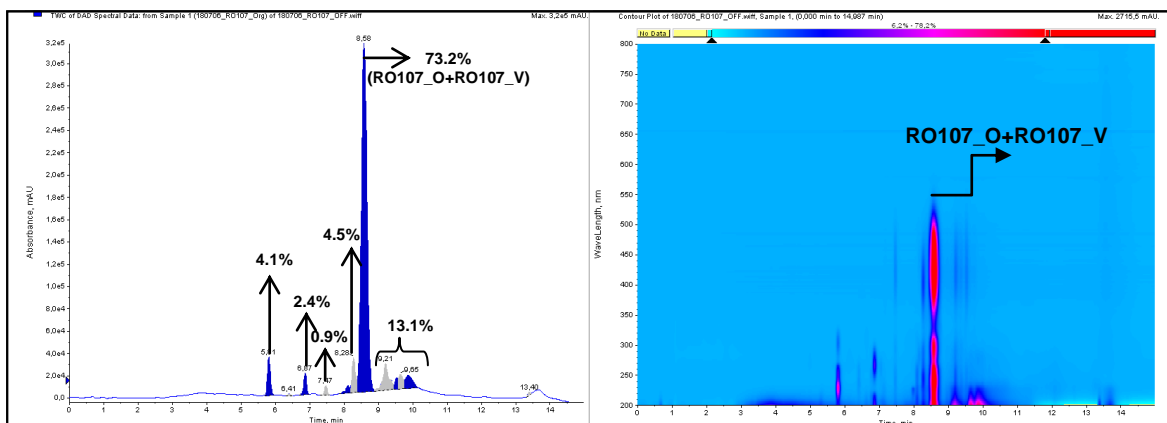


Figure 4.1 Total wavelength chromatogram and DAD chromatogram of commercial azo reactive dye RO107.

From the total wavelength chromatogram, it was detected that 73% of RO107 is the original (RO107_O) and vinyl (RO107_V) forms of the dye. It can be seen from DAD chromatogram, the main compounds in visible region (380-720 nm) are RO107_O and RO107_V. The other components formed during the dissolution are listed in Table 4.1.

Table 4.1 The composition of commercial (original) azo reactive dye RO107.

Compounds	Abbreviation	m/z	Molecular Mass (g/mol)	Retention time (min)
4-Acetylamino-2-amino-benzenesulfonic acid	NA-ABSA	229	230	5.81
2-amino-5-(2-hydroxy-ethanesulfonyl)-benzenesulfonic acid or p-Base Sulfone ester	PBSA	280	281	6.87
Reactive Orange 107-Hydrolyzed	RO107_H	441	442	7.47
Reactive Orange 107-Hydrolyzed with one Acetyl group	RO107_H+NA	482	483	8.28
Reactive Orange 107- Vinyl form	RO107_V	423	424	8.58
Reactive Orange 107-Original	RO107_O	520	521	8.58

The negative ionization mode used in the LC/MS-MS analysis is the most suitable ionization technique for determination of molecular weight and total number of sulphonic and carboxylic acid groups in (poly)-sulphonated dyes. The spectra produced via this method are easy to interpret, because they contain only decationized molecular ions with different number of charges. Characterization of

the azo dyes could be achieved by observing typical fragment ions formed by cleavage of the C-N bonds (azo-type fission) on either side of the azo linkage, and cleavage of the N=N double (keto-type fission) bond with transfer of one or two hydrogen atoms to form an imine or amine (Holcapek et al., 1999; Straub et al., 1992; Plum and Rehorek, 2005; Poiger and Baughman, 2000; Reemtsma, 2001; Epolito et al., 2005 and Smyth et al., 1999).

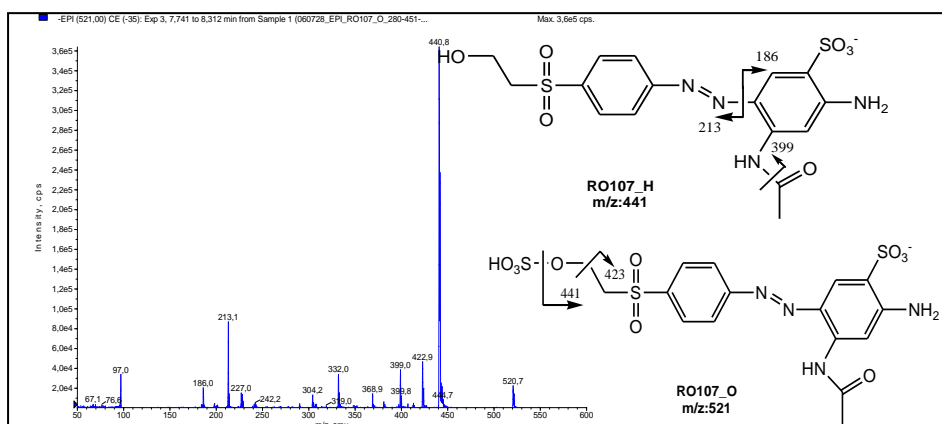


Figure 4.2 Enhanced Product Ion (EPI) spectrum and fragmentation pattern of RO107 original form (RO107_O).

In Figure 4.2, the enhanced product ion spectrum and the fragmentation pattern of RO107 original form are shown. There are two intensive signals, one of which belongs to $m/z:441$, and the other to $m/z:213$. The signal $m/z:441$ represents the hydrolyzed form of RO107 (RO107_H) and formed by the secession of SO_3^- group from RO107 original form. The other intensive peak $m/z:213$ points to an azo-type fission.

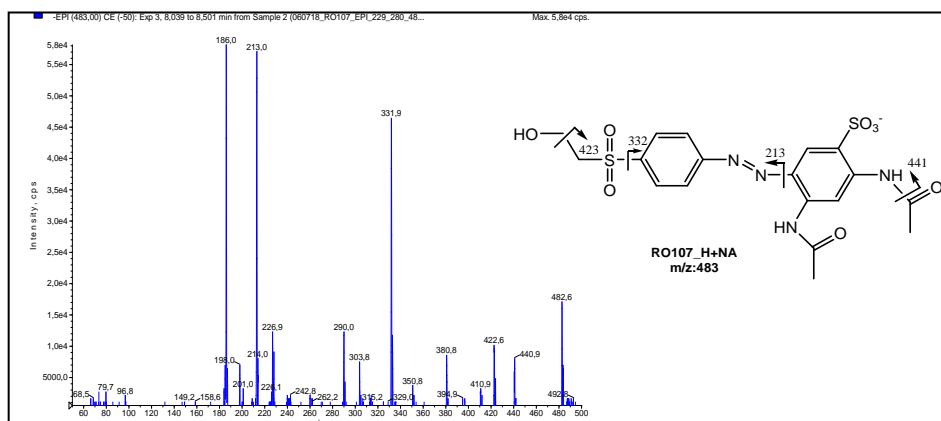


Figure 4.3 Enhanced Product Ion (EPI) spectrum and fragmentation pattern of hydrolyzed RO107 with one acetyl group (RO107_H+NA).

The enhanced product ion spectrum and the fragmentation pattern of hydrolyzed RO107 with one acetyl group (RO107_H+NA) were given in Figure 4.3. The two intensive signals point to both azo (m/z : 186) and keto (m/z : 213) types cleavages.

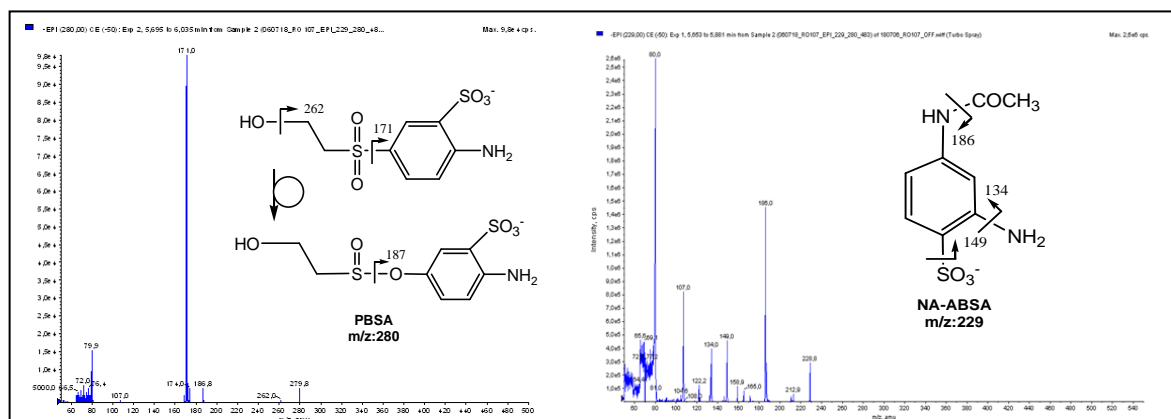


Figure 4.4 Enhanced Product Ion (EPI) spectrum and fragmentation pattern of original dye components of PBSA and NA-ABSA.

In Figure 4.4, the enhanced product ion spectrum and the fragmentation pattern of two important compounds of original dye RO107, 2-amino-5-(2-hydroxyethanesulfonyl)-benzenesulfonic acid (p-base sulfone ester-PBSA) and 4-acetylamino-2-amino-benzenesulfonic acid (NA-ABSA) were indicated. NA-ABSA is one of the main group constituting the original dye (RO107_O, m/z :521).

4.2. The Structural Analysis of Hydrolyzed RO107

Reactive azo dyes are generally used to dye cellulosic fibres. The dyes are firstly absorbed onto the cellulose and then react with the fibre. The reaction occurs by direct nucleophilic substitution or addition as shown in Figure 4.5.

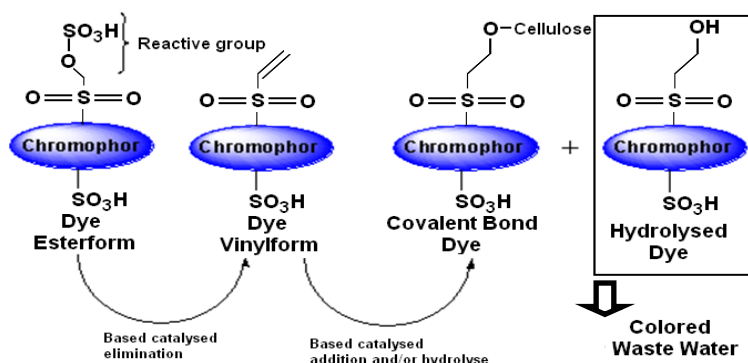


Figure 4.5 Hydrolysis of dye during dyeing process.

The reactive groups of the dye react with ionized hydroxyl groups on the cellulose substrate. However, hydroxyl ions present in the dye bath due to alkaline dyeing conditions compete with the cellulose substrate, resulting in a percentage of hydrolyzed dye which can no longer react with the fibre. Thus, between 10-50% of the initial dye load will be present in the dyebath effluent giving a highly coloured effluent (Al-Degs et al., 2000).

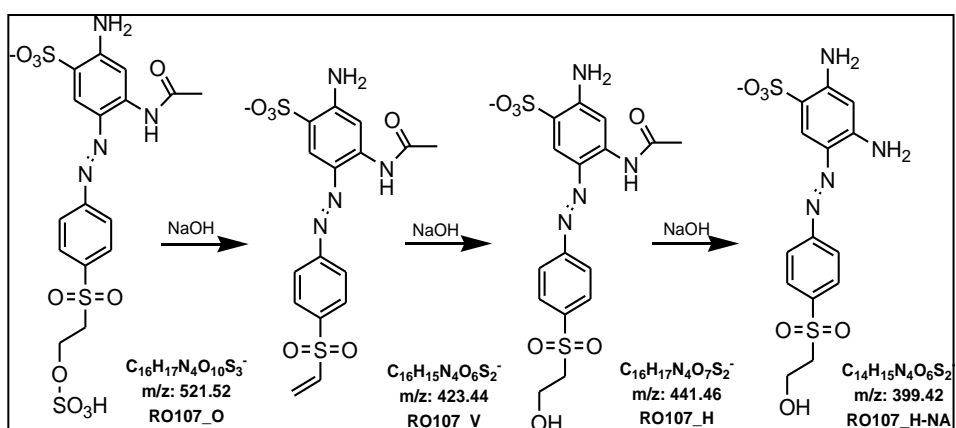


Figure 4.6 The hydrolysis way of RO107 original dye.

The hydrolysis way of RO107 original dye was explained in Figure 4.6. Because elimination and addition reactions occurred during the hydrolysis process, vinyl form (RO107_V), hydrolyzed form (RO107_H) and hydrolyzed form without acetyl group (RO107_H-NA) of RO107 were observed. The hydrolyzed form without acetyl group (RO107_H-NA, $m/z:399$) is the main compound in the starting hydrolyzed dye solution used for experimental studies

Total wavelength chromatogram and DAD chromatogram of hydrolyzed RO107 are given in Figure 4.7.

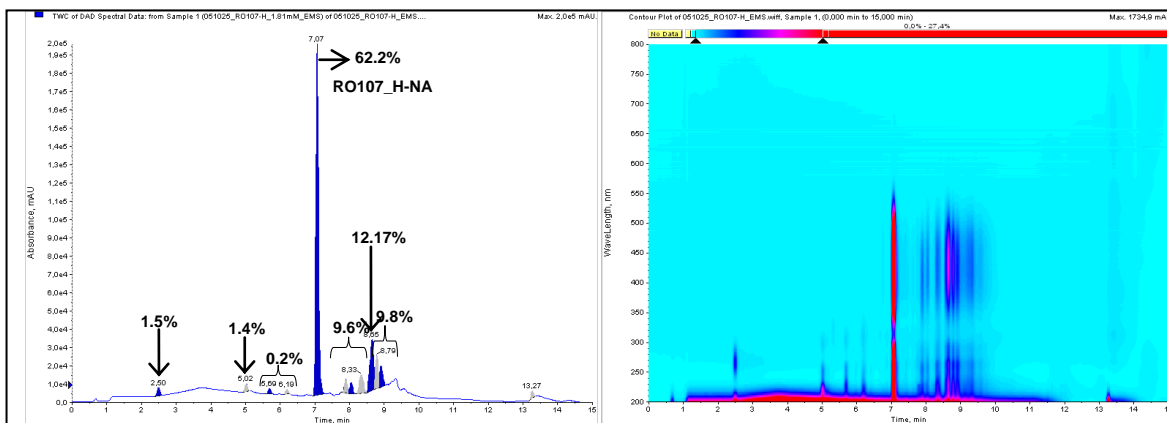


Figure 4.7 Total wavelength chromatogram and DAD chromatogram of hydrolyzed RO107.

From total wavelength chromatogram it was evaluated that approximately 62% of RO107 is in the hydrolyzed form without acetyl group (RO107_H-NA). The other components are listed in Table 4.2.

The enhanced product ion spectrum and fragmentation pattern of hydrolyzed RO107 without acetyl group (RO107_H-NA) are presented in Figure 4.8.

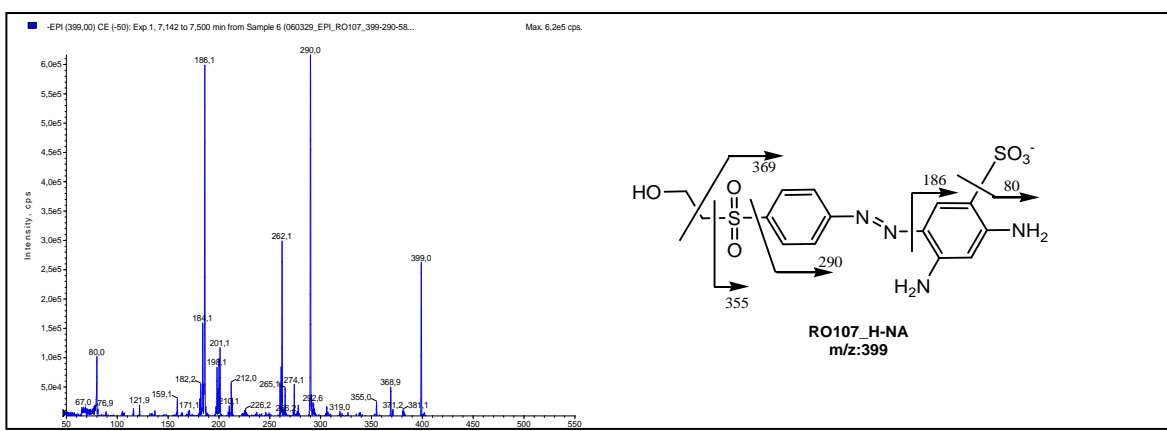


Figure 4.8 Enhanced Product Ion (EPI) spectrum and fragmentation pattern of RO107 hydrolyzed form without acetyl group (RO107_H-NA).

From the figure, one of the intensive two signals which belongs to $m/z:290$ was formed by secession of sulfonylethanol group from main dye structure of RO107_H-NA. The sulfonylethanol group is split off under hydrogen transmission from the phenol ring as neutral particle. The other signal ($m/z:186$) points to azo-type cleavage. The signal of $m/z:80$ belongs to SO_3^- group which may split as neutral particle and also appears as radical.

The enhanced product ion spectrum and fragmentation patterns of other components represented in Table 4.2 are given in Appendix 4.

Table 4.2 The composition of hydrolyzed RO107.

Compounds	Abbreviation	m/z	Molecular Mass (g/mol)	Retention Time (min)
p-base	PB	200	201	2.49
2,4-Diaminobenzenesulfonic acid	DA-BSA	187	188	5.02
4-Acetylamino-2-amino-benzenesulfonic acid	NA-ABSA	229	230	5.69
Reactive Orange 107-Hydrolyzed without ethylene	RO107_H-C ₂ H ₄	413	414	6.19
Reactive Orange 107-Hydrolyzed without acetyl group	RO107_H-NA	399	400	7.07
Reactive Orange 107 Hydrolyzed	RO107_H	441	442	7.23
Reactive Orange 107-Hydrolyzed without acetyl group+p-base	(RO107_H-NA)+PB	581	582	7.89
Reactive Orange 107-Hydrolyzed without amino +Phenol sulfonic acid (PSA)	(RO107_H-NH ₂)+PSA	610	611	8.05
5-[4-(2-{2-[4-(2-Acetylamino-3-sulfo-phenylazo)-benzenesulfonyl]-ethoxy}-ethanesulfonyl)-phenylazo]-2-hydroxy-benzenesulfonic acid	(Dimer RO107_H-NH ₂ +OH)-NA-OH	794	795	8.33
Dimer-Reactive Orange 107-Hydrolyzed without acetyl group ether form	DimerRO107_H-NA	780	781	8.65
Dimer-Reactive Orange 107-Hydrolyzed without acetyl group and sulfonic acid	Dimer RO107_H-NA-SO ₃ ⁻	700	701	8.79
2,4-Diamino-5-[4-(2-{2-[4-(3-hydroxy-5-sulfo-phenylazo) – benzenesulfonyl]-exhoxy}-phenylazo)-benzenesulfonic acid	(Dimer RO107_H-NA)-2NH ₂ +OH	767	768	8.91
UNK 541	UNK 541	541	542	9.33

4.3. Ultrasonic Decolourization Studies of Hydrolyzed RO107

4.3.1. Effect of frequency on ultrasonic degradation of hydrolyzed dye

To investigate the effect of frequency on the removal of hydrolyzed dye, experiments were performed with 50 mg/l initial dye concentration at three different frequencies changing from 378 to 992 kHz and at 20 °C. The working conditions (power value, working volume, radical formation rate, etc.) of ultrasound systems are described in Part 3. Data evaluation was done by taking into consideration RO107_H-NA, m/z:399, the main compound of hydrolyzed RO107, from DAD results of LC/MS-MS analysis and the variation of relative decolourization% with respect to frequency are indicated in Figure 4.9.

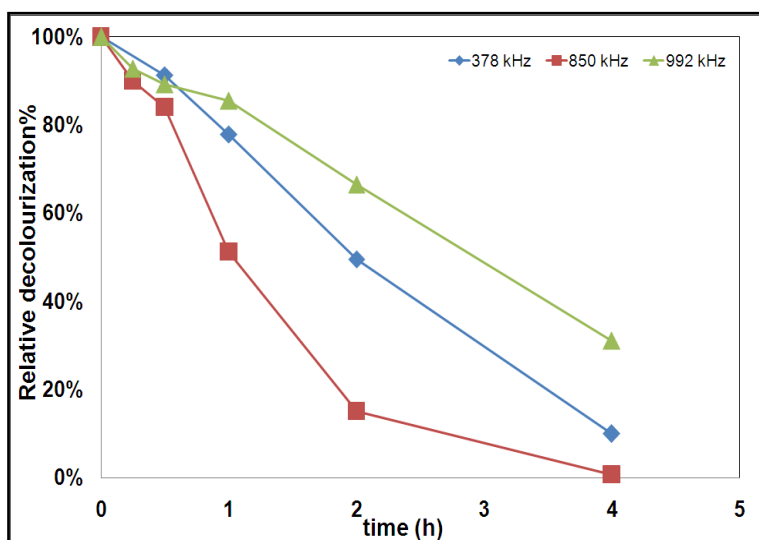


Figure 4.9 The variation of relative decolourization% of RO107_H-NA, m/z: 399, the main compound of hydrolyzed RO107, with frequency (C_0 : 50 mg/l, T: 20 °C).

As seen from figure decolourization of hydrolyzed dye solution increased with increasing frequency from 378 kHz to 850 kHz. The percentage of removal was obtained as 90% at 378 kHz. When the frequency enhanced to 850 kHz, the removal percentage reached to 99%. Further increase in frequency to 992 kHz, the removal percentage diminished to 69%. As a result, the optimum frequency value was chosen as 850 kHz for this system and further studies were performed at this frequency.

As known the frequency of the ultrasound has a significant effect on dye removal influencing the cavitation processes as it alters the critical size of the cavitation bubble. At lower frequency, ultrasound produces a more violent cavitation, leading to higher localized temperatures and pressures at the cavitation site. However, higher frequencies may actually increase the number of free radicals in the system; indirectly increase the dye removal, although cavitation is less violent. It is claimed that the optimum frequency is system specific (Thompson and Doralswamy, 1999).

4.3.2. Effect of temperature on ultrasonic degradation of hydrolyzed RO107

The effect of temperature on the removal of RO107_H-NA; m/z: 399, the main compound of hydrolyzed RO107, was investigated at 20 and 30 °C at a frequency value of 850 kHz with 50 mg/l initial dye concentration. The change in relative percentage dye removal with respect to temperature is shown in Figure 4.10.

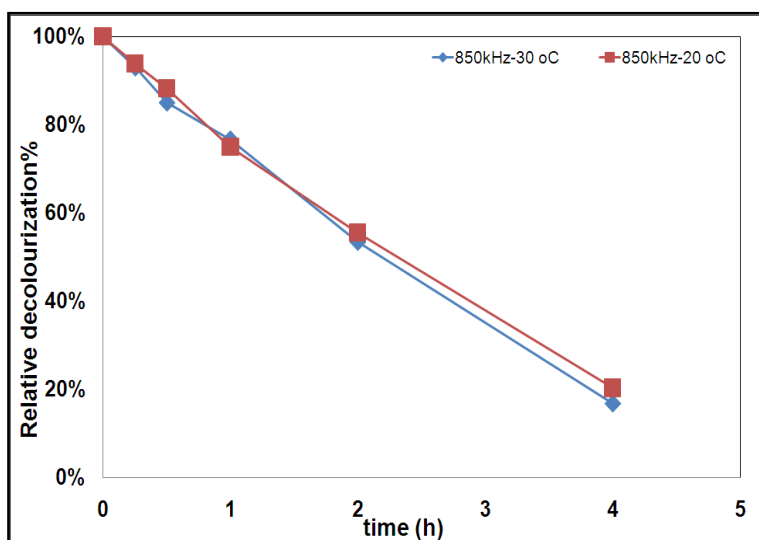


Figure 4.10 The effect of temperature on relative concentration of RO107_H-NA; m/z: 399, the main compound of hydrolyzed RO107, (C_0 : 50 mg/l, f: 850 kHz).

As seen from the figure with increasing the temperature from 20 to 30 °C percentage of main dye component removal increased from 80% to 83%. Temperature affected the dye removal slightly. It is expected that the rate of a reaction enhances with temperature. However, in sonochemical reactions an increase in the temperature results in an overall decrease in the cavitation

violence. Because higher external temperature reduces the intensity necessary to induce cavitation due to the increased vapor pressure of the liquid. At higher external temperatures more vapor diffuses into the cavity, and the cavity collapse is cushioned and less violent (Vajnhandl and Le Marechal, 2005 and Thompson and Doralswamy, 1999).

4.3.3. Determination of the sonication mechanism in the degradation of hydrolyzed RO107

In aqueous solution, degradation of organic pollutants by sonolysis occurs via two possible mechanisms:

- 1) Direct pyrolysis in the gas phase of the cavitation bubbles due to high-localized temperature and pressure
- 2) Reactions with free radicals, formed as a result of water molecules thermolysis during the collapse of the cavitation bubble, in the bubble interfacial region or in the bulk solution (Shemer and Narkis, 2004 and Peller et al., 2001)

In order to determine whether the sonodegradation of hydrolyzed RO107 occurs via pyrolysis or by free radicals oxidation, sonolysis experiments were carried out in the presence of tert-butanol (t-BuOH), which is known as $\cdot\text{OH}$ radical scavenger. t-BuOH scavenges $\cdot\text{OH}$ radicals inside the cavitation bubble and prevents their accumulation at the interfacial region of the bubble. Hence, t-BuOH suppresses degradation of the dye by radicals (Shemer and Narkis, 2004).

In order to investigate the degradation mechanisms of hydrolyzed RO107, experiments were performed with 50 mg/l initial dye concentration at a frequency value of 850 kHz at 20 °C. Varying amounts of t-BuOH were added to the dye solutions. The change in relative relative RO107_H-NA, m/z:399 removal in the absence and presence of changing amounts of t-BuOH from 0 to 0.004 (v/v) was shown Figure 4.11. The results showed that the sonolysis of dye was indeed inhibited by the addition of t-BuOH. In the absence of t-BuOH, approximately 60% of RO107_H-NA dye was sonodegraded within 4 hours. In the presence of t-BuOH at changing levels, approximately 30% sonolysis was observed for each

case. The increase in the amount of t-BuOH did not show any significant effect on the dye sonolysis. It can be concluded that the main degradation of hydrolyzed RO107 proceeds via reaction with free radicals together with pyrolysis whose effect is much more less than free radicals.

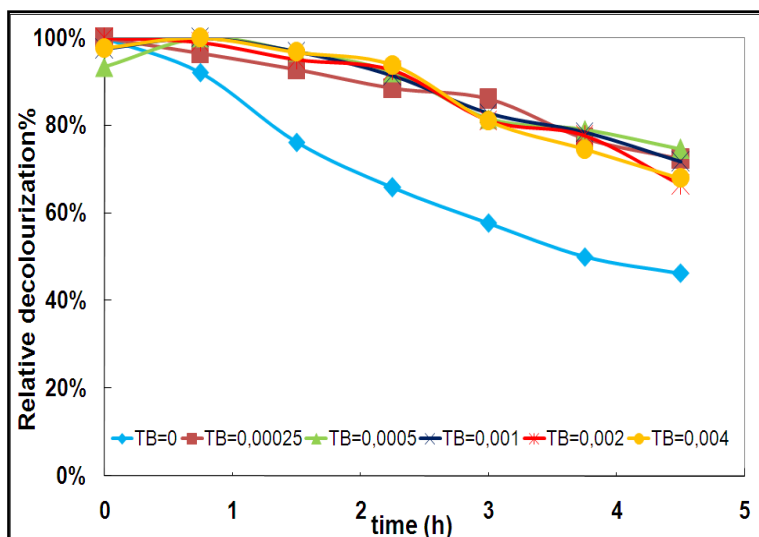


Figure 4.11 The effect of the addition of t-BuOH on the degradation of RO107_H-NA, main compound of hydrolyzed RO107 (C_0 : 50 mg/l, f:850 kHz, T: 20 °C).

4.3.4. Effect of initial hydrolyzed dye concentration on ultrasonic degradation

The effect of initial dye concentration on the removal of hydrolyzed RO107 was examined at 50, 100 and 200 mg/l initial dye concentrations at a frequency value of 850 kHz and at 30 °C. The DAD chromatogram of hydrolyzed form of RO107 obtained at 50 mg/l initial dye concentration for 24 hours sonication time was given in Figure 4.12.

The intensive coloured peak at 6.80 retention time (RT) represents RO107_H-NA, m/z:399, the main compound of hydrolyzed RO107. At the end of 6 h, nearly the complete decolourization of this coloured peak was achieved. There are also some other less intensive peaks of coloured compounds formed between 8.0 and 9.0 RTs and another important peak was also observed around 2.4 RT, p-base, m/z:200. The complete decolourization of these peaks was also achieved at the end of 6 h. It is notable that an increase the peak area around 4.6 RT (m/z:177) was appeared during 24 h sonication period.

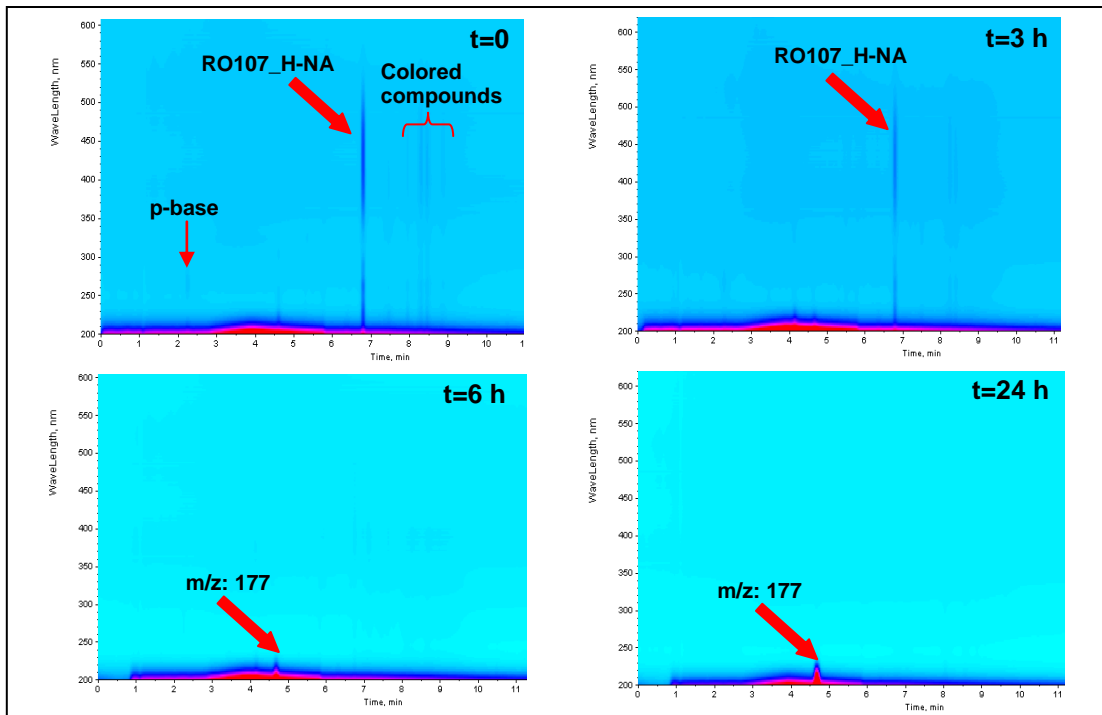


Figure 4.12 DAD chromatograms of hydrolyzed RO107 at 50 mg/l initial dye concentration.

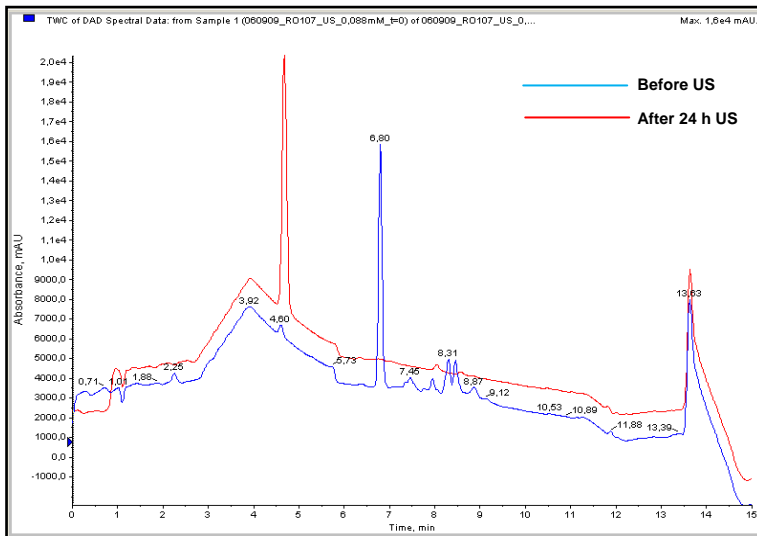


Figure 4.13 The comparison of TWC of DAD spectral data for hydrolyzed RO107 before and after 24 h sonication time (C_0 :50 mg/l, f:850 kHz).

From the total wavelength chromatogram (TWC) of DAD spectral data analyses of hydrolyzed RO107 showed that after 3 h sonication time, the degradation of RO107_H-NA, m/z:399, main compound, was approximately 60%. The amount of degraded RO107_H-NA increased with sonication time; 97% removal was

observed after 6 h sonication. After 24 h, nearly no RO107_H-NA, m/z :399 was detected. The comparison of total wavelength chromatogram (TWC) of DAD spectral data for hydrolyzed RO107 before and after 24 h sonication time was represented in Figure 4.13. While the blue line represents TWC of DAD spectral data before sonication, the red one shows TWC of DAD spectral data after 24 h sonication. From the figure, again the increase in the peak area of compound at 4.60 RT was observed after 24 h sonication. This peak is referred to an intermediate compound of m/z :177 (UNK177) increase in the area of this peak also indicates the increase in the amount of this compound during sonication.

The DAD chromatograms of hydrolyzed RO107 obtained at 100 and 200 mg/l initial dye concentrations are presented in Figure 4.14 and 4.15, respectively.

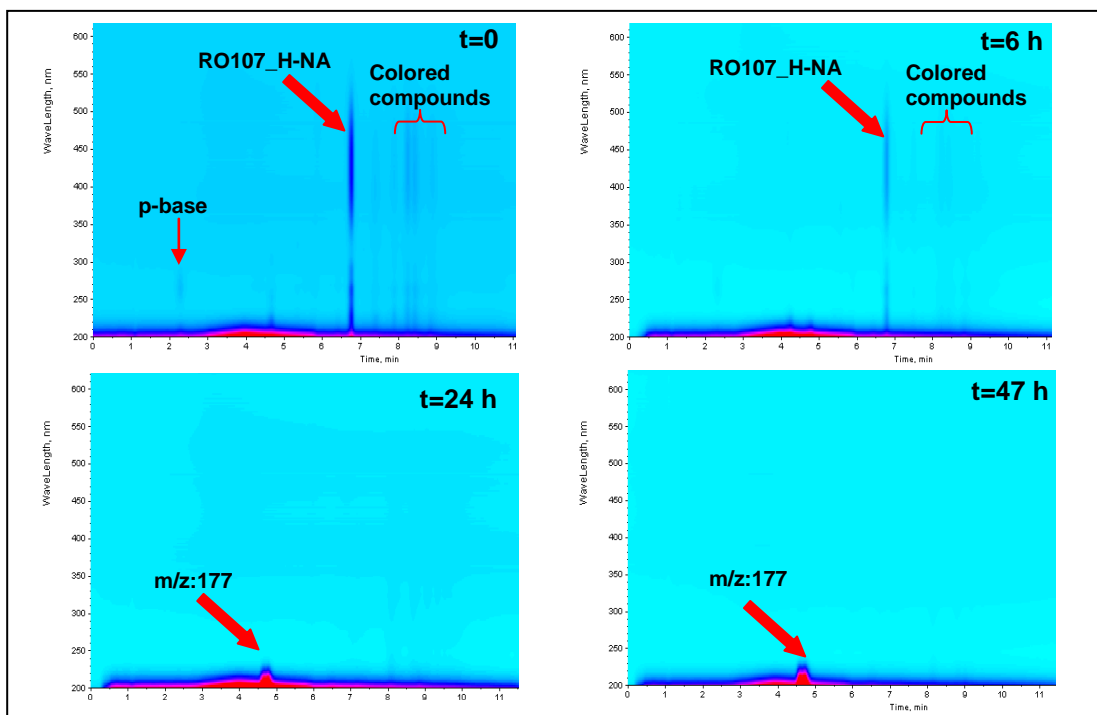


Figure 4.14 DAD chromatograms of hydrolyzed RO107 at 100 mg/l initial dye concentration.

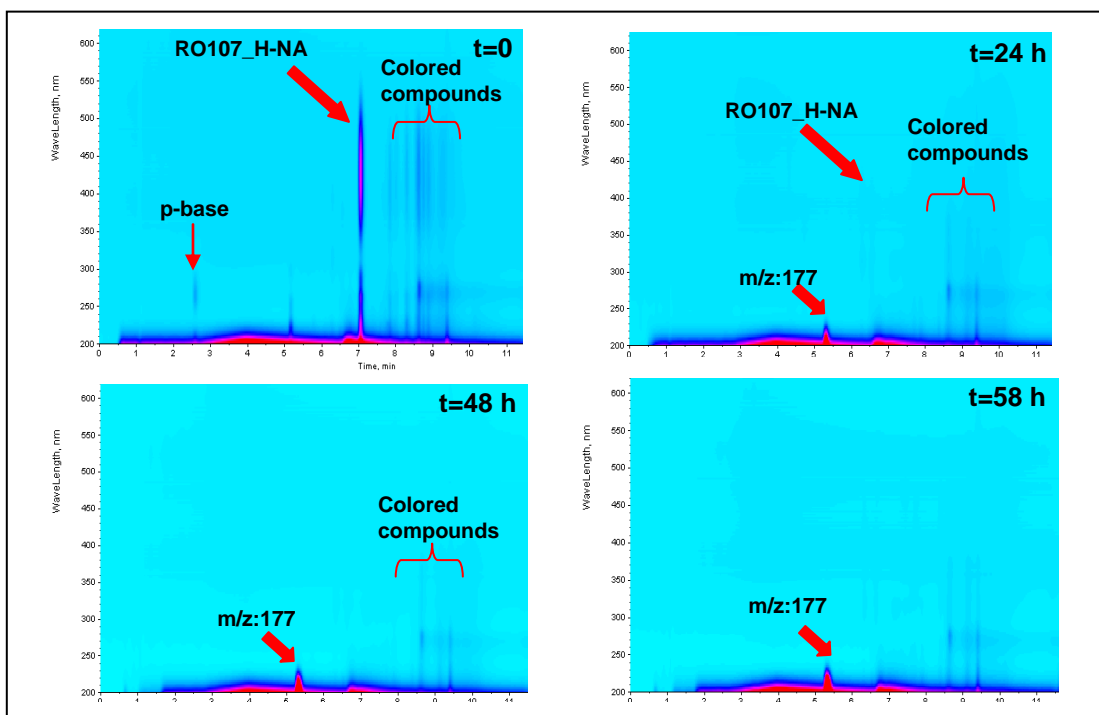


Figure 4.15 DAD chromatograms of hydrolyzed RO107 at 200 mg/l initial dye concentration.

From the figures, the time for the complete removal of RO107_H-NA, m/z:399, the main compound of hydrolyzed RO107, prolonged with increasing initial dye concentration. The total decolourization of RO107_H-NA, m/z:399 was achieved after 24 h for 100 mg/l initial dye concentration and after 48 h for 200 mg/l initial dye concentration.

The comparison of total wavelength chromatograms (TWC) of DAD spectral data obtained for 100 and 200 mg/l initial hydrolyzed RO107 concentrations are given in Figures 4.16 and 4.17, respectively.

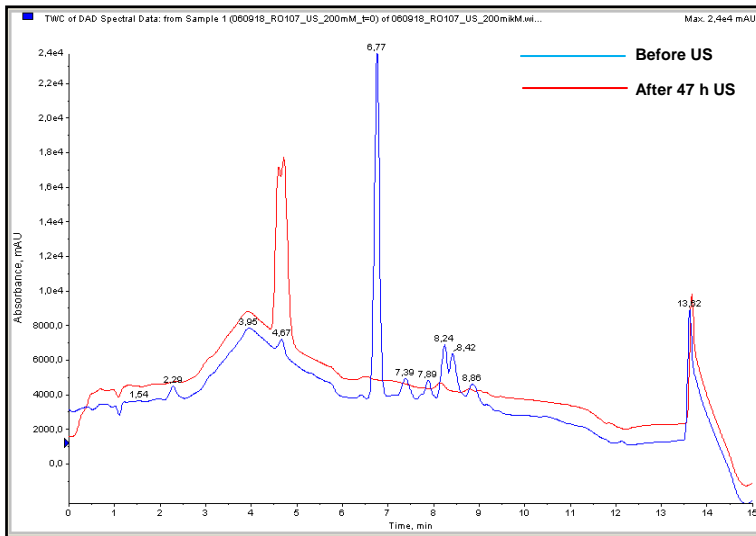


Figure 4.16 The comparison of TWC of DAD spectral data for hydrolyzed RO107 before and after 47 h sonication time (C_0 :100 mg/l, f:850 kHz).

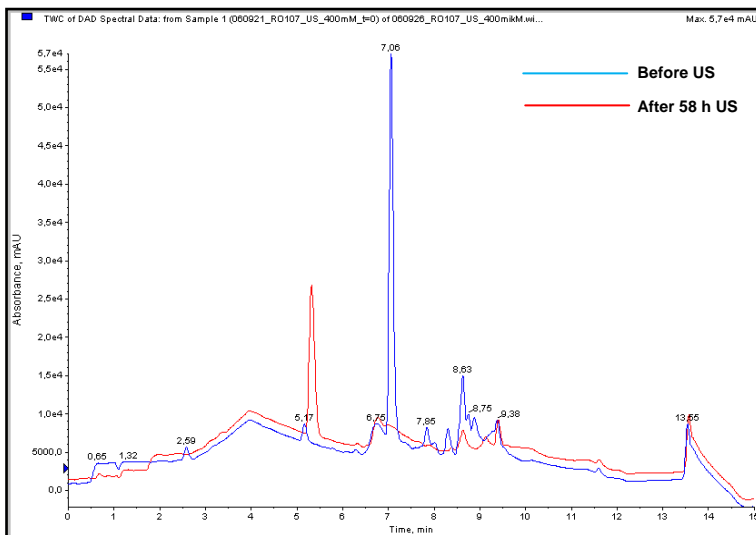


Figure 4.17 The comparison of TWC of DAD spectral data for hydrolyzed RO107 before and after 58 h sonication time (C_0 :200 mg/l, f:850 kHz).

For both figures, while the blue lines represent TWC of DAD spectral data before sonication, the red ones represent TWC of DAD spectral data of 100 mg/l dye degradation after 47 h sonication and of 200 mg/l dye degradation after 58 h sonication.

Some important compounds of hydrolyzed RO107 detected before and after ultrasound (US) treatment are listed in Table 4.3.

Table 4.3 Some important compounds of hydrolyzed RO107 detected before and after ultrasound (US) treatment.

Compounds	Abbreviation	m/z	Molecular weight (g/mol)	RT (min)	Before US	After US
p-base	PB	200	201	2.49	+	-
UNK177	UNK177	177	178	4.60	+	++
Reactive Orange 107-Hydrolyzed without acetyl group	RO107_H-NA	399	400	7.07	++	-
Reactive Orange 107-Hydrolyzed without acetyl group+p-base	(RO107_H-NA)+PB	581	582	7.89	+	-
Reactive Orange 107-Hydrolyzed without amino +Phenol sulfonic acid (PSA)	(RO107_H-NH ₂)+ PSA	610	611	8.05	+	-
5-[4-(2-{2-[4-(2-Acetylamino-3-sulfo-phenylazo)-benzenesulfonyl]-ethoxy}-ethanesulfonyl)-phenylazo]-2-hydroxy-benzenesulfonic acid	(Dimer RO107_H-NH ₂ +OH)-NA-OH	794	795	8.33	+	-
Dimer-Reactive Orange 107-Hydrolyzed without acetyl group ether form	DimerRO107_H-NA	780	781	8.65	+	+-
Dimer-Reactive Orange 107-Hydrolyzed without acetyl group and sulfonic acid	Dimer RO107_H-NA-SO ₃ ⁻	700	701	8.79	+	-
2,4-Diamino-5-[4-(2-(2-[4-(3-hydroxy-5-sulfo-phenylazo) – benzenesulfonyl]-exhoxy)-phenylazo]-benzenesulfonic acid	(Dimer RO107_H-NA)-2NH ₂ +OH	767	768	8.91	+	-

+exist, ++much exist +-less exist – non-exist

The proposed mechanism for the degradation of hydrolyzed dye during ultrasonic treatment is shown in Figure 4.18 (Rehorek et al., 2007; He et al., 2007; Donlagic and Levec, 1997; Joseph et al., 2000 and Tauber et al., 2005).

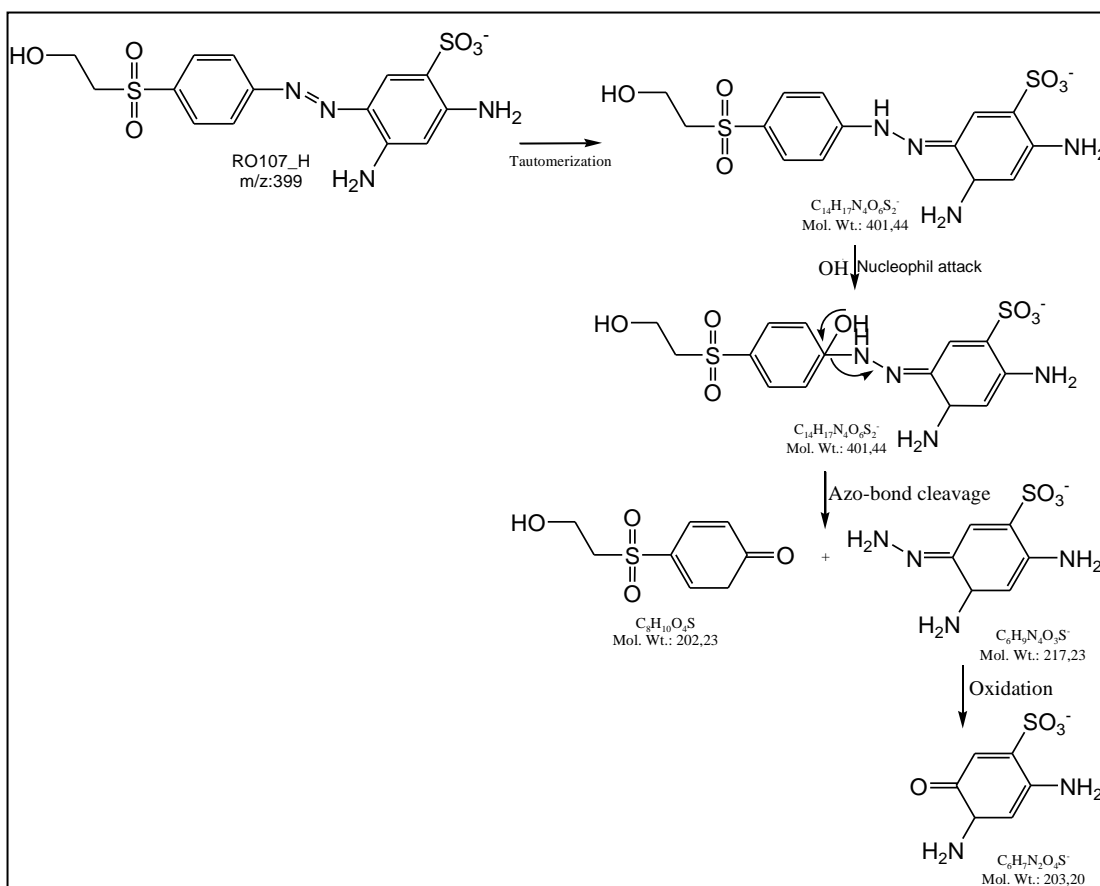


Figure 4.18 The proposed mechanism for the degradation of hydrolyzed dye during ultrasonic treatment.

The change of relative RO107_H-NA, m/z:399, the main compound of hydrolyzed dye, removal was plotted as a function of time for the three dye concentrations (Figure 4.19). As seen, with increasing the initial RO107_H-NA concentration, the removal rate diminished. Assuming the sonical degradation of hydrolyzed dye component RO107_H-NA is pseudo first order (Eq.4.1), rate constants obtained from by plotting $\ln(C/C_0)$ vs t , were presented in Table 4.4. The degradation rate constants also reduced with increasing initial RO107_H-NA concentration.

$$\frac{dC}{dt} \bigg|_{C_0} = -kC \quad \text{Eq. 4.1}$$

where

C: relative bulk dye concentration

C₀: relative initial dye concentration

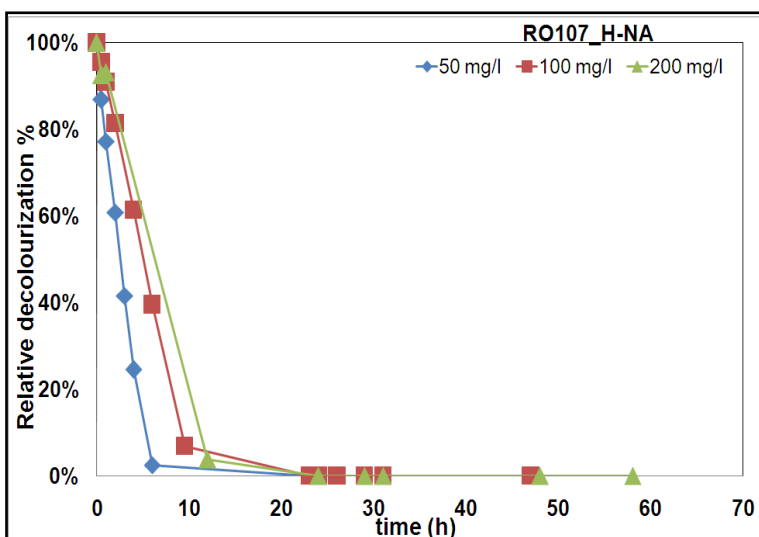


Figure 4.19 Effect of initial hydrolyzed RO107 concentration on relative RO107_H-NA removal percentage (f: 850 kHz, T:30 °C).

Table 4.4 Pseudo first order degradation rate constants of RO107_H-NA, m/z:399 obtained at different initial dye concentrations.

Initial dye concentration (mg/l)	50	100	200
k (1/h)	0.0046	0.0019	0.0015
R ²	0.988	0.988	0.780

p-base, m/z:200, another important compound of hydrolyzed RO107, consumed during sonication, and unknown compound, UNK177 (RT 4.6), formed during sonication, were selected in order to examine the effect of initial hydrolyzed dye concentration on their consumption and formation kinetics, respectively. In Figures 4.20 and 4.21, the change of relative concentration of each component with time as a function of initial hydrolyzed dye concentration was indicated.

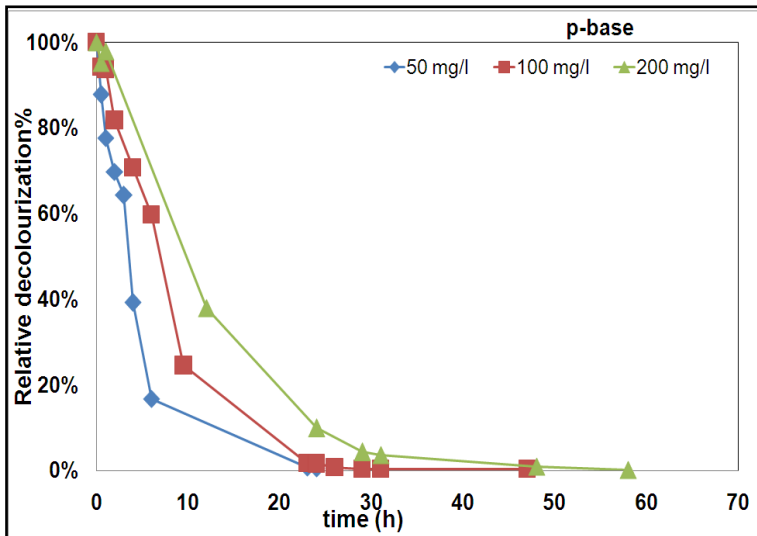


Figure 4.20 Effect of initial hydrolyzed RO107 concentration on relative p-base removal percentage (f: 850 kHz, T:30 °C).

From Figure 4.20, for p-base, the removal rate of decreased and the time for the complete decolourization enhanced with increasing initial hydrolyzed dye concentration.

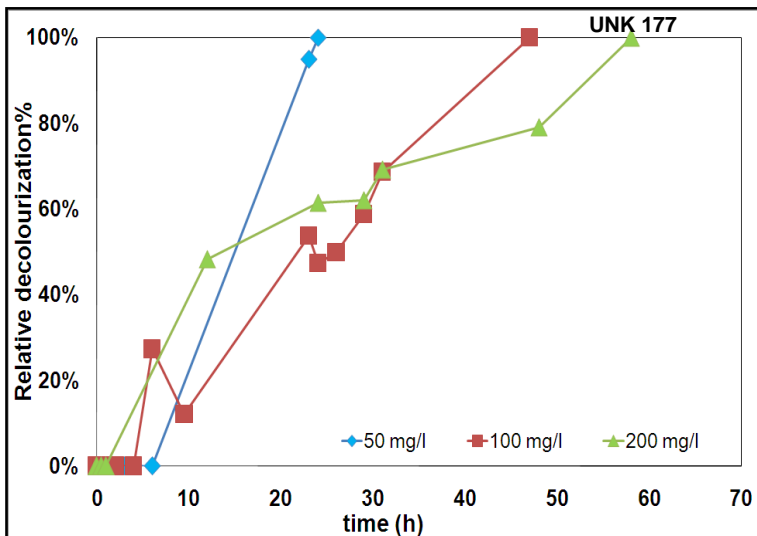


Figure 4.21 Effect of initial hydrolyzed RO107 concentration on relative UNK177 removal percentage (f: 850 kHz, T:30 °C).

From Figure 4.21, for compound UNK177, the formation rate diminished and the time for the complete decolourization enhanced with increasing initial hydrolyzed dye concentration

The UV-visible spectra of the dye solutions were recorded during the sonication and spectrum profiles of dye solutions were compared in Figures 4.22, 23 and 24 for each initial hydrolyzed dye concentration.

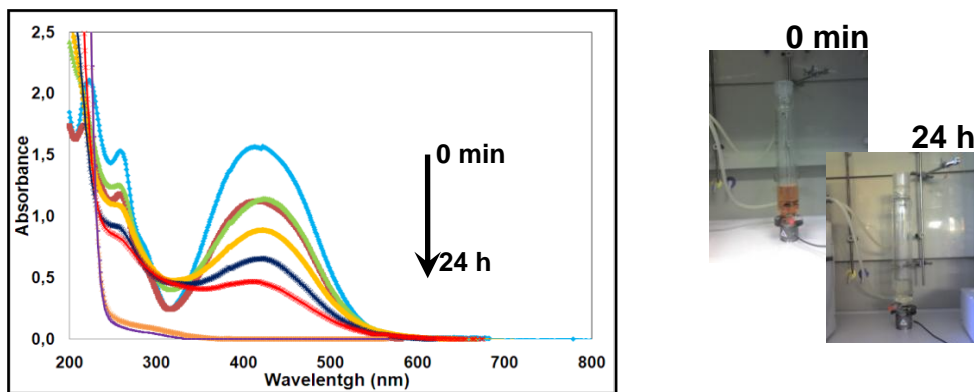


Figure 4.22 Spectral changes during 12 h sonication of 50 mg/l hydrolyzed dye solution.

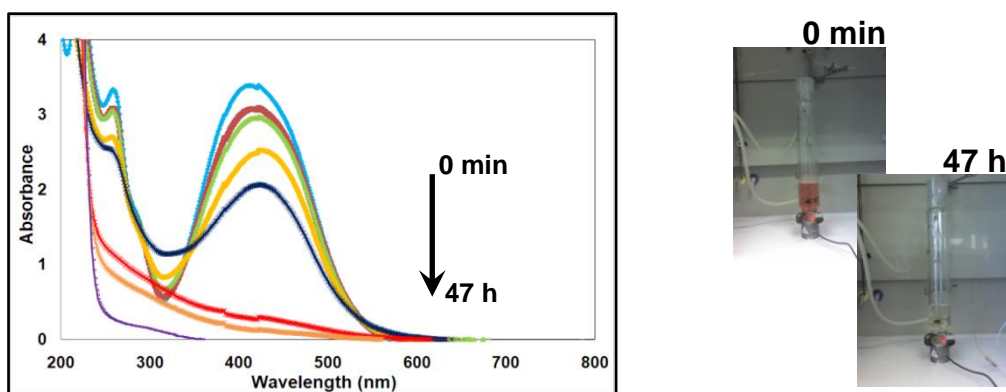


Figure 4.23 Spectral changes during 47 h sonication of 100 mg/l dye solution.

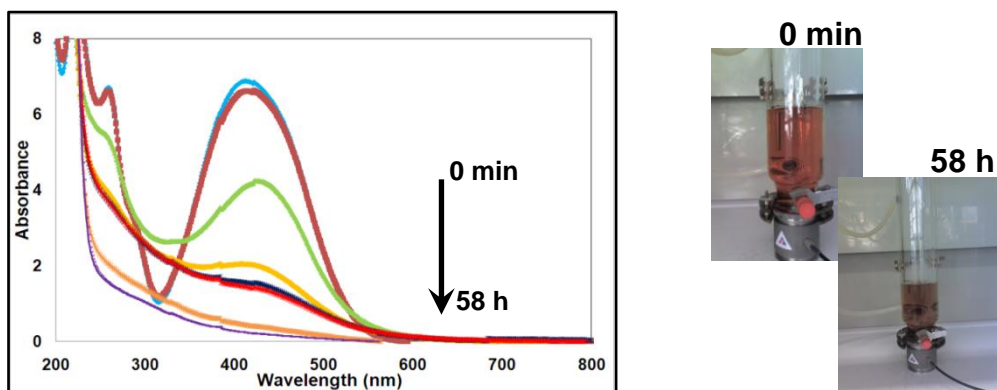


Figure 4.24 Spectral changes during 58 h sonication of 200 mg/l dye solution.

As seen from the figures, the magnitude of absorbance increased with increasing dye concentration. Moreover, there is one visible absorption peak in the spectrum at 400 nm for all dye concentrations studied. This peak is due to the azo form of the dye which absorbs typically at 400-440 nm (Ince and Guyer, 2004). The UV-visible spectrum of the dye solutions also indicated the reduction in the colour.

Chemical oxygen demand (COD) is a measure of oxygen consumption, which is needed to oxidize the organic compounds, during the decomposition of organic matter. The variation of chemical oxygen demand (COD) with time is shown in Figure 4.25 for each initial hydrolyzed dye concentration studied.

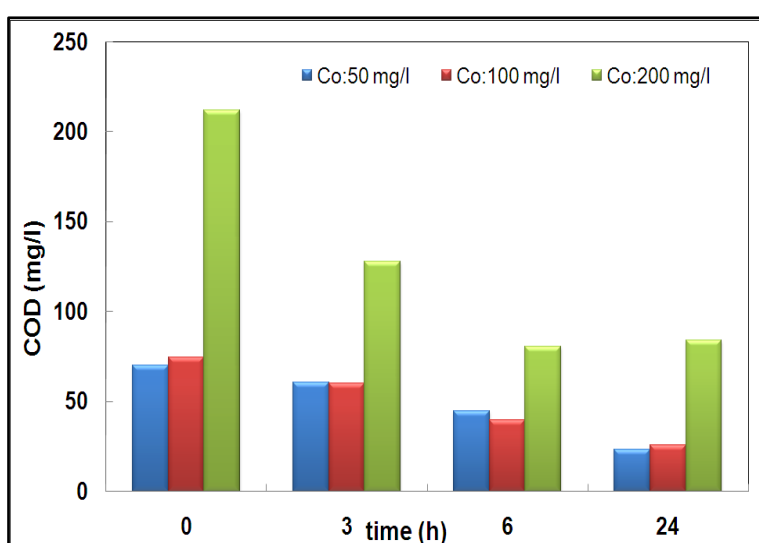


Figure 4.25 Variation of chemical oxygen demand as a function of time obtained at three different initial dye concentrations.

As seen from the figure, the COD value of the most concentrated dye solution is the highest. The COD of dye solution decreased with sonication due to degradation of dye. The COD value became half of its initial value after 24 h sonication for all initial dye concentrations.

4.4. Microbial Biodegradation Studies of Hydrolyzed RO107

4.4.1. Biodegradation of RO107 hydrolyzed dye by using bacterial sludge

Bacterial sludge experiments were performed in sequential anaerobic-aerobic batch bioreactors. For anaerobic degradation studies hydrolyzed dye solution was used. After anaerobic treatment, the effluent was used in the aerobic reactor.

4.4.1.1. Anaerobic (AN) biodegradation of hydrolyzed RO107

The anaerobic biodegradation of hydrolyzed RO107 was performed in a batch system with an initial dye concentration of 3400 mg/l. Anaerobic experiments were carried out in two trials with the same concentrations. After the first trial, which was carried on for 4 days, the second one was started and continued for 10 days in the same system with the same load of dye solution.

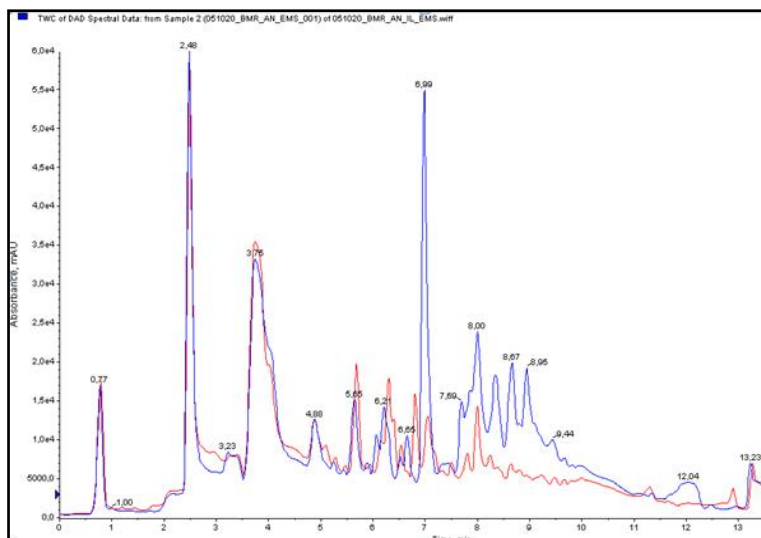


Figure 4.26 The comparison of TWC of DAD spectral data for hydrolyzed RO107 at the beginning and at the end of anaerobic treatment (1st trial: 4 days).

The comparison of TWC of DAD spectral data for hydrolyzed RO107 at the beginning and at the end of anaerobic treatment for the first trial is given in Figure 4.26. While the blue line represents TWC of DAD spectral data before anaerobic degradation, the red one indicates TWC of DAD spectral data after 4 days. From Figure 4.26 hydrolyzed dye contained mainly RO107_H-NA and p-base before anaerobic degradation. During anaerobic degradation, azo bond cleavage occurs and aromatic amines are formed. From the same figure, the main compounds detected during anaerobic biodegradation were p-base, NA-DABSA and NA-ABSA. All the compounds detected during anaerobic treatment of hydrolyzed RO107 were listed in Table 4.5.

The proposed formation mechanisms of p-base (m/z :200), NA-DABSA (4-Acetylamino-2-5-Diamino-benzenesulfonic acid) (m/z : 244) and NA-ABSA (4-

Acetylamino-2-amino-benzenesulfonic acid) (m/z : 229) were indicated in Figure 4.27. The removal of amine group ($-NH_2$) from NA-DABSA gives the main degradation product of anaerobic biodegradation, NA-ABSA.

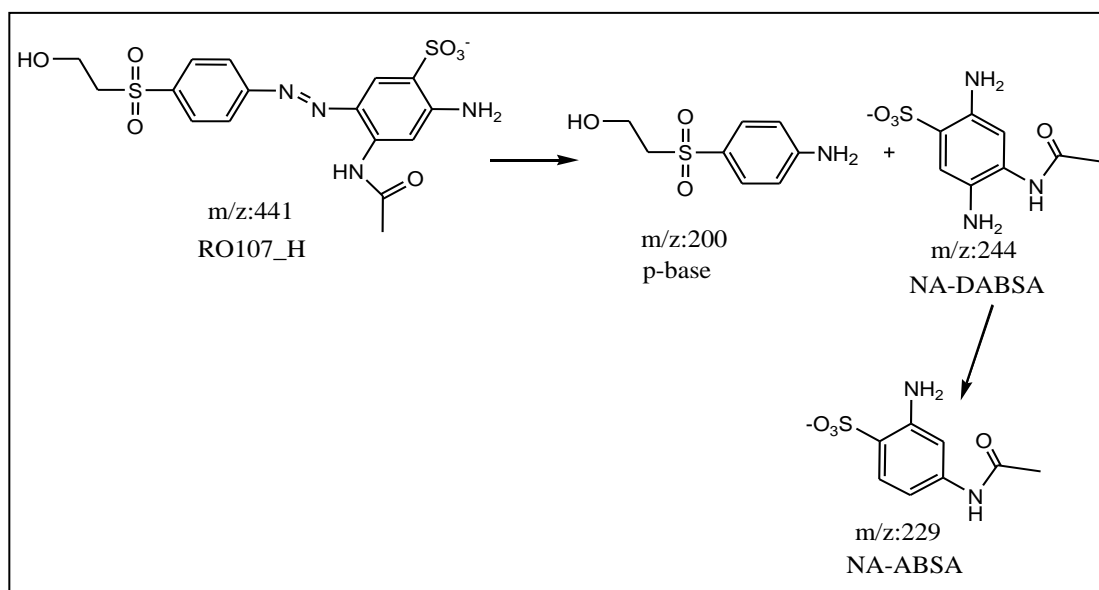


Figure 4.27 The mechanism of degradation of hydrolyzed RO107 in anaerobic reactor.

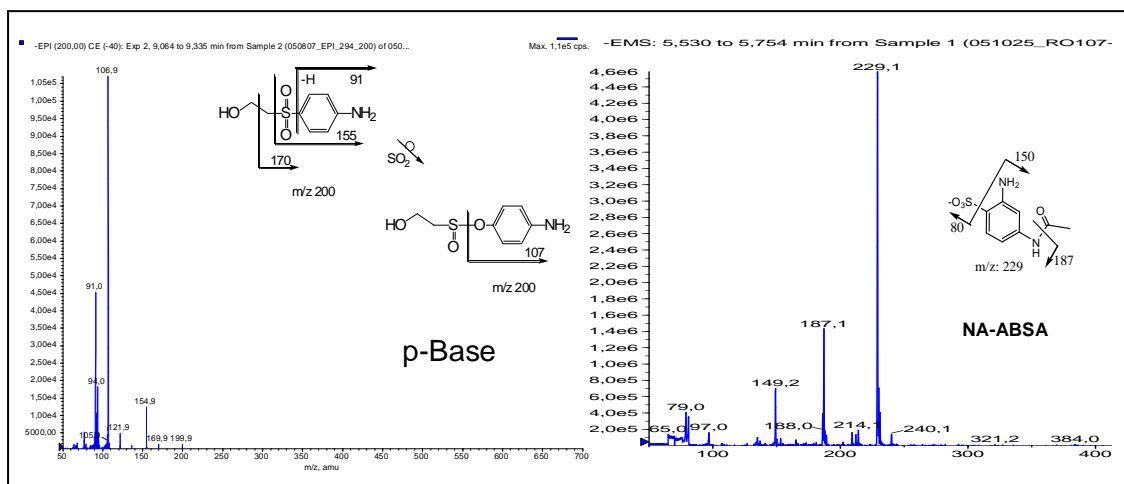


Figure 4.28 Enhanced product ion (EPI) spectrum and fragmentation patterns of p-base and NA-ABSA intermediates.

The enhanced product ion (EPI) spectrum and fragmentation patterns of p-base and NA-ABSA intermediates were represented in Figure 4.28. From the figure, the p-base splits methanol CH_3OH and $HOCH_2CH_2\cdot$, $HOCH_2CH_2SO_2\cdot$ radicals. By the rearrangement of sulphonyl group, the second form of p-base formed and the occurrence of the signal m/z :107 is due to the secession of SOC_2H_4OH group from

p-base. For NA-ABSA, the appearance of the signals of m/z:187 and m/z:149 are due to the splitting of C₂H₄OH and SO₃⁻ groups from NA-ABSA.

Table 4.5 All the compounds detected during anaerobic treatment of hydrolyzed RO107.

Compounds	Abbreviations	m/z	Molecular Weight (g/mol)	RT (min)	Before AN	After AN
2-(4-Aminobenzenesulfonyl)-ethanol, para Base (PB)	p-Base	200	201	2.48	++	++
N-[4-(2-Hydroxyethansulfonyl)-phenyl]-acetamide, Vinyl para Base acetamide	NAPB	242	243	3.74	+	+
4-Acetylamino-2-5-Diaminobenzenesulfonic acid	NA-DABSA	244	245	4.50	-	+
Sulfanilic acid	s-Acid	172	173	4.88	+	+
2,4-Diaminobenzenesulfanilic acid	DABSA	187	188	5.20	+	+
4-Acetylamino-2-amino-benzenesulfonic acid	NA-ABSA	229	230	5.66	+	+
4-Acetylamino-2-hydroxy-benzenesulfonic acid	NA-HBSA	230	231	6.21	+	+
4-Acetylamino-2-[4-(2-hydroxy-ethansulfonyl)-phenylamino]-benzenesulfonic acid	NA-HES-PABSA	414	415	6.52	-	+
4-Acetylamino-2-[4-(2-amino-ethansulfonyl)-phenylamino]-benzenesulfonic acid	NA-AES-PABSA	412	413	6.65	+	+
Reactive Orange 107-Hydrolyzed without acetyl group	RO107_H-NA	399	400	6.98	++	+-

+exist, ++much exist +-less exist – non-exist

The change in relative concentration of RO107_H-NA; m/z: 399, the main compound of hydrolyzed RO107, was plotted as a function of time and given in Figure 4.29 for the both trials of anaerobic treatments. From the figure, RO107_H-NA was completely decolourized in 1 day in the first trial and in 1.5 days in second trial. The removal rate was faster in the 1st trial than the 2nd trial. The rate constants obtained from the pseudo first order degradation kinetics are presented in Table 4.6. The rate constant was higher for the 1st trial than that of 2nd trial. This may be due to the decrease of microbial activity after the 1st trial.

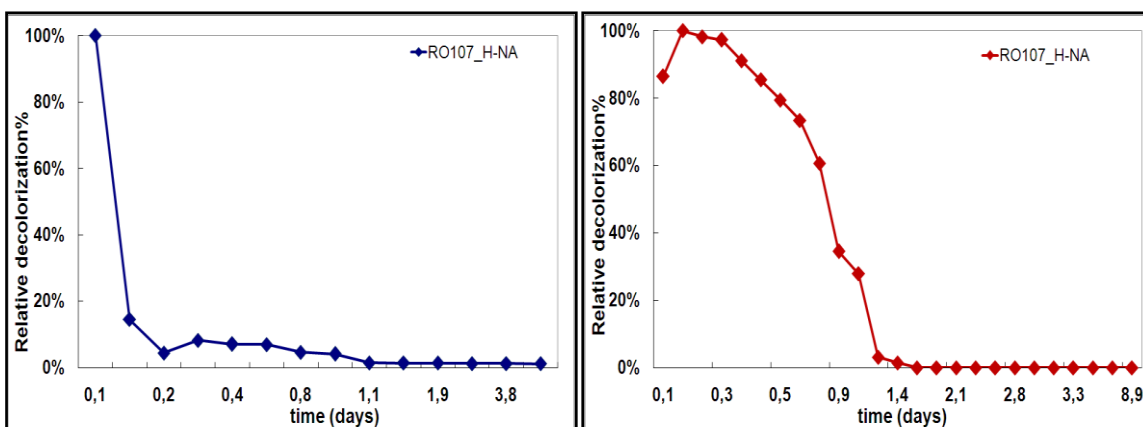


Figure 4.29 The change in relative decolorization percentage of RO107_H-NA; m/z: 399, during anaerobic biodegradation (Left:1st trial, Right:2nd trial).

Table 4.6 Pseudo 1st order degradation rate constants for anaerobic degradation of RO107_H-NA.

	1 st trial	2 nd trial
k (1/h)	22.16	1.14
R²	0.980	0.985

The change in relative decolorization percentage of p-base and NA-ABSA, the two significant intermediates, with time is indicated in Figure 4.30 for both trials. As seen, p-base intermediate remained unchanged during anaerobic degradation.

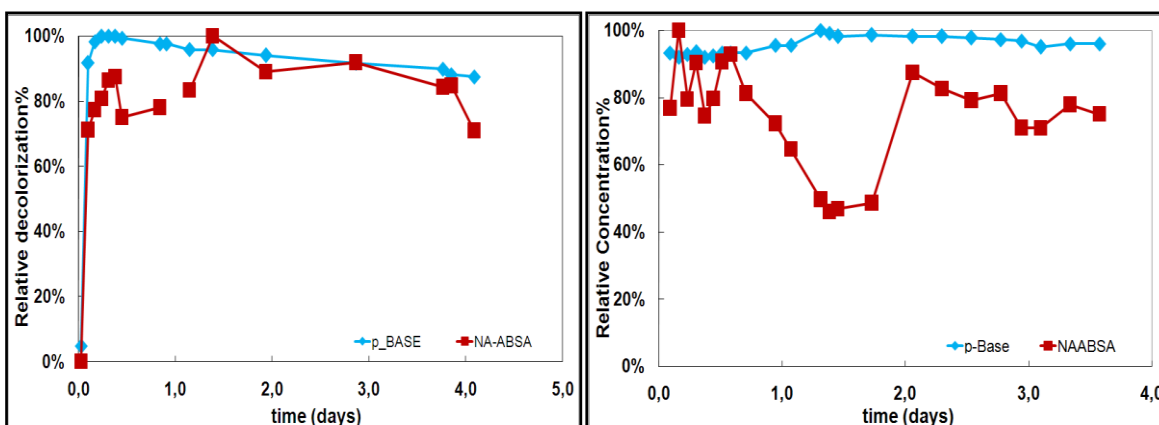


Figure 4.30 The change in decolorization percentage of p-base and NA-ABSA during anaerobic biodegradation (Left:1st trial, Right:2nd trial).

The UV-visible spectrum of the dye solution for both trials was recorded during the anaerobic degradation and spectrum profiles of dye solution were compared in Figure 4.31.

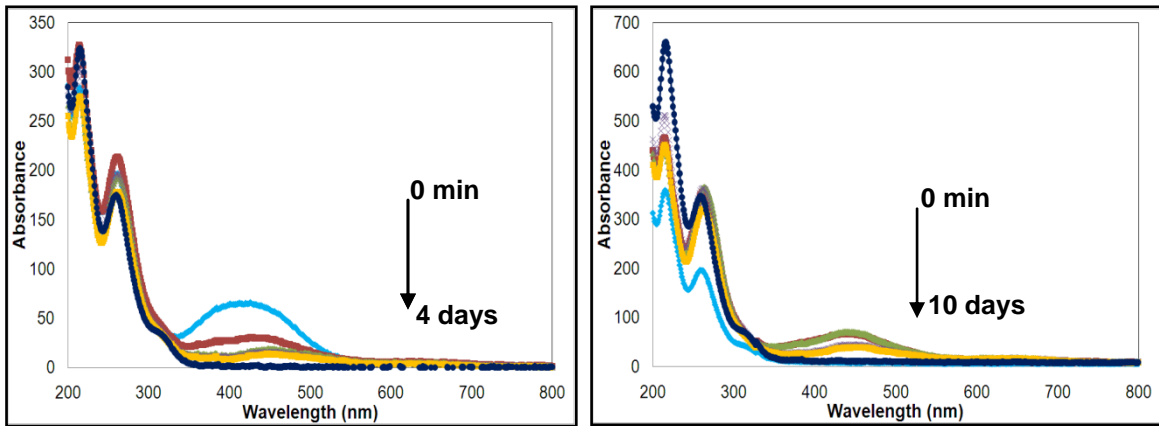


Figure 4.31 Spectral changes during anaerobic biodegradation (C_0 :3400 mg/l 1st trial:4 days, 2nd trial:10 days).

From the figure, there are two UV and visible absorption peaks in the spectrum for each case which point intensively at the existence of p-base at 270 nm and the azo form of the dye (colourization) at 400 nm. The certain reduction in the magnitude of the peak at 400 nm showed the complete decolourization of dye solution. The little change in the magnitude of peak at 270 nm showed slightly degradation of p-base.

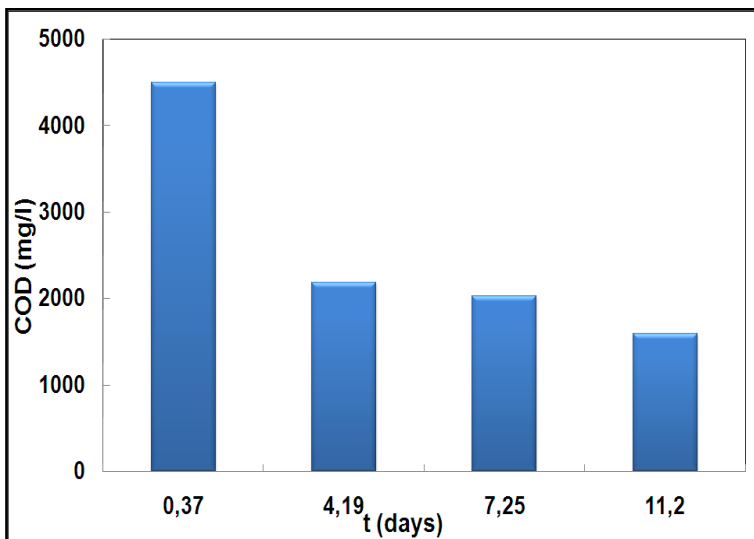


Figure 4.32 Variation of chemical oxygen demand as a function of time obtained for anaerobic batch treatment.

The variation of chemical oxygen demand (COD) with time was shown in Figure 4.32 for anaerobic batch treatment of hydrolyzed dye. As seen, COD of dye

solution decreased with anaerobic treatment and the COD value became half of its beginning value after 4 days treatment.

4.4.1.2. Aerobic (AE) degradation of anaerobic (AN) effluent

The aerobic degradation studies were carried out in a batch system for 10 and 11 days in two trials by using the anaerobic effluents as the initial dye solution. The comparison of TWC of DAD spectral data for the dye solution before and after aerobic treatment for the first trial was given in Figure 4.33.

In the figure, the blue line represents TWC of DAD spectral data before aerobic degradation; the red one indicates TWC of DAD spectral data after 10 days. From the figure, at the beginning of aerobic treatment, p-base (PB) and a compound (RT:5.91) that recolourized the solution were detected. During aerobic degradation, p-base was completely degraded and most of RT:5.91 compound was removed. All the compounds detected before and during aerobic treatment were listed in Table 4.7.

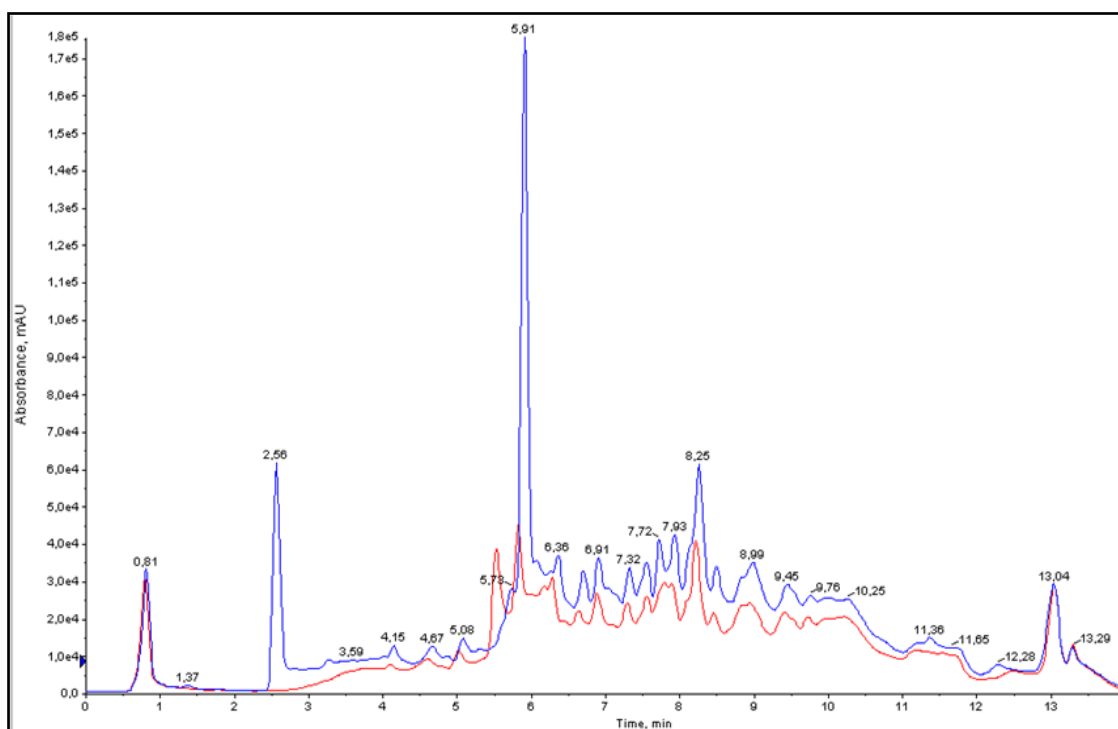


Figure 4.33 The comparison of TWC of DAD spectral data for the dye solution before and after aerobic treatment (1st trial: 10 days).

Table 4.7 All the compounds detected before and during aerobic treatment.

Compounds	Abbreviations	m/z	Molecular Weight (g/mol)	RT (min)	Before AE	After AE
2-(4-Aminobenzenesulfonyl)-ethanol, para Base	p-Base	200	201	2.56	++	-
Vinyl para Base with Acetylamino Group	VPB+NA	240	241	5.51	-	+
4-[2-(4-Diazenyl-benzenesulfonyl)-ethoxy]-benzene-1,3-diamine	DABSE+BDA	319	320	5.91	++	+/-
4-Acetylamino-3-(4-{2-[2-(4-amino-benzenesulfonyl)-ethoxy]-ethanesulfonyl}-phenylazo)-benzenesulfonic acid	RO107_H-NH ₂ +PSA	610	611	8.25	+	+

+exist, ++much exist +/-less exist - non-exist

It was considered a new compound (DABSE+BDA, m/z:319) was formed at 5.91 RT at the beginning and during aerobic treatment. Enhanced product ion (EPI) spectrum and fragmentation patterns of the compound with m/z:319 were given in Figure 4.34.

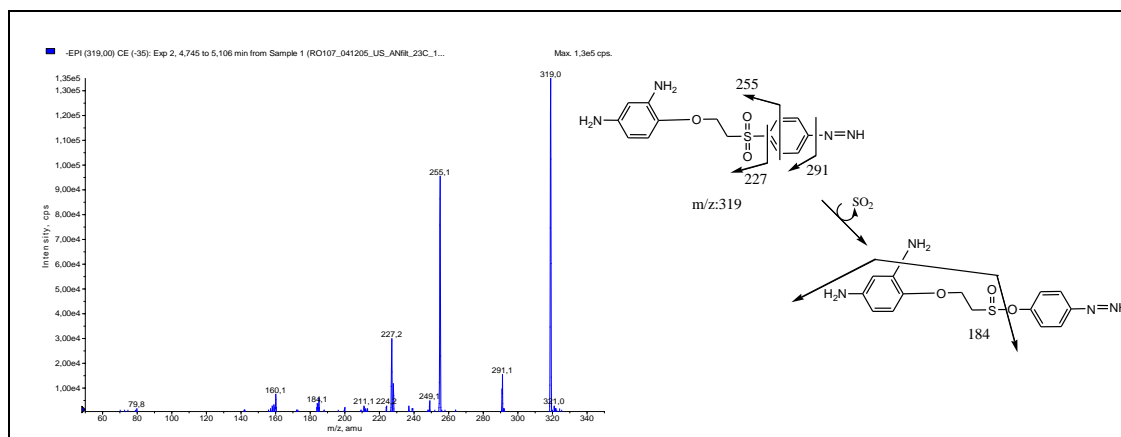


Figure 4.34 Enhanced product ion (EPI) spectrum and fragmentation patterns of DABSE+BDA.

The proposed mechanism for the formation of this coloured compound is indicated in Figure 4.35.

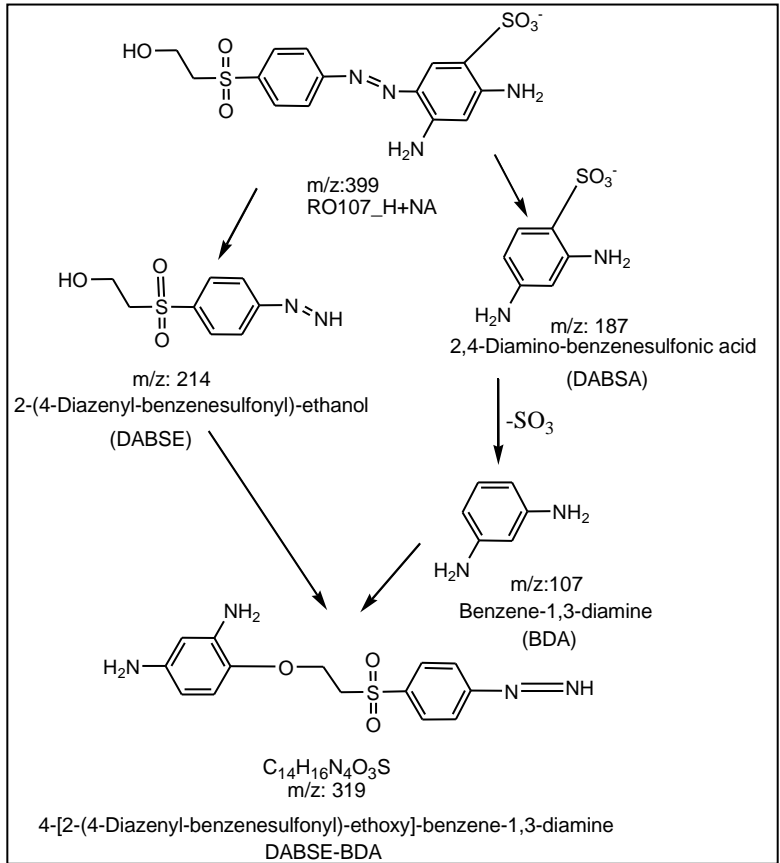


Figure 4.35 The proposed mechanism for the formation of coloured compound m/z:319.

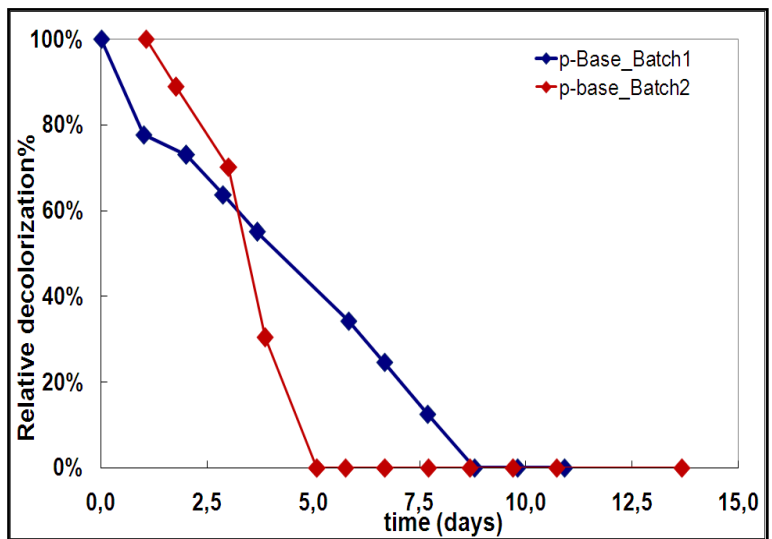


Figure 4.36 The change in relative concentration of p-base during aerobic biodegradation.

The variation of relative concentration of p-base; m/z: 200, one of the main compounds of anaerobic effluent, with time was given in Figure 4.36 for the both

trials of aerobic treatments. As seen from the figure, p-base was completely removed after 8 days for the first trial and time decreased to 5 days for the second trial.

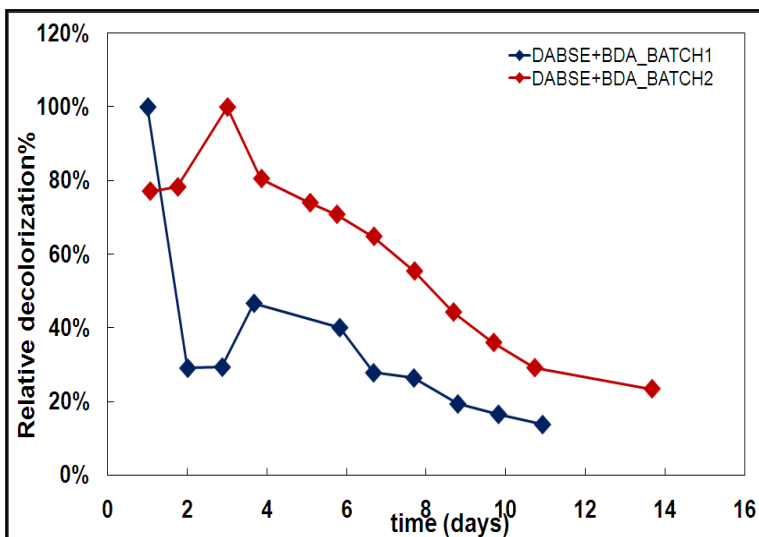


Figure 4.37 The change in relative concentration of DABSE+BDA during aerobic biodegradation.

The change in relative concentration of DABSE+BDA, another important compound which caused the recolourization problem, with time is given in Figure 4.37. From the figure, DABSE+BDA, existing in the dye solution at the beginning of aerobic degradation, was both degraded and formed during aerobic treatment. The decolourization of dye solution pointed out that degradation was higher than formation.

The UV-visible spectrum of the dye solution for both trials was recorded during the aerobic degradation and spectrum profiles of dye solution were compared in Figure 4.38.

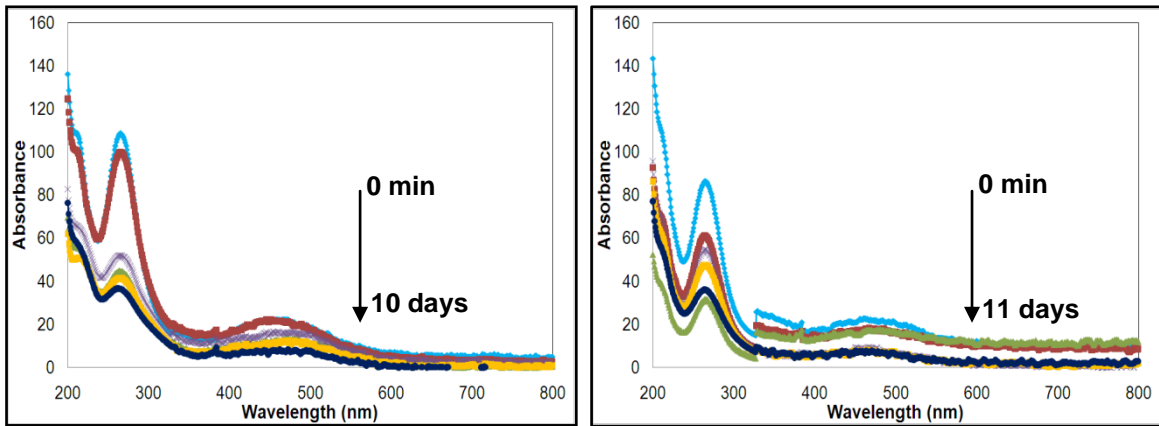


Figure 4.38 Spectral changes during aerobic biodegradation.

From the figure, there are two visible and UV absorption peaks in the spectrum for each case which point intensively at the existence of p-base at 270 nm and coloured compounds at 400 nm. The reduction in the magnitude of these peaks showed the degradation of both p-base and coloured compounds.

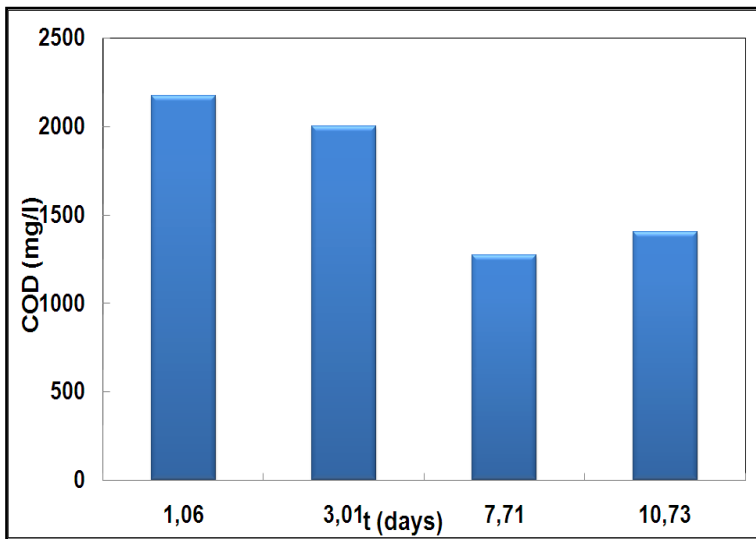


Figure 4.39 Variation of chemical oxygen demand as a function of time obtained for aerobic batch treatment.

The variation of chemical oxygen demand (COD) with time was shown in Figure 4.39 for aerobic batch treatment. As seen, the COD value of dye solution was higher than the anaerobic dye solution. The COD value decreased with time but not as much as anaerobic treatment.

4.4.2. Fungal Biodegradation of hydrolyzed RO107

4.4.2.1. Effect of pH on fungal growth and dye decolourization

For this part of studies, the white rot fungus *T. versicolor* was used for the aerobic biodegradation of hydrolyzed RO107 azo reactive dye. The effect of pH on fungal growth and dye biodegradation was investigated between pH 3.0-5.5 in no dye and in dye containing medium in order to find the suitable pH for the effective fungal growth and dye decolourization. Initial substrate (glucose) concentration was 10 g/l for each case and initial dye concentration was chosen as 50 mg/l for fungal growth studies in dye containing medium. The variation of dry maximum cell concentration obtained at the end of growth period (21 days) with pH is indicated in Figure 4.40. From the figure, while the maximum fungus concentration was obtained at pH 4.0 in no dye containing medium as 1.567 g dry weight/l, optimum pH for dye containing medium was determined as 5.0 (X_{\max} : 1.607 g dry weight/l).

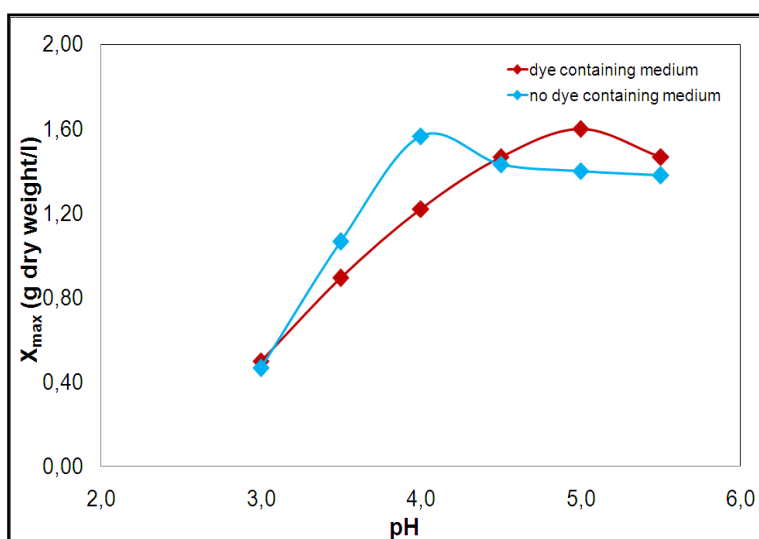


Figure 4.40 The effect of pH on fungal growth in no dye and in dye containing growth medium (S_{G0} :10 g/l, T:30 °C, ST: 150 rpm).

The percentage of glucose consumption and the percentage of dye removal determined for each pH studied at the end of growth period are presented in Table 4.8. From the table, 98.5 % glucose consumption was obtained at pH 4.0 in no dye containing growth medium. For dye containing growth medium, the dye removal and glucose consumption were found as 83.1% and 98.1%, respectively at the

end of 21 days growth period. For the further fungus studies performed by using *T. versicolor*, working pH was chosen as 5.0.

Table 4.8 Percentage of glucose consumption and percentage of dye removals obtained at different pH values (S_{G0} :10 g/L).

	No dye containing medium	50 mg/l dye containing medium	
pH	Glucose consumption %	Dye removal %	Glucose consumption %
3.0	98.4	42.5	66.3
3.5	98.3	53.5	75.8
4.0	98.5	73.8	90.8
4.5	98.5	78.6	94.9
5.0	98.3	83.1	98.1
5.5	98.6	80.0	95.5

4.4.2.2. Effect of initial glucose concentration on fungal growth in the absence of dye

Fungal growth and dye decolourization experiments were performed by using two different substrates; glucose and molasses sucrose. For fungal growth and dye decolourization studies glucose was firstly used as the main carbon source at different levels. The effect of initial glucose concentration on fungal growth was investigated between 2.5-20 g/l initial glucose concentrations in the absence of dye. The fungal growth and glucose consumption curves are represented in Figure 4.41. As seen from the figure, dry fungus concentration increased and glucose consumption was prolonged with initial glucose concentration. In general, the point at which all the glucose was used up referred to maximum fungal growth. So, glucose consumption curves may give an idea about fungal growth.

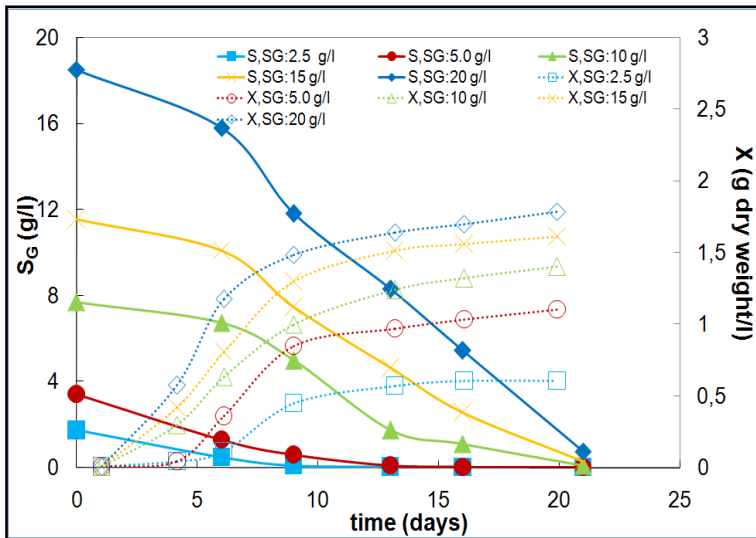


Figure 4.41 Fungal growth and glucose consumption curves at different initial glucose concentrations in no dye containing medium.

Percentage of glucose consumptions, maximum dried fungus concentrations and growth periods are given in Table 4.9. As seen, at all glucose concentrations studied, almost all glucose in the growth medium was consumed. With raising initial glucose concentration to 20 g/l, fungus concentration increased and maximum fungal growth was obtained at the maximum glucose concentration of 20 g/l as 1.787 g dry weight/l at the end of 21 days incubation period. Both glucose consumption and microbial growth were completed in a shorter growth period at lower substrate concentrations.

Table 4.9 Glucose consumption and maximum fungal growths obtained at different initial glucose concentrations after 21 days incubation period.

S_{G0} (g/l)	Glucose consumption%	X_{max} (g dry weight /l)	Incubation time (h)
2.5	99.1	0.607	9
5.0	99.0	1.103	13
10	98.8	1.401	16
15	97.5	1.613	16
20	95.9	1.787	21

4.4.2.3. Effect of dual substrate (glucose+molasses sucrose) concentration on fungal growth in the absence of dye

Molasses sucrose was also used as a second carbon source for the fungal growth and dye removal studies and added at different levels to the growth medium containing reduced glucose quantity. Percentage of glucose consumptions, maximum dried fungus concentrations and incubation periods obtained for the different binary combinations of glucose+molasses sucrose were given in Table 4.10. As seen from the table, glucose consumption was found nearly 98-99% for each binary glucose+molasses sucrose combination studied. It was also observed that increasing the concentrations of both substrates, especially sucrose, in the growth medium significantly increased the fungal growth. The maximum fungal growth was obtained in the growth medium containing maximum glucose and molasses sucrose concentrations.

Table 4.10 Percentage of glucose consumptions, maximum fungus concentrations and incubation periods obtained at each glucose+molasses sucrose combination.

$S_{(G+S)0}$ (g/l)	Glucose consumption%	X_{max} (g dry weight/l)	Incubation time (h)
2.5+2.5	98.4	1.233	8
2.5+5.0	98.4	1.353	14
2.5+10	99.0	1.540	21
5.0+2.5	98.9	1.701	8
5.0+5.0	99.4	1.793	14
5.0+10	99.2	1.980	21

The glucose consumption curves obtained at different binary combinations of glucose+molasses sucrose are also given in Figure 4.42. As seen from the figure, increasing the concentrations of both glucose and molasses sucrose prolonged the glucose consumption period.

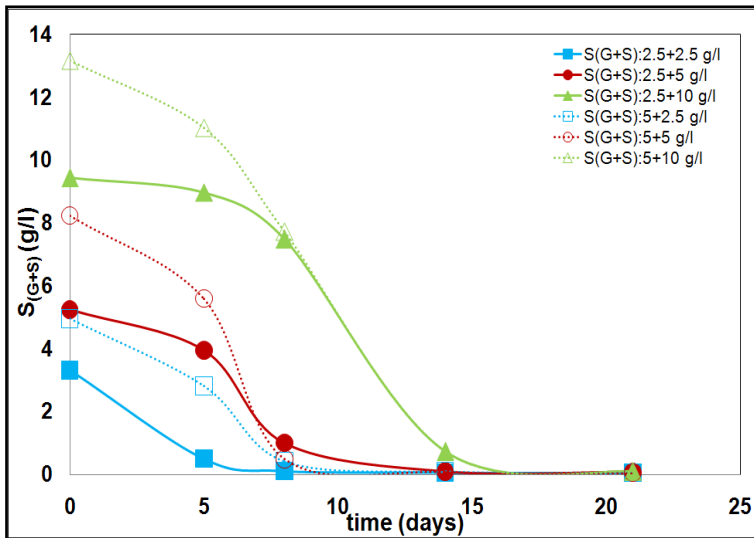


Figure 4.42 Glucose consumption curves obtained at different binary combinations of glucose+molasses sucrose.

4.4.2.4. Effects of initial glucose and dye concentrations on fungal growth and dye decolourization in the presence of dye

The effects of initial substrate and dye concentrations on fungal growth and dye biodegradation were studied in both glucose and glucose+molasses sucrose containing growth media. For each case, the initial dye concentration was varied between 25-300 mg/l at a constant substrate concentration. For the studies with using only glucose as carbon source, initial glucose concentration was changed between 2.5-30 g/l. Table 4.11 was arranged to give glucose consumption percentage, percentage of dye removal and maximum fungus concentration obtained at the end of growth period at changing substrate concentrations for a constant dye level. From the table, in general, glucose consumption and dye removal percentages and maximum fungus concentration enhanced with increasing glucose concentration up to 20 g/l. However, while both the glucose consumption and fungal growth were reduced by further increase in glucose concentration, dye removal was not affected.

From the same table, at all constant glucose concentrations with changing the dye concentration from 25 to 100 mg/l, dye removal percentage increased. Further increase in dye concentration up to 300 mg/l resulted in a reduction of dye

removal. In general, the dye concentration positively affected the fungal growth due to the usage of dye by *T. versicolor*.

Table 4.11 Percentage of glucose consumption, percentage of dye removal and maximum fungus concentrations obtained at different initial glucose and dye concentrations.

	C ₀ : 25 mg/l			C ₀ : 50 mg/l			C ₀ : 100 mg/l		
S _{G0} (g/l)	Glucose consump.%	Dye removal%	X _{max} g dry weight/l	Glucose consump.%	Dye removal%	X _{max} g dry weight/l	Glucose consump.%	Dye removal%	X _{max} g dry weight/l
2.5	98.7	63.3	0.653	98.6	66.5	0.673	98.9	71.4	0.680
5.0	99.4	74.1	1.160	99.4	77.6	1.253	99.3	80.8	1.347
10	99.5	81.6	1.480	99.6	83.1	1.600	99.7	87.3	1.707
20	99.6	85.7	1.833	96.2	87.9	1.887	93.4	89.3	2.013
30	70.2	84.8	1.793	68.3	87.6	1.840	66.5	87.9	2.040
	C ₀ : 200 mg/l			C ₀ : 300 mg/l					
S _{G0} (g/l)	Glucose consump.%	Dye removal%	X _{max} g dry weight/l	Glucose consump.%	Dye removal%	X _{max} g dry weight/l			
2.5	98.8	48.9	0.687	98.2	36.1	0.700			
5.0	99.2	65.3	1.413	99.0	45.8	1.513			
10	99.6	77.5	1.813	99.5	56.5	1.967			
20	91.1	81.0	2.167	86.6	65.5	2.307			
30	67.9	79.5	2.100	63.5	65.8	2.240			

The variations of glucose and dye concentrations with time at different levels of dye were presented in Figure 4.43 at a representative glucose concentration of 10 g/l. From the figure, glucose consumption rate slightly diminished with dye concentration. However, all the glucose was consumed nearly in the same period (21 days) for all dye concentrations studied. At lower dye concentrations, dye removal was succeeded in a short time while dye removal at higher concentrations took a longer time. For example, at the end of 14 days, 17.5 mg/l dye (75.5% efficiency) was removed by the fungus at 25 mg/l initial dye concentration. When initial dye concentration was raised to 300 mg/l, at the same time period, 85.4 mg/l dye (32.9% efficiency) was degraded.

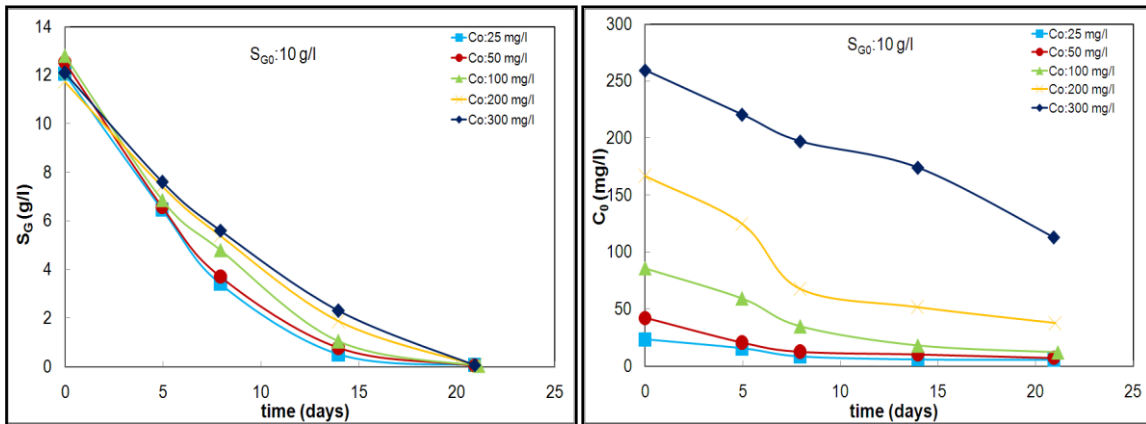


Figure 4.43 The effect of initial dye concentration on glucose and dye consumptions (S_{G_0} :10 g/l).

The DAD chromatograms of hydrolyzed dye obtained at 50 and 200 mg/l initial dye concentrations at representative 10 g/l glucose concentration for 21 days biodegradation time are given in Figures 4.44 and 4.45. The intensive coloured peak at 7.23 RT represented RO107_H-NA, m/z :399, the main compound of hydrolyzed dye for both concentrations studied. At the end of 14 days, nearly the complete decolourization of this coloured peak was achieved. There are also some other less intensive peaks of formed at RT: 4.4 and 6.30 besides p-base (RT:2.28).

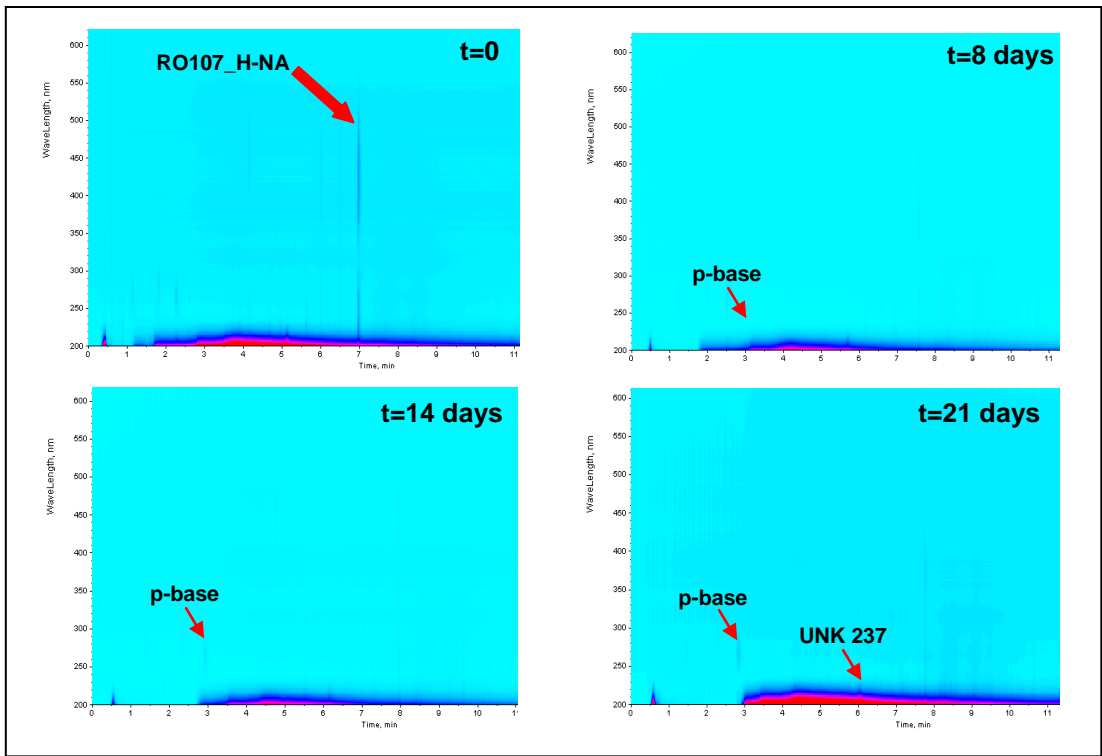


Figure 4.44 DAD chromatograms of hydrolyzed RO107 at 50 mg/l initial dye concentration (S_{G0} : 10 g/l).

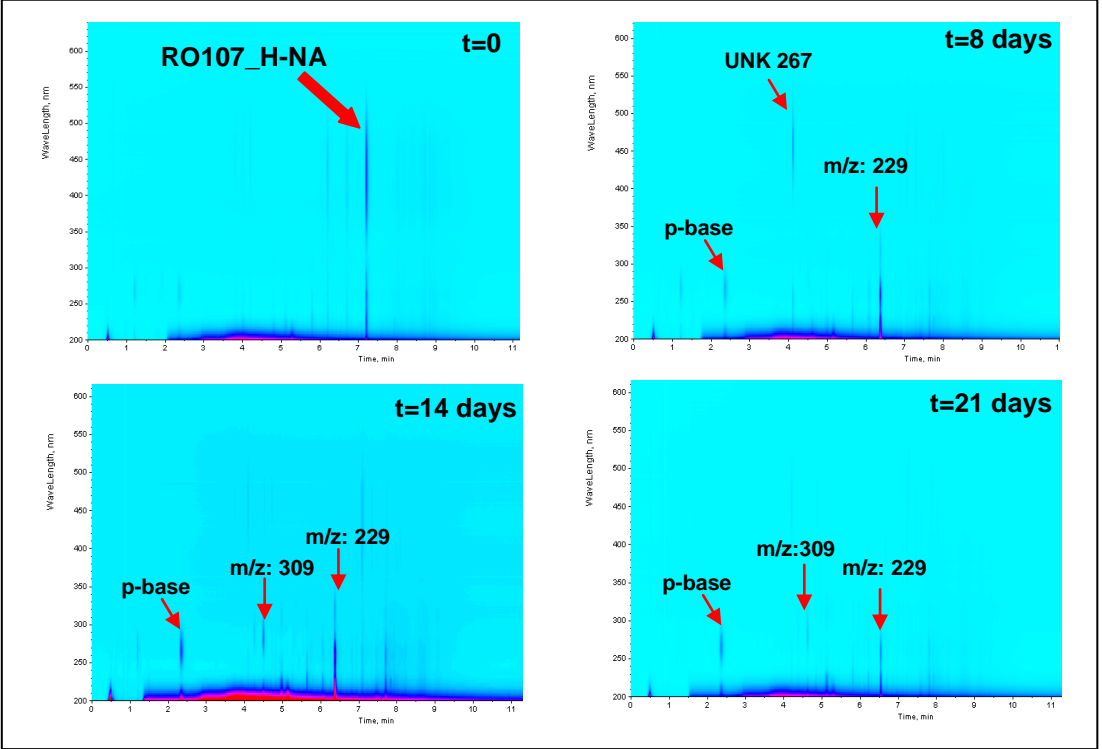


Figure 4.45 DAD chromatograms of hydrolyzed RO107 at 200 mg/l initial dye concentration (S_{G0} : 10 g/l).

The comparisons of total wavelength chromatograms (TWC) of DAD spectral data for hydrolyzed RO107 obtained at 50 and 200 mg/l initial dye concentrations before and after 20 days biodegradation period are represented in Figs.4.46 and 4.47.

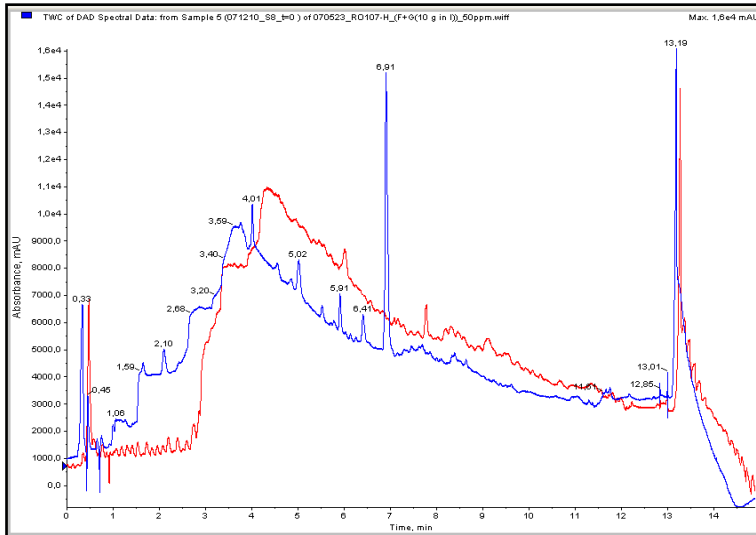


Figure 4.46 The comparison of TWC of DAD spectral data for hydrolyzed RO107 before and after 21 days biodegradation period (C_0 :50 mg/l, S_{G0} :10 g/l).

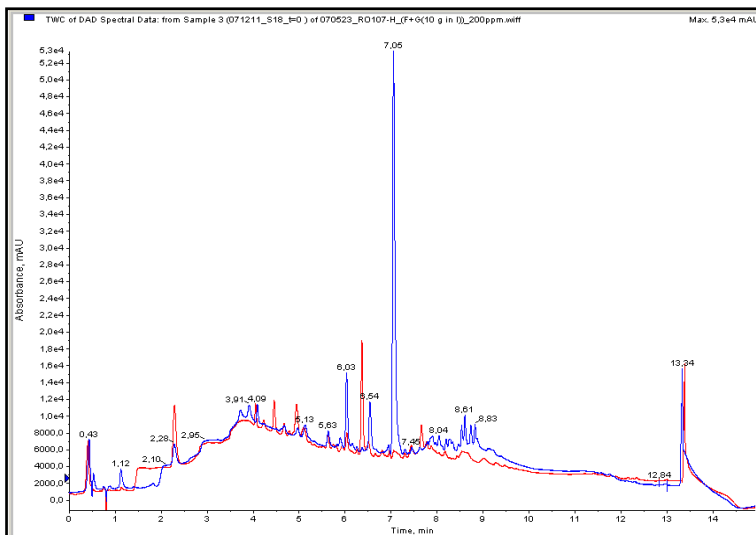


Figure 4.47 The comparison of TWC of DAD spectral data for hydrolyzed RO107 before and after 21 days biodegradation period (C_0 :200 mg/l, (S_{G0} : 10 g/l).

While the blue lines represent TWC of DAD spectral data before biodegradation, the red ones show TWC of DAD spectral data after 21 days biodegradation period.

From the same figures, the main compounds detected during fungal biodegradation were RO107_H-NA, p-base, and RT:6.30. The important compounds detected during the fungal treatment of hydrolyzed RO107 were listed in Table 4.12.

Table 4.12 Some important compounds of hydrolyzed RO107 detected before and after fungal treatment.

Compounds	Abbreviation	m/z	Molecular Weight (g/mol)	RT (min)	Before Fungal Treat.	After Fungal Treat.
2-(4-Aminobenzenesulfonyl)-ethanol, para Base	p-Base	200	201	2.28	+	+
UNK 267	UNK 267	267	268	4.04	+	+
2,4-Dihydroxy-5-(4-hydroxy-phenylazo)-benzenesulfonic acid	DH-HPA-BSA	309	310	4.46	-	+
UNK 237	UNK 237	237	238	6.04	+	+-
(4-Nitro benzenesulfonyl)-acetaldehyde	BSAA	229	230	6.36	-	+
UNK 280	UNK 280	280	281	6.51	+	+-
Reactive Orange 107-Hydrolyzed without acetyl group	RO107_H-NA	399	400	7.05	++	-

+exist, ++much exist +-less exist - non-exist

Mechanisms for the fungal degradation of hydrolyzed dye were proposed as shown in Figure 4.48 (Tauber et al., 2005 and Adosinda et al., 2003).

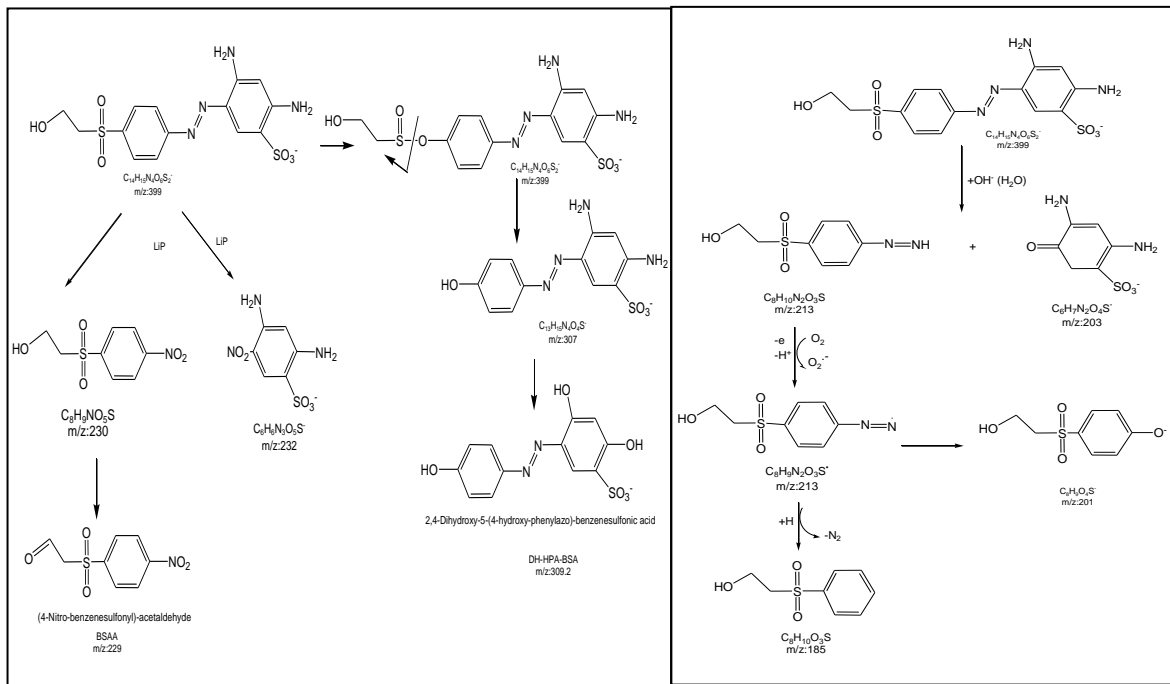


Figure 4.48 Two proposed mechanisms for the fungal degradation of hydrolyzed dye.

The relative removal of RO107_H-NA, m/z:399, the main compound of hydrolyzed dye, was plotted as a function of time for the two selected dye concentrations (Figure 4.49).

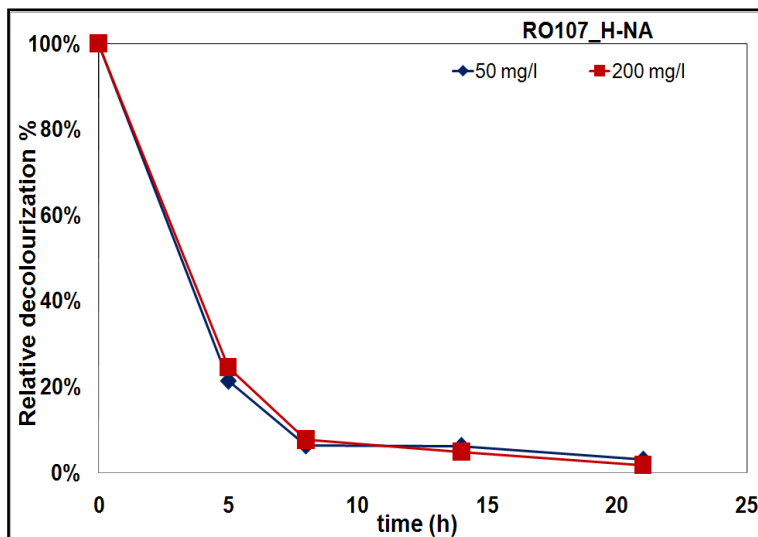


Figure 4.49 The change in relative RO107_H-NA removal with time obtained at two different hydrolyzed dye concentrations.

As seen, with increasing the initial RO107_H-NA concentration from 50 to 200 mg/l, the removal rate slightly changed. Assuming the fungal degradation of hydrolyzed dye component RO107_H-NA is pseudo first order, rate constants obtained from $\ln(C/C_0)$ vs t plot, were presented in Table 4.13 for both concentrations. The degradation rate constants were also reduced with increasing initial RO107_H-NA concentration.

Table 4.13 Pseudo first order degradation rate constants of RO107_H-NA, m/z:399 obtained at two different initial dye concentrations.

Initial dye concentration (mg/l)	50	200
k (1/h)	0.013	0.012
R ²	0.993	0.991

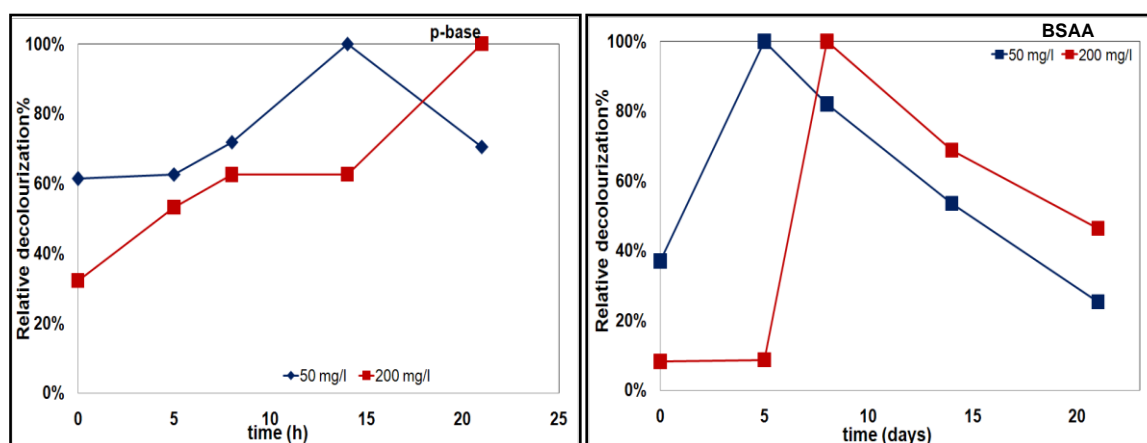


Figure 4.50 The change in relative p-base and BSAA removal with time obtained at two different hydrolyzed dye concentrations.

The effect of initial hydrolyzed dye concentration on the removal of p-base, m/z:200, and BSAA, m/z:229, relative decolourization is shown in Figure. 4.49. From figure, while the amount of p-base increased with time and formation rate was reduced with increasing initial hydrolyzed dye concentration, BSAA was firstly formed and then started to degrade for both concentration. While the removal percentage was 75% for 50 mg/l initial dye concentration, it was found as 55% for 200 mg/l initial dye concentration.

The UV-visible spectrums of the dye solutions were recorded during the fungal

biodegradation and spectrum profiles of dye solutions were compared in Figs. 4.51 and 52 for two selected initial hydrolyzed dye concentrations.

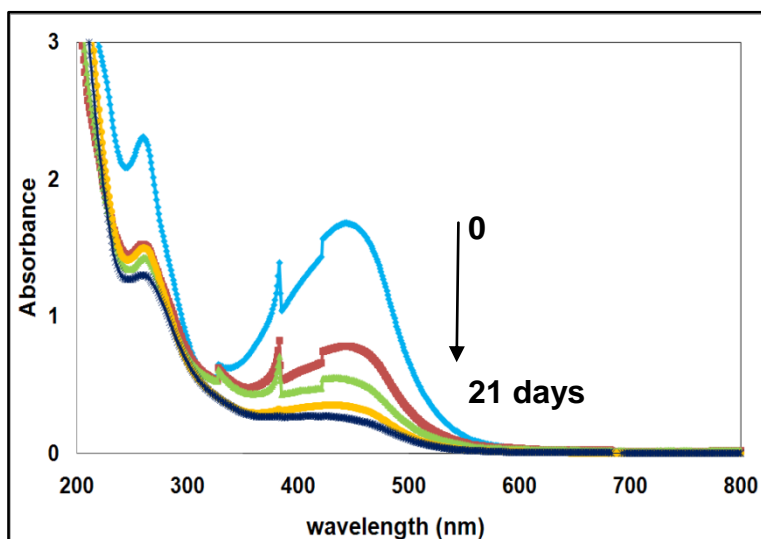


Figure 4.51 Spectral changes during fungal biodegradation for 50 mg/l initial dye concentration.

As seen from the figures, the magnitude of absorbance increased with increasing dye concentration. Moreover, there is one visible absorption peak in the spectrum at 400 nm referring to azo group in the dye structure for both the selected dye concentrations. The UV-visible spectrum of the dye solutions also indicated the reduction in the colour with time.

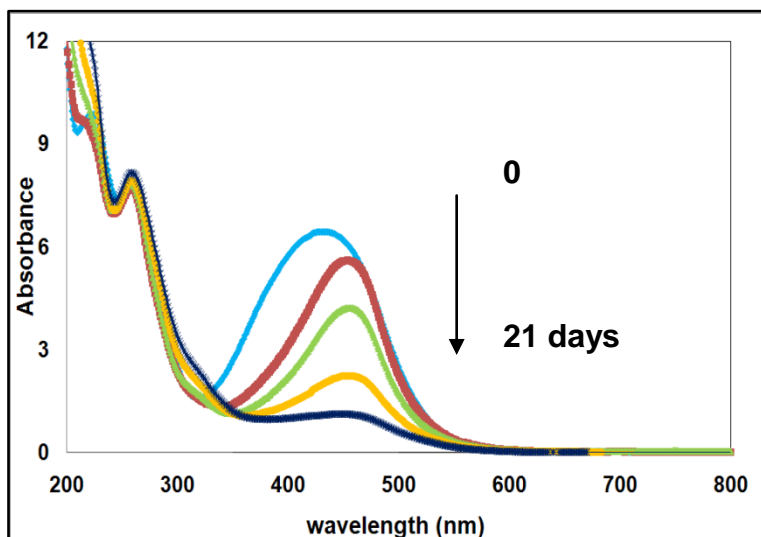


Figure 4.52 Spectral changes during fungal biodegradation for 200 mg/l initial dye concentration.

4.4.2.5. Effects of dual substrate (glucose+molasses sucrose) and dye concentrations on fungal growth and dye decolourization in the presence of dye

For the studies performed with different combinations of glucose+molasses sucrose concentrations, two selected media were used: First growth medium contained 2.5 g/l glucose and 10 g/l molasses sucrose and the second growth medium was consisted of 5 g/l glucose and 10 g/l molasses sucrose. For each medium; glucose consumption and dye removal percentages, and maximum fungus concentration obtained at the end of 21 days incubation period were compared in Table 4.14. From the table, while the addition of molasses sucrose considerably increased the fungal growth, it affected the dye removal slightly in a positive manner.

Table 4.14 Percentage of glucose consumption, percentage of dye removal and maximum fungus concentrations obtained at the end of 21 days incubation.

C ₀ (mg/l)	S _{(G+S)0} :2.5+10 g/l			S _{(G+S)0} :5+10 g/l		
	Glucose consump.%	Dye removal %	X _{max} (g dry weight/l)	Glucose consump.%	Dye removal %	X _{max} (g dry weight/l)
25	95.3	63.3	1.567	98.5	77.6	2.033
50	95.9	66.5	1.633	98.7	80.8	2.073
100	96.9	71.4	1.687	98.5	84.8	2.120
200	96.1	48.9	1.747	97.5	68.3	2.207
300	97.0	36.1	1.840	98.0	49.4	2.300

The variations of glucose in glucose+molasses sucrose mixture and dye concentrations with time at changing dye concentrations were presented in Figure 4.53 at a representative combination of 5 g/l glucose+10 g/l molasses sucrose. From the figure, glucose consumption rate was not affected by the dye concentration and all the glucose was consumed nearly in the same period (10 days) for each case. At lower dye concentrations, dye removal was succeeded in a short time while dye removal at higher concentrations took a longer time. For example, at the end of 14 days, 14.1 mg/l dye (65.1% efficiency) was removed by the fungus at 25 mg/l initial dye concentration. When initial dye concentration was raised to 300 mg/l, at the same time period, 104.2 mg/l dye (38.4% efficiency) was degraded.

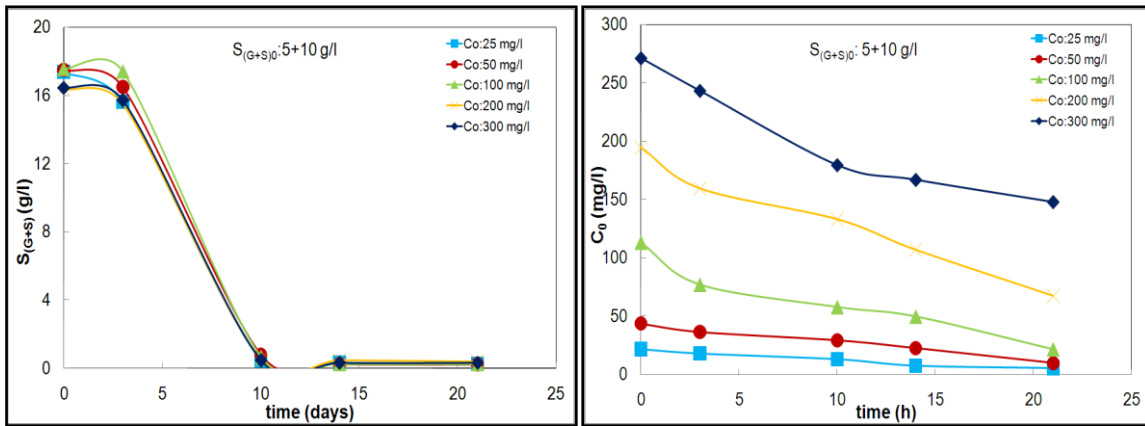


Figure 4.53 The effect of initial dye concentration on glucose and dye consumptions ($S_{(G+S)0}:5+10$ g/l).

4.5. Using of Ultrasound and Microbial Systems in Series

The degradation of hydrolyzed dye was also investigated in combined ultrasound and microbial degradation systems expecting to further degraded initial and intermediate products and to achieve higher dye removal rates and efficiencies. Ultrasound and microbial degradation systems were studied in four different combinations:

- Anaerobic biodegradation (AN)+ ultrasound (US)
- Aerobic biodegradation (AE) + ultrasound (US)
- Fungal biodegradation (F)+ ultrasound (US)
- Ultrasound (US) + fungal biodegradation (F)

Data evaluations were done by taking into consideration some important compounds at the beginning, consumed and occurred during the degradation for each case from DAD results of LC/MS-MS analysis and the results were compared.

4.5.1. Combined anaerobic (AN) + ultrasound (US) degradation system

In this system the effluent from anaerobic biodegradation of hydrolyzed dye was used as the initial dye solution of ultrasound treatment. Data evaluation was done by taking into consideration the three important compounds of hydrolyzed dye and anaerobic biodegradation: RO107_H-NA, m/z:399, and p-base, m/z:200, the main compounds of hydrolyzed dye, and intermediate NA_ABSA, m/z:229. The change

in relative removal of RO107_H-NA with time is given in Figure 4.54 for AN, US, and AN+US systems in series.

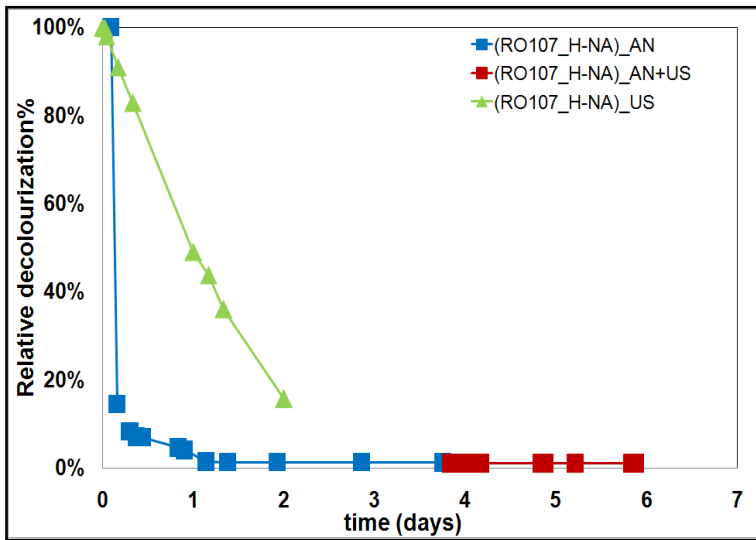


Figure 4.54 The comparison of the change in relative concentration of RO107_H-NA with time in each AN and AN+US system (C_0 :3400 mg/l, f :850 kHz).

From the figure, as the complete decolourization of RO107_H-NA was achieved within 2 days during anaerobic treatment, when anaerobic effluent was used as the feed dye solution of US system, no RO107_H-NA was detected in this solution. Therefore, no further degradation of RO107_H-NA was observed during US treatment of AN effluent. The changes in relative concentrations of p-base and NA_ABSA with time were also given in Figure 4.55 for AN, US, and AN+US systems in series.

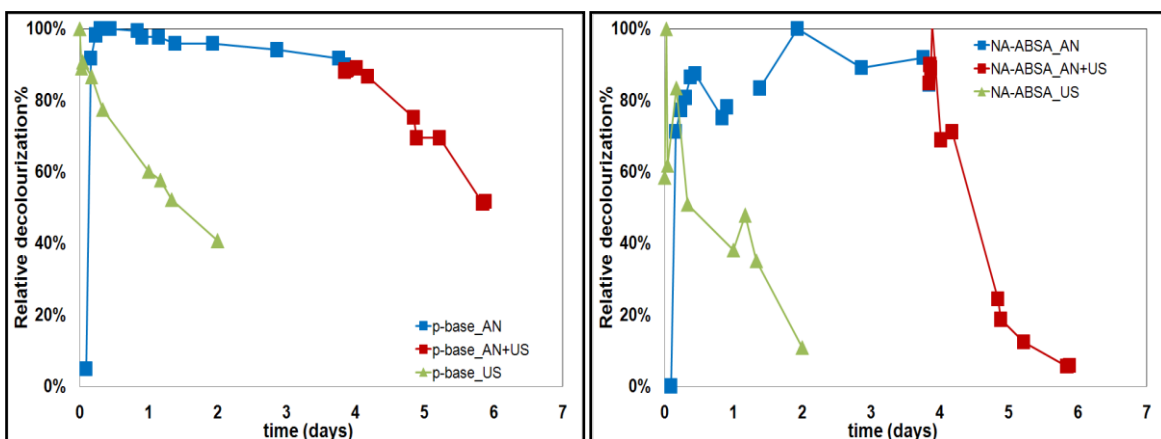


Figure 4.55 The comparison of the change in relative concentration of p-base and NA_ABSA with time in each AN and AN+US system (C_0 :3400 mg/l, f :850 kHz).

From the figure, while 8% removal of p-base was obtained at the end of 4 days of AN treatment, the decolourisation percentage of p-base in sequential US treatment was 49% at the end of 2 days of AN effluent treatment. The removal percentage of p-base was 59% in single US system. For NA_ABSA, the decolourization percentage was 8% at the end of 4 days of anaerobic treatment, and nearly the complete decolourization (94%) was achieved within 2 days in sequential ultrasound treatment. For single ultrasound system, this value was 89%. It is clear that degradation rates and yields were higher for both compounds in combined system than that of AE system and lower than that of US system.

4.5.2. The combined aerobic (AE) + ultrasound (US) degradation system

For this system, the effluent from aerobic biodegradation of hydrolyzed dye was used as the feed dye solution of ultrasound treatment. Data evaluation was done by taking into consideration two important intermediate compounds of aerobic biodegradation: DAPSE+BDA, m/z:319 and p-base, m/z:200. The change in relative removal of DABSE_BDA with time is given in Figure 4.56 for AE and AE+US systems in series.

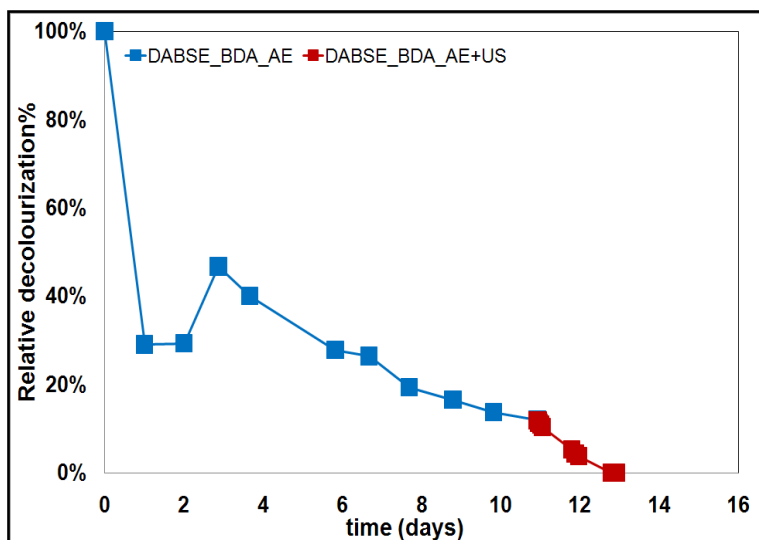


Figure 4.56 The comparison of the change in relative concentration of DABSE_BDA with time in each AE and AE+US system.

From the figure, while 89% decolourization of DABSE_BDA was achieved at the end of 10 days aerobic treatment, the complete decolourization was obtained within 2 days of sequential US treatment. It is clear that removal rate and yield of

DABSE_BDA were higher in combined AE+US system than that of single AE system. The change in relative removal of p-base with time was also given in Figure 4.57 for AE, US, and AE+US systems in series.

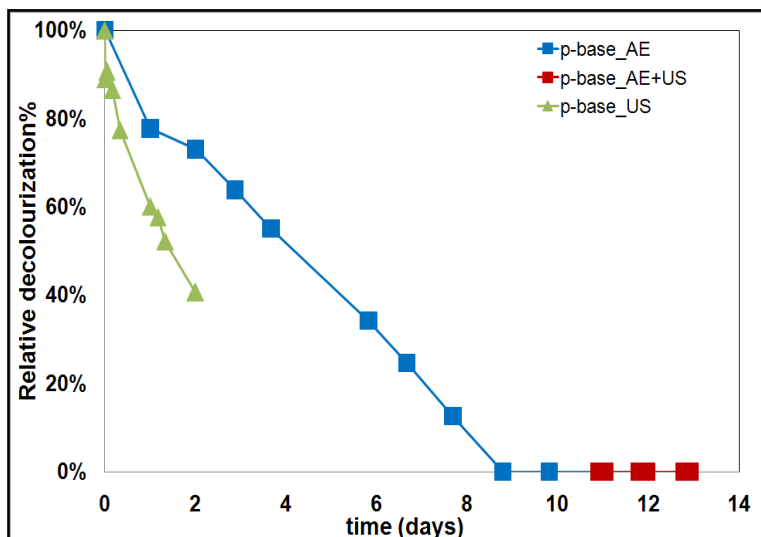


Figure 4.57 The comparison of the change in relative concentration of p-base with time in each AE and AE+US system.

From the figure, as the complete decolourization of p-base was achieved in 9 days during aerobic treatment, when aerobic effluent was used as a feed dye solution of US system, no p-base was detected in the feed dye solution. Therefore, no further degradation of p-base was observed during US treatment of AE effluent. 60% removal of p-base was obtained for single ultrasound system within 2 days.

4.5.3. The combined fungal (F) + ultrasound (US) degradation system

In this system, the dye solution obtained at the end of fungal treatment was used as the feed dye solution of ultrasound treatment. Data evaluation was done by taking into consideration three important compounds of hydrolyzed dye and fungal biodegradation: RO107_H-NA, m/z:399, p-base, m/z:200 and BSAA, m/z:229. The change in relative concentration of RO107_H-NA with time was given in Figure 4.58 for F and F+US systems in series.

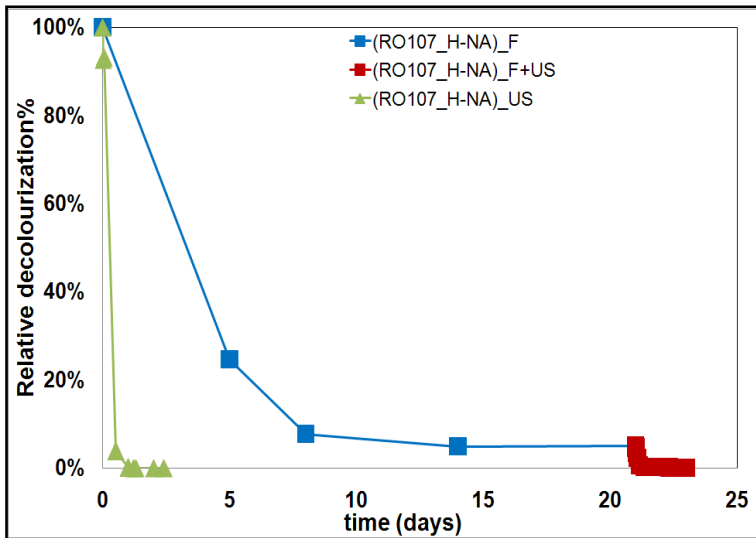


Figure 4.58 The comparison of the change in relative concentration of RO107_H-NA with time in each F and F+US system (C_0 :200 mg/l, T :30 °C).

From the figure, 95% decolourization of RO107_H-NA was achieved at the end of 21 days of fungal treatment. The effluent of fungal treatment was then treated with sequential US system and complete decolourization was observed within 2 days. The removal rate of RO107_H-NA was occurred much more rapidly in sequential US system than the single F system. The change in relative concentration of p-base and BSAA with time was given in Figure 4.59 for F and F+US systems in series.

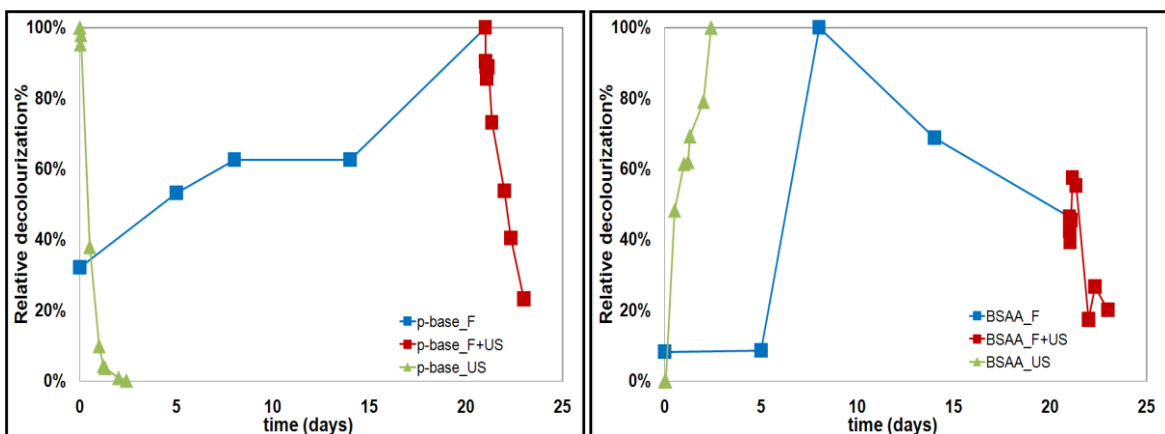


Figure 4.59 The comparison of the change in relative concentration of p-base and BSAA with time in each F and F+US system.

From the figure, it is evident that p-base was formed during the fungal treatment. 77% of this p-base was degraded within 2 days by sequential US system. On the

other hand, the compound BSAA, also formed during the fungal treatment, started to degrade after 8 days of fungal treatment and 64% degradation was achieved at the end of 21 days fungal treatment. This value increased to 75% by sequential US system within 2 days. Degradation rates and yields of both the compounds were found to be higher in combined F+US system than that of single F system.

4.5.4. The combined ultrasound (US) + fungal (F) biodegradation

In this reverse bounded system, the effluent solution from ultrasound system was used as the feed dye solution for fungal treatment. Data evaluation was done by taking into consideration two important compounds of hydrolyzed dye and ultrasound degradation: RO107_H-NA, m/z:399 and p-base, m/z:200. The change in relative concentration of RO107_H-NA with time was given in Figure 4.60 for single US system and F+US system in series.

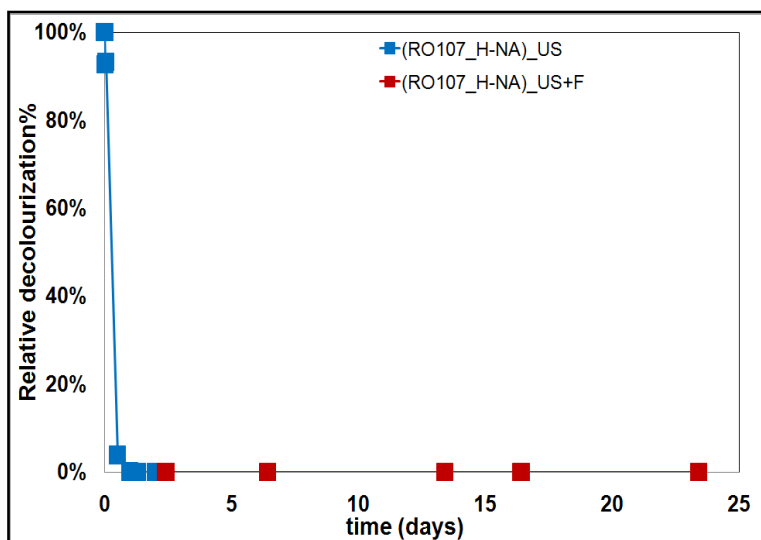


Figure 4.60 The comparison of the change in relative concentration of RO107_H-NA with time in each US and US+F system. (C_0 :200 mg/l, T:30 °C).

From the figure, complete decolourization of RO107_H-NA was achieved at the end of 2.5 days ultrasound treatment. So no degradation of RO107_H-NA was observed in sequential F system. The change in relative concentration of p-base with time was given in Figure 4.61 for US and US+F systems.

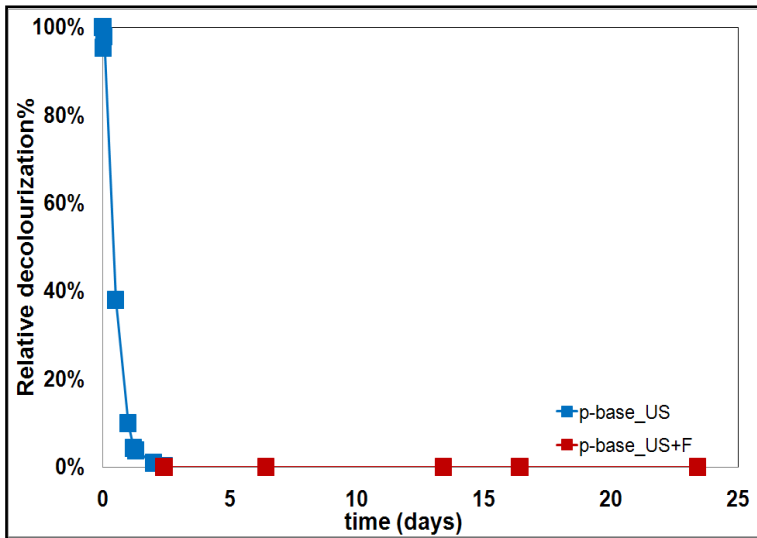


Figure 4.61 The comparison of the change in relative concentration of p-base with time in each US and US+F system. (C_0 :200 mg/l, T :30 °C).

From the figure, as p-base was completely removed from the dye solution in single US system, again sequential F system had no effect on p-base degradation

5. CONCLUSIONS

In this thesis study, the removal of Reactive Orange 107 (RO107) mono-azo reactive dye, an important pollutant in textile wastewaters, was investigated by using ultrasonic and microbial methods in single and in series system. The degradation mechanisms were proposed after analyzing the original and hydrolyzed form of dye and ultrasonic and microbial formation and degradation products by using LC/MS-MS and Analyst Software and Chem Draw 7.0 programmes.

Since the RO107 dye is found in wastewaters in its hydrolyzed form, hydrolyzed form of the dye was used in the experimental studies. For this purpose, firstly, the structural analysis of original and hydrolyzed form of RO107 was done by LC-MS/MS and it was detected that original dye contains 73.2% RO107_O and RO107_V components, and hydrolyzed dye contains mainly 63.7% RO107_H-NA, m/z:399, and p-base, m/z:200 compounds. The results of degradation studies were evaluated mainly.

Ultrasonic dye removal studies were performed at three different frequencies (378, 850 ve 992 kHz), at two different temperatures (20, 30 °C) and at three different initial dye concentrations (50, 100, 200 mg/l). The highest dye removal was obtained at 850 kHz frequency and at 50 mg/l initial dye concentration and it was observed that temperature has no significant effect on dye removal. Under these conditions, 99% dye removal was achieved after 6 h sonication. It was observed that while RO107_H-NA and p-base were removed during ultrasonic degradation, an important compound UNK 177, m/z:177, was formed.

The removal of 3400 mg/l initial hydrolyzed dye concentration was investigated in sequential anaerobic-aerobic batch bioreactors by using anaerobic-aerobic bacterial sludge. For this purpose, hydrolyzed dye solution was hold in the anaerobic reactor for a while and then fed to aerobic reactor. The degradation mechanisms for both processes were investigated. During anaerobic process, the main compound of hydrolyzed dye RO107_H-NA was cleaved totally from azo bond and converted to p-base and NA_ABSA, m/z:229. The compound p-base was remained unchanged during anaerobic process. At the beginning of aerobic

process an important amount of DABSE_BDA, m/z:319 was formed due to the oxidation by oxygen in air. P-base was totally removed and DABSE_BDA was degraded during aerobic process.

Microbial degradation studies were carried out by using *Trametes versicolor*, a white rot fungus and the results were compared with the findings obtained by anaerobic-aerobic bacterial sludge. In fungal degradation, glucose was used as the single and binary carbon source together with the molasses waste. When the effect of medium pH on the fungal dye removal was examined in the medium containing 10 g/l glucose and 50 mg/l hydrolyzed dye, maximum dye removal (83.1%) was obtained at pH 5.0. At this pH value, in no dye containing medium, by increasing the initial glucose concentration up to 20 g/l, the weight of fungal biomass increased from 0.607 to 1.787 g/l. In hydrolyzed dye containing medium, the effect of initial dyestuff concentration changing between 25-250 mg/l on the fungal growth and dye removal at a constant glucose concentration, varied for each experimental set from 2.5 to 30 g/l, was studied and it was found that dye removal and fungal biomass increased with both glucose concentration up to 20 g/l and dye concentration up to 100 mg/l. Maximum dye removal was obtained as 89.3 % in 20 g/l initial glucose and 100 mg/l initial dye concentrations containing medium. Maximum fungal biomass concentration was determined as 2.307 g/l at 20 g/l initial glucose concentration in 300 mg/l initial dye concentration including medium. The increase in fungal biomass represents the use of dye by the fungus as a nutrient source.

In the second part of fungal biodegradation studies, molasses sucrose was used as an additional carbon source besides glucose. For this purpose, while the glucose concentration was kept constant at 2.5 or 5.0 g/l, 2.5, 5.0 or 10 g/l molasses sucrose concentration was added to the medium. Fungal biomass increased significantly with increasing both the glucose and molasses sucrose concentrations in the growth medium. While 1.980 g/l dried biomass was obtained in no dye and 5 g/l glucose+10 g/l molasses sucrose containing medium, 2.300 g/l dried biomass was achieved for the same combination of glucose + molasses sucrose in 300 mg/l initial hydrolyzed dye containing medium. Maximum dye

removal (84.8%) was observed for the same combination of glucose + molasses sucrose with 100 mg/l hydrolyzed dye. When molasses was added to growth medium, it was observed that the weight of fungal biomass increased considerably, but dye removal was changed insignificantly. In fungal degradation, the main compound of hydrolyzed dye, RO107_H-NA was completely removed and converted to p-base and BSAA, m/z:229. While p-base cannot be degraded during fungal process, 78-80% of BSAA, which was formed during the first 5 days of fungal processes, was removed.

The main degradation compounds with respect to the method used were given in Table 5.1. The results obtained for each method were compared in Table 6.2.

Table 5.1 The main degradation compounds with respect to the method used

Name of The Method	The main hydrolyzed dye components	Degradation compounds
Ultrasound	RO107_H_NA, m/z:399 p-base, m/z:200	UNK 177, m/z:177
Anaerobic Degradation		p-base, m/z:200 NA-ABSA, m/z:229 NA-DABSA, m/z:244
Aerobic Degradation		VPB+NA, m/z:240 DABSE+BDA, m/z:319
Fungal Degradation		BSAA, m/z:229 DH-HPA-BSA, m/z:309

In the last part of studies, it was aimed to use microbial and ultrasonic systems in series in order to further degrade initial and intermediate products and to achieve higher dye removal rates and efficiencies. Because RO107_H-NA was degraded during single AN system, sequential US system had no effect. While p-base was unchanged in AN system, 49% of it was degraded in sequential US system within two days. Another degradation compound of AN system, NA_ABSA, was also completely removed within 2 days in sequential US system.

Within 10 days 85% aerobic degradation of coloured compound DABSE_BDA was achieved. The complete removal of DABSE_BDA was achieved within 2 days sequential US system. 60% of p-base was removed within 2 days in US system. For the single AE system complete removal of p-base was achieved within 8 days. Combined AE-US had no effect on the removal of this compound.

The removal of RO107_H-NA in single F system was 95% within 14 days while 99% removal was accomplished in US system within 2 days. The use of sequential US system provided the complete degradation of this compound remained after F treatment. While p-base was removed totally in US system within 2 days, its quantity increased during 21 days F treatment. For F+US combined system, 80% of p-base removal was achieved in sequential US system within 2 days.

When the removals of RO107_H-NA ve p-base, the main compounds of hydrolyzed dye, were investigated in reverse bounded US+F system, as the total removals of both compounds were achieved in US system within 2 days, this reverse bound system was not thought to be effective.

In this thesis study the usage of single and binary ultrasonic and microbial methods, which have been proposed repeatedly in recent years for the treatment of reactive dye containing textile wastewaters, for the removal of Reactive Orange 107 (RO107), a mono-azo reactive dye, was investigated. Moreover degradation mechanisms and the structures of hydrolysis and degradation processes were tried to be explained by using new analytical techniques. Experimental results showed that both the single and binary ultrasonic and anaerobic-aerobic bacterial sludge treatments were very effective for the decolourization of RO107 dye and fungal decolourization was slow and depended on growth nutrients.

Table 5.2 Comparison of the results with respect to the method used

Name of The Method	Working Conditions	Duration	Pseudo 1st order degradation rate constants, k (1/h)	COD Removals	Percentage removals of the main compounds
Ultrasound	f:850 kHz, T:30 °C, Initial dye concentrations, C ₀ : 50,100,200 mg/l	24 h for C ₀ : 50 mg/l 47 h for C ₀ : 100 mg/l 58 h for C ₀ : 200 mg/l	k:0.0046 for C ₀ : 50 mg/l k:0.0019 for C ₀ : 100 mg/l k:0.0015 for C ₀ : 200 mg/l	66.6% for C ₀ : 50 mg/l 65.4% for C ₀ : 100 mg/l 60.4% for C ₀ : 200 mg/l	*100% removal of RO107_H-NA *100% removal of p-base
Anaerobic Degradation	Initial dye concentration, C ₀ : 3400 mg/l	1 st trial: 4 days 2 nd trial: 10 days	k:22.16 for 1 st trial k:1.14 for 2 nd trial	51.6% for 1 st trial 64.6% for 2 nd trial	*100% removal of RO107_H-NA *Very little removals of p- base and NA-ABSA
Aerobic Degradation	Feed solution (AN effluent)	1 st trial: 10 days 2 nd trial: 11 days	-	34.1% for 1 st trial 35.3% for 2 nd trial	*No RO107_H-NA *100% removal of p-base *86% removal of colored compound, DABBSE+BDA
Fungal Degradation	pH:5.0, T: 30 °C, S _{G0} :10 g/l Initial dye concentrations, C ₀ : 25-300 mg/l	21 days	k:0.013 for 50 mg/l k:0.012 for 200 mg/l	-	*98% removal of RO107_H-NA

6. SONUÇLARIN TARTIŞILMASI

Bu tez çalışmasında, tekstil atıksularının önemli bir kirleticisi olan Reactive Orange 107 (RO107) mono-azo reaktif boyarmaddesinin ultrasonik ve mikrobiyal yöntemlerle giderimi tekli ve ardışık sistemlerde incelenmiş, boyarmaddenin orijinal ve hidroliz formları ile ultrasonik ve mikrobiyal oluşum ve yıkım ürünlerinin LC/MS-MS ve Analyst Software ve Chem Draw 7.0 programları kullanılarak yapısal analizleri yapılarak giderim mekanizmaları önerilmiştir.

RO107 atıksuda hidrolize formda bulunduğundan, deneysel çalışmalarda boya hidrolize edilerek kullanılmıştır. Çalışmaların ilk kısmında orijinal ve hidrolize formdaki RO107 boyarmaddesinin LC/MS-MS kullanılarak yapı analizi yapılmış ve orijinal boyanın %70 oranında RO107_O ve RO107-vinil'den oluştuğu; hidrolize boyanın ise yoğunluklu olarak (62,2%) RO107_H-NA, m/z:399,'yı ve p-base,m/z:200,'i içerdiği gözlenmiştir. Degredasyon çalışmaları sonuçları RO107_H-NA ve p-base bileşikleri temel alınarak değerlendirilmiştir.

Ultrasonik yöntemle renk giderim çalışmaları üç farklı frekans (378, 850 ve 992 kHz), iki farklı sıcaklık (20, 30 °C) ve üç farklı başlangıç boyarmadde derişimi (50, 100, 200 mg/l) değerinde gerçekleştirilmiş ve en yüksek giderimin 850 kHz frekans ve 50 mg/l derişim değerinde sağlandığı gözlenmiş, sıcaklığın ise önemli bir etkisi görülmemiştir. Bu koşullarda 6 saat sonunda gözlenen renk giderimi %99 olmuştur. Hidrolize RO107'nin ultrasonik parçalanması sonucu RO107_H-NA ve p-base'in giderildiği, önemli bir bileşik olan UNK 177, m/z:177'nin oluştuğu gözlenmiştir.

Kesikli ardışık anaerobik-aerobik biyoreaktör sisteminde anaerobik-aerobik bakteri çamuru kullanılarak 3400 mg/l başlangıç hidrolize boyarmadde derişiminin giderimi incelenmiştir. Bu amaçla anaerobik reaktöre verilen hidrolize boya çözeltisi bu reaktörde belli bir süre alıkonulduktan sonra aerobik reaktöre beslenmiş ve boyanın her iki prosesteki yıkım mekanizmaları araştırılmıştır. Anaerobik proseste hidrolize boyanın ana bileşeni RO107_H-NA azo bağından tamamen yıkılarak p-base ve NA-ABSA, m/z:229,'a dönüşmüştür. p-base bileşiği anaerobik degredasyon boyunca değişmeden kalmıştır. Aerobik prosesin başında ise havanın oksijeni ile oksidasyon sonucu önemli miktarda DABSE_BDA, m/z:319

oluşmuştur. Oluşan DABSE_BDA ise proses boyunca yıkıma uğramıştır. p-base'in ise tamamı yıkılmıştır.

Mikrobiyal degradasyon çalışmaları beyaz çürükçül fungus *Trametes versicolor*'la gerçekleştirilmiş, sonuçlar anaerobik-aerobik bakteri çamuru ile elde edilenlerle karşılaştırılmıştır. Fungal giderimde glukoz tek başına ve bir atık olan melasla birlikte karbon kaynağı olarak kullanılmıştır. 10 g/l glukoz ve 50 mg/l hidrolize boya içeren besin ortamında boya giderimine ortam pH'ının etkisi incelendiğinde, pH 5,0'da en yüksek giderim (% 83,1) gözlenmiştir. Bu pH değerinde, boya içermeyen ortamda glukoz derişiminin 20 g/l'ye kadar artması ile biyokütlenin 0.607'den 1.787 g/l'ye arttığı gözlenmiştir. Boya içeren ortamda 2,5 ila 30 g/l arasında sabit tutulan her bir glukoz derişiminde, 25-300 mg/l aralığında deęiştirilen başlangıç hidrolize boyarmadde derişiminin fungusun üremesine ve boyarmadde giderimine etkileri araştırıldığında ise, glukoz derişiminin 20 g/l'ye, boyarmadde derişiminin ise 100 mg/l'ye kadar artmasıyla boyarmadde gideriminin ve biyokütlenin arttığı görülmüştür. Maksimum boyarmadde giderimi 20 g/l başlangıç glukoz ve 100 mg/l başlangıç boyarmadde derişiminde çalışıldığında % 89,3 olarak elde edilmiştir. Maksimum biyokütle derişimi ise 20 g/l başlangıç glukoz ve 300 mg/l başlangıç boyarmadde derişiminde 2,307 g/l olarak bulunmuştur. Fungal kütledeki artış boyarmaddenin fungus tarafından besin kaynağı olarak kullanıldığını göstermektedir.

Fungal biyodegradasyon çalışmalarının ikinci kısmında glukozun yanısıra melas sakkarozu da besin ortamına ek karbon kaynağı olarak katılmıştır. Bu amaçla glukoz derişimi 2,5 veya 5,0 g/l'de tutulurken melas sakkarozu derişimi 2,5, 5,0 veya 10 g/l olarak ortama eklenmiştir. Glukoz ve melas sakkarozu derişimlerinin artması ile biyokütlenin önemli ölçüde arttığı gözlenmiştir. 5,0 g/l glukoz+10 g/l melas sakkarozu karışımı ile boyasız ortamda yapılan çalışma sonucunda 1.980 g/l kuru hücre elde edilmiştir. Aynı kombinasyonda glukoz+melas sakkarozu ve 300 mg/l başlangıç boyarmadde derişimi içeren boyalı ortamda ise 2,300 g/l kuru hücrenin oluştuęu gözlenmiştir. Maksimum boya giderimi (% 84,8) ise yine aynı glukoz+melas sakkarozu kombinasyonunda ve 100 mg/l boyarmadde ile çalışıldığında bulunmuştur. Melasın fungal biyokütleyi arttırmakla birlikte boya

giderim verimini çok fazla deęiřtirmedięi gözlenmiřtir. Fungal proste hidrolize boyanın ana bileřeni RO107_H-NA tamamen yıkılarak p-base ve BSAA, m/z: 229,'ya dönüřmüřtür. p-base bileřięi fungal degradasyonda yıkıma uğratılamazken, ilk 5 gün boyunca oluřan BSAA, 75-80% oranında parçalanmıřtır.

Temel degradasyon ürünleri kullanılan yöntemlere göre Table 6.1'de verilmiřtir. Her bir yöntem için elde edilen sonuçlar Tablo 6.2'de karşılařtırılmıřtır.

Table 6.1 Kullanılan yöntemlere göre elde edilen temel degradasyon ürünleri

Metod İsmi	Hidrolize boyanın temel bileřenleri	Degradasyon ürünleri
Ultrasound	RO107_H_NA, m/z:399 p-base, m/z:200	UNK 177, m/z:177
Anaerobic Degradasyon		p-base, m/z:200 NA-ABSA, m/z:229 NA-DABSA, m/z:244
Aerobik Degradasyon		VPB+NA, m/z:240 DABSE+BDA, m/z:319
Fungal Degradasyon		BSAA, m/z:229 DH-HPA-BSA, m/z:309

Çalıřmaların son kısmında mikrobiyal ve ultrasonik sistemler seri halde kullanılarak boya ara yıkım ürünlerinin daha ileri parçalanması ve boya giderim hız ve veriminin artırılması hedeflenmiřtir. AN-US seri baęlı sistemde hidrolize boyanın temel bileřenini RO107_H-NA AN sistemde zaten tamamen yıkıldıęından seri baęlı US'in bir katkısı gözlenmemiřtir. AN sistemde yıkılmayan p-base ise seri baęlı US sistemde % 49 oranında yıkıma uğratılmıřtır. AN sistemin dięer bir yıkım ürünü olan NA_ABSA ise seri baęlı US sistemde 2 gün içinde neredeyse tamamen tüketilmiřtir.

Renkli bileřik DABSE_BDA'nın 10 günlük AE yıkımı (85%) sonrası tamamen giderimi seri baęlı US sistemde 2 gün içinde saęlanmıřtır. p-base'in tekli US

sistemde 2 gün sonunda %60 oranında giderimi sağlanırken, p-base'in tekli AE sistemde yaklaşık 8 gün sonunda tamamen giderimi sağlanmıştır. AE-US seri bağlı sistemin p-base giderimine bir katkısı görülmemiştir.

RO107_H-NA'nın tekli F sistemde giderimi 14 günde % 95 olarak gerçekleşirken, tekli US sistemde ise 2 günde RO107_H-NA giderimi % 99 olarak bulunmuştur. F+US seri bağlı sistemin kullanılması, F sistem sonrası çözeltide çok az miktarda bulunan RO107_H-NA'nın tamamen giderimini sağlamıştır. p-base'in miktarı tekli US sistemde 2 gün içinde tamamen giderilirken, tekli F sistemde ise 21 gün boyunca artmıştır. F+US ikili sistemin kullanıldığı durumda seri bağlı US sistemde p-base 2 gün içinde yaklaşık 80% oranında giderilmiştir.

Ters bağlı US+F sistemle yine hidrolize boyanın ana bileşenlerinden RO107_H-NA ve p-base'in giderimi incelendiğinde, tekli US sistem 2 günün sonunda hem RO107_H-NA'yı hem de p-base'i tamamen yıktığından, bu bileşiklerin gideriminde US+F seri bağlı sistemin bir katkısının olmadığı gözlenmiştir.

Tez çalışmasında tekstil endüstrisi atıksularının en önemli kirleticilerinden olan reaktif boyarmaddelerin giderimi için son yıllarda üzerinde oldukça durulan ve önerilen ultrasonik ve mikrobiyal yöntemlerin tekli ve kombine olarak mono-azo reaktif boyarmaddesinin gideriminde kullanılabilirliği araştırılmıştır. Çalışmada ayrıca yeni analiz teknikleri kullanılarak yıkım mekanizmaları ve hidrolizin ve yıkımın çeşitli aşamalarındaki yapılar da aydınlatılmaya çalışılmıştır. Deneysel sonuçlar tekli ve ikili ultrasonik ve aerobik-anaerobik ardışık bakteri çamuruyla muamele yöntemlerinin RO107'nin oluşturduğu rengin gideriminde oldukça hızlı ve verimli çalıştığını, fungal renk gideriminin ise çok yavaş ve besin ortamı bileşenlerine oldukça bağımlı olduğunu göstermiştir. Temel degradasyon ürünleri ve deneylerde kullanılan yöntemler sırasıyla Tablo 6.1 ve 6.2'de karşılaştırılmalı olarak sunulmuştur.

Table 6.2 Kullanılan yöntemlere göre elde edilen sonuçların karşılaştırılması.

Metod İsmi	Çalışılan Koşullar	Süre	Pseudo 1. derece degradasyon hız sabitleri, k (1/h)	KOİ Giderimi	Temel bileşiklerin yüzde giderim değerleri
Ultrasound	f:850 kHz, T:30 °C, Başlangıç boya derişimi, C ₀ : 50,100,200 mg/l	C ₀ : 50 mg/l için 24 saat C ₀ : 100 mg/l için 47 saat C ₀ : 200 mg/l için 58 saat	C ₀ : 50 mg/l için k:0,0046 C ₀ : 100 mg/l için k:0,0019 C ₀ : 200 mg/l için k:0,0015	C ₀ : 50 mg/l için %66,6 C ₀ :100 mg/l için %65,4 C ₀ :200 mg/l için %60,4	* RO107_H-NA:%100 giderim * p-base:%100 giderim
Anaerobik Degredasyon	Başlangıç boya derişimi , C ₀ : 3400 mg/l	1. deneme: 4 gün 2. deneme: 10 gün	1. deneme için k:22,16 2. deneme için k:1,14	1. deneme için %51,6 2. deneme için %64,6	* RO107_H-NA:% 100 giderim *p-base veNA-ABSA: çok az giderim
Aerobik Degredasyon	Besleme Çözeltisi (AN çıkış çözeltisi)	1. deneme: 10 gün 2. deneme: 11 gün	-	1. deneme için %34,1 2. deneme için %35,3	*RO107_H-NA:yok *p-base:%100 giderim *renkli bileşik, DABBSE+BDA: %86 giderim
Fungal Degredasyon	pH:5.0, T: 30 °C, S _{G0} :10 g/l Başlangıç boya derişimi, C ₀ : 25-300 mg/l	21 gün	C ₀ : 50 mg/l için k:0,013 C ₀ : 200 mg/l için k:0,012 l	-	* RO107_H-NA:%98 giderim

REFERENCES

- Adewuyi, Y.G., 2005, Sonochemistry in environmental remediation. 2. Heterogeneous Sonophotocatalytic Oxidation Processes for the Treatment of Pollutants in Water, *Environ. Sci. Technol.* 39, 8557-8570.
- Adosinda, M., Martins, M., Lima, N., Silvestre, A.J.D. and Queiroz, M. J., 2003, Comparative studies of fungal degradation of single or mixed bioaccessible reactive azo dyes, *Chemosphere.* 52, 967-973.
- Aksu, Z., 2005, Application of biosorption for the removal of organic pollutants: a review, *Process Biochem.* 40, 997-1026.
- Aksu, Z., and Isoglu I.A., 2006, Use of agricultural waste sugar beet pulp for the removal of Gemazol turquoise blue-G reactive dye from aqueous solution, *Journal of Hazardous Materials.* 137, 418-430.
- Aksu, Z., Kilic, N.K., Ertugrul, S. and Donmez G., 2006, Inhibitory effects of chromium(VI) and Remazol Black B on chromium(VI) and dyestuff removals by *Trametes versicolor*, *Enzyme and Microbial Technology.* 40, 1167-1174
- Al-Degs Y., Khraisheh, M.A.M., Allen, S.J., and Ahmad, M.N., 2000, Effect of carbon surface chemistry on the removal of reactive dyes from textile effluent, *Water Research.* 34, 927-935.
- Allen, S.J. and Koumanova, B., 2005, Decolourization of waste/wastewater using adsorption: Review, *Journal of the University of Chemical Technology and Metallurgy.* 40, 175-192.
- Arora, D.S. and Gill, P.K., 2000, Laccase production by some white rot fungi under different nutritional conditions, *Bioresource Technology.* 73, 283-285.
- Arora, D.S. and Gill, P.G., 2001, Effects of various media and supplements on laccase production by some white rot fungi, *Bioresource Technology.* 77, 89-91.
- Cetin, D. and Dönmez, G., 2006, Decolourization of reactive dyes by mixed cultures isolated from textile effluent under anaerobic conditions, *Enzyme and Microbial Technology.* 38, 926-930.
- Chinwetkitvanich, S., Tuntolvest, M. and Panswad, T., 2000, Anaerobic Decolourization of Reactive Dyebath Effluents by a Two-stage UASB System with Tapioca as a Co-substrate, *Water Research.* 34, 2223-2232.
- Chitra, S., Paramasivam, K., Sinha, P.K. and Lal K.B., 2004, Ultrasonic treatment of liquid waste containing EDTA, *Journal of Cleaner Production.* 12, 429-435.
- Crini G., 2006, Non-conventional low-cost adsorbents for dye removal: A review, *Bioresource Technology.* 97, 1061-1085.
- Colour-Index, 2008, <http://www.colour-index.org/newusr1.asp>.

Dawen, G., Xianghua, W. and Yi, Q., 2004, Decolourization of reactive brilliant red K-2BP with the white rot fungi under non-sterile conditions, *Chinese Science Bulletin*.49, 981-982.

Donlagic J. and Levec, J., 1997, Oxidation of an Azo Dye in Subcritical Aqueous Solutions, *Ind. Eng. Chem. Res.* 36, 3480-3486.

Druding, S.C., 1982, A bi-annual gathering of weavers, dyers and spinner, Seminar presented in Seattle, <http://www.straw.com/sig/dyehist.html> .

D'Souza, D.T., Tiwari, R., Sah, A.K. and Raghukumar, C., 2006, Enhanced production of laccase by a marine fungus during treatment of colored effluents and synthetic dyes, *Enzyme and Microbial Technology.* 38, 504-511.

DyesPigments, 2008, <http://www.dyespigments.com/what-is-dye.html>.

Eichlerova, I., Homolka, L. and Nerud, F., 2006, Synthetic dye decolourization capacity of white rot fungus *Dichomitus squalens*, *Bioresource Technology.* 97, 2153-2159.

Ekici, P., Leupold, G. and Parlar, H., 2001, Degradability of selected azo dye metabolites in activated sludge systems, *Chemosphere.* 44, 721-728.

Entezari, M.H. and Z. Sharif A. H., 2007, Sono-sorption as a new method for the removal of methylene blue from aqueous solution, *Ultrasonics Sonochemistry.* 14, 599-604.

Epolito, W.J., Lee, Y.H., Bottomley, L.A. and Pavlostathis, S.G., 2005, Characterization of the textile anthraquinone dye Reactive Blue 4, *Dyes and Pigments.* 67, 35-46.

Forgacs, E., Cserhati, T. and Oros, G., 2004, Removal of synthetic dyes from wastewaters: a review, *Environment International.* 30, 953-971.

Frömer, R., 2005, Machbarkeitsstudie zur sonochemischen Behandlung organophosphathaltiger Abwässer der ADO Gardinenwerke, Master Thesis, Fachhochschule Köln, Cologne, 71 p.

He, Z., Song, S., Zhou, H., Ying, H. and Chen, J., 2007, C.I. Reactive Black 5 decolourization by combined sonolysis and ozonation, *Ultrasonics Sonochemistry.* 14, 298-304.

Hildenbrand, S., 1999, Azo dyes and carcinogenic aromatic amines in cell cultures, *Int Arch Occup Environ Health.* 72, 52-56.

Ge J. and Qu, J., 2004, Ultrasonic irradiation enhanced degradation of azo dye on MnO₂, *Applied Catalysis B: Environmental.* 47, 133-140.

Goskondaa, S., Catallob, W.J. and Junka, T., 2002, Sonochemical degradation of aromatic organic pollutants, *Waste Management.* 22, 351-356.

Holcapek, M., Jandera, P. and Prikryl, J., 1999, Analysis of sulphonated dyes and intermediates by electrospray mass spectrometry, *Dyes and Pigments.*, 43, 127-137.

Ince, N.H. and Guyer, G.T., 2004, Impacts of pH and molecular structure on ultrasonic degradation of azo dyes, *Ultrasonics.* 42, 591-596.

Inoue, M., Okada, F., Sakurai, A. and Sakakibara, M., 2006, A new development of dyestuffs degradation system using ultrasound, *Ultrasonics Sonochemistry.* 13, 313–320.

Isik M., Sponza, D.T., 2004, Monitoring of toxicity and intermediates of C.I. Direct Black 38 azo dye through decolourization in an anaerobic/aerobic sequential reactor system, *Journal of Hazardous Materials,* B114, 29-39.

Isik, M. and Sponza, D.T., 2006, Biological treatment of acid dyeing wastewater using a sequential anaerobic/aerobic reactor system, *Enzyme and Microbial Technology.* 38, 887-892.

Joseph J.M., Destailats, H., Hung, H.M. and Hoffman, M.R, 2000, The Sonochemical Degradation of Azobenzene and Related Azo Dyes: Rate Enhancements via Fenton' s Reactions, *J. Phys. Chem. A.* 104, 301-307.

Jozwiak, W.K., Mitros, M., Kaluzna-Czaplinska, J. and Tosik, R.,2007, Oxidative decomposition of Acid Brown 159 dye in aqueous solution by H₂O₂/Fe²⁺ and ozone with GC/MS analysis, *Dyes and Pigments.* 74, 9-16.

Kapdan, I.K., Kargi, F., McMullan, G. and Marchant, R., 2000, Effect of environmental conditions on biological decolourization of textile dyestuff by *C. versicolor*, *Enzyme and microbial technology.* 26, 381-387.

Kim, T.H., Lee, Y., Yang, J., Lee, B. and Park, C., 2004, Decolourization of dye solutions by a membrane bioreactor (MBR) using white-rot fungi, *Desalination.* 168, 287-293.

Kirk-Othmer, Dialog, 2001, Dialog Ondisk Books v3.21 and Kirk-Othmer Encyclopedia of Chemical Technology. [CD-ROM].The Dialog Cor. USA.

Kusic, H., Koprivanac, N. and Srsan, L., 2006, Azo dye degradation using Fenton type processes assisted by UV irradiation: A kinetic study, *Journal of Photochemistry and Photobiology A: Chemistry.* 181, 195-202.

Kusic, H., Bozic A.L. and Koprivanac, N., 2007, Fenton type processes for minimization of organic content in coloured wastewaters: Part I: Process optimization, *Dyes and Pigments.* 74, 380-387.

Libra, J.A, Borchert, M., Banit, S., 2003, Competition strategies for the decolourization of a textile-reactive dye with the white-rot fungi *Trametes versicolor* under non-sterile conditions, *Biotechnol Bioeng.* 82, 736-744.

Libra, J., Borchert, M., Vigelahn, L. and Storm, T., 2004, Two stage biological treatment of a diazo reactive textile dye and the fate of the dye metabolites, *Chemosphere*. 56, 167-180.

Lorimer, J.P., Mason, T.J., Plattes, M., Phull, S.S. and Watson, D.J., 2001, Degradation of dye effluent, *Pure Appl. Chem.* 73, 1957-1968.

Lorenzo, M., Moldes, D. and Sanroman, M.A., 2006, Effect of heavy metals on the production of several laccase isoenzymes by *Trametes versicolor* and on their ability to decolourise dyes, *Chemosphere*. 63, 912-917.

Lorenzo, M., Moldes, D., Couto, S.R. and Sanroman, M.A., 2002, Improving laccase production by employing different lignocellulosic wastes in submerged cultures of *Trametes versicolor*, *Bioresource Technology*. 82, 109-113.

Ma, C.Y., Xu, J.Y. and Liu, X.J., 2006, Decomposition of an azo dye in aqueous solution by combination of ultrasound and visible light, *Ultrasonics*. 44, 375-378.

Manu, B. and Chaudhari, S., 2002, Anaerobic decolourisation of simulated textile wastewater containing azo dyes, *Bioresource Technology*. 82, 225-231.

Mason, T.J., 2007, Developments in ultrasound-Non-medical, *Progress in Biophysics and Molecular Biology*. 93, 166-175.

McMullan, G., Meehan, C., Conneely, A., Kirby, N., Robinson, T., Nigam, P., Banat, I. M., Marchant, R., and Smyth, W.F., 2001, Microbial decolourisation and degradation of textile dyes, *Appl Microbiol Biotechnol*. 56, 81-87.

Neppolian, B., Park, J.S., Choi, H., 2004, Effect of Fenton-like oxidation on enhanced oxidative degradation of para-chlorobenzoic acid by ultrasonic irradiation, *Ultrasonics sonochemistry*. 11, 273-279.

Nilsson, I., Möller, A., Rubindamayugi, M.S.T. and Welander, U., 2006, Decolourization of synthetic and real textile wastewater by the use of white-rot fungi, *Enzyme and Microbial Technology*. 38, 94-100.

Nigam, P., Banat, I.M., Singh, D. and Marchant R., 1996, Microbial Process for the Decolourization of Textile Effluent Containing Azo, Diazo and Reactive Dyes, *Process Biochemistry*. 31, 435-442.

Novotny, C., Svobodova, K., Erbanova, P., Cajthaml, T., Kasinath, A., Lang, E. and Sasek, V., 2004, Ligninolytic fungi in bioremediation: extracellular enzyme production and degradation rate, *Soil Biology and Biochemistry*. 36, 1545-1551.

Peller, J., Wiest, O. and Kamat, P.V., 2001, Sonolysis of 2,4-Dichlorophenoxyacetic acid in aqueous solutions. Evidence for OH-Radical-Mediated Degradation, *J. Phys. Chem. A*. 105, 3176-3181.

Plum A. and Rehorek, A., 2005, Strategies for continuous on-line high performance liquid chromatography coupled with diode array detection and electrospray tandem mass spectrometry for process monitoring of sulfonated azo dyes and their intermediates in anaerobic-aerobic bioreactors, *Journal of Chromatography A*. 1084, 119-133.

Plum, A., 2005, Prozessanalytische und verfahrenstechnische Methodenentwicklung zur Optimierung der biologischen Entfärbung azofarbstoffhaltiger Textilabwasserkonzentrate, PhD Thesis, Der Fakultät für Chemie und Mineralogie der Universität Leipzig, 126 p.

Poiger, S.D.R. and Baughman, G.L., 2000, Identification of reactive dyes in spent dye baths and wastewater by capillary electrophoresis-mass spectrometry, *Journal of Chromatography A*. 886, 271-282.

Reemtsma, T., 2001, The use of liquid chromatography-atmospheric pressure ionization-mass spectrometry in water analysis-Part I: Achievements, *Trends in analytical chemistry*. 20, 500-517.

Rehorek, A., Hoffman, P., Frömer, R., Gornacka, B. and Györgyicze, C., 2004, ULTRATEC Project Training Course, Basics of Ultrasound, The Uses of Ultrasound in Processing and Chemistry/Applied Sonochemistry, Cologne, 231 p.

Rehorek, A., Tauber, M. and Gübitz, G., 2004, Application of power ultrasound for azo dye degradation, *Ultrasonics Sonochemistry*. 11, 177-182.

Rehorek, A. and Plum, A., 2006, Online LC-MS-MS process monitoring for optimization of biological treatment of wastewater containing azo dye concentrates, *Anal Bioanal Chem*. 384, 1123-1128.

Rehorek, A., Hoffmann, P., Kandelbauer, A., Gübitz, G.M., 2007, Sonochemical substrate selectivity and reaction pathway of systematically substituted azo compounds, *Chemosphere*. 67, 1526-1532.

Sanghi, R., Dixit, A. and Guha, S., 2006, Sequential batch culture studies for the decolorization of reactive dye by *Coriolus versicolor*, *Bioresource Technology*. 97, 396-400.

Santos, A.B., Cervantes, F.J. and Lier, J.B., 2007, Review paper on current technologies for decolorisation of textile wastewaters: Perspectives for anaerobic biotechnology, *Bioresource Technology*. 98, 2369-2385.

Sayan, E., 2006, Optimization and modelling of decolorization and COD reduction of reactive dye solutions by ultrasound-assisted adsorption, *chemical engineering Journal*. 119, 175-181.

Shaw, C.B., Carliell, C.M. and Wheatley, A.D., 2002, Anaerobic/aerobic treatment of coloured textile effluents using sequencing batch reactors, *Water Research*. 36, 1993-2001.

Shemer, H. and Narkis, N., 2004, Mechanisms and inorganic byproducts of trihalomethane compounds sonodegradation, *Environ. Sci. Technol.* 38, 4856-4859.

Sivakumar, V. and Rao, P.G., 2003, Studies on the use of power ultrasound in leather dyeing, *Ultrasonics Sonochemistry* . 10, 85-94.

Smyth, W.F., McClean, S., O'Kane, E., Banat, I. and McMullan, G., 1999, Application of electrospray mass spectrometry in the detection and determination of Remazol textile dyes, *Journal of Chromatography A*. 854, 259-274.

Slokar, Y.M. and Marechal, M.L., 1998, Methods of Decolouration of Textile Wastewaters, *Dyes and Pigments*. 37, 335-356.

Sood, V.K., Research into the effect of ultrasound in dyeing of cotton fabrics with reactive dyes", PhD Thesis, Graduate Faculty of North Carolina State University, Fiber and Polymer Science, Raleigh, 367p.

Sponza, D.T. and Işik, M., 2005, Toxicity and intermediates of C.I. Direct Red 28 dye through sequential anaerobic/aerobic treatment, *Process Biochemistry*. 40, 2735-2744.

StainsFile, 2005, <http://www.stainsfile.info/StainsFile/dyes/dyes.htm>.

Straub, R. Voyksner, R.D. and Keever, J.T., 1992, Thermospray, particle beam and electrospray liquid chromatography-mass spectrometry of azo dyes, *Journal of Chromatography A*. 627, 173-186.

Suslick, K.S., Hammerton, D.A. and Cline, R.E., 1986, The sonochemical hot spot, *J. Am. Chem. Soc.* 108, 5641-5642.

Suslick K., 1994, The Chemistry of Ultrasound, *The Yearbook of Science & the Future*; Encyclopaedia Britannica: Chicago, pp. 138-155..

Svobodova, K., Senholdt, M., Novotny, C. and Rehorek, A., 2007, Mechanism of Reactive Orange 16 degradation with the white rot fungus *Irpex lacteus*, *Process Biochemistry*. 42, 1279-1284.

Swamy, J. and Ramsay, J.A., 1999, Effects of glucose and NH₄⁺ concentrations on sequential dye decoloration by *Trametes versicolor*, *Enzyme and Microbial Technology*. 25, 278-284.

Swamy, J. and Ramsay, J.A., 1999, The evaluation of white rot fungi in the decolouration of textile dyes, *Enzyme and Microbial Technology*. 24, 130-137.

Tauber, M.M., Guebitz, G.M. and Rehorek A., 2005, Degradation of azo dyes by laccase and ultrasound treatment, *Applied and Environmental Microbiology*. 71, 2600-2607.

Tatli, I., 2003, Çeşitli Tekstil Boyarmaddelerin Adsorpsiyon/Biyosorpsiyonunun Karşılaştırmalı Olarak Kesikli Sistemde İncelenmesi, Master Thesis, Hacettepe University, Chemical Engineering Department, Ankara, p 1991.

Tezcanli-Guyer, G. and Ince, N.H., 2004, Individual and combined effects of ultrasound, ozone and UV irradiation: a case study with textile dyes, *Ultrasonics*. 42, 603-609.

Tezer, S., 2003, *Tekstil Endüstrisi Atıksularında Yer Alan Reaktif Boyaların Biyosorpsiyonun İncelenmesi*, Master Thesis, Hacettepe University, Chemical Engineering Department, Ankara, p 199.

Thompson, L.H. and Doralswamy, L. K., 1999, Sonochemistry: Science and Engineering, In. *Eng. Chem. Res.* 38, 1215-1249.

Vajnhandl, S. and Le Marechal, A.M., 2005, Ultrasound in textile dyeing and the decolourization/mineralization of textile dyes, *Dyes and Pigments*. 65, 89-101.

Vajnhandl, S. and Le Marechal, A. M., 2007, Case study of the sonochemical decolouration of textile azo dye Reactive Black 5, *Journal of Hazardous Materials*. 141, 329–335.

Van der Zee, F.P. and Villaverde, S., 2005, Combined anaerobic-aerobic treatment of azo dyes-A short review of bioreactor studies, *Water Research*. 39, 1425-1440.

Vinodgopal, K., Peller, J., Makogon, O. and Kamat P.V., 1998, Ultrasonic Mineralization of Reactive Textile Azo Dye Remazol Black B, *Wat. Res.* 32, 3646-3650.

Voncina, D.B. and Le Marechal, A.M., 2003, Reactive dye decolourization using combined ultrasound/H₂O₂, *Dyes and Pigments*. 59, 173-179.

Wang, L., Zhu, L., Luo, W., Wu, Y. and Tang, H., 2007, Drastically enhanced ultrasonic decolourization of methyl orange by adding CCl₄, *Ultrasonics Sonochemistry* . 14, 253-258.

Wesenberg, D., Kyriakides, I. and Agathos, S.N., 2003, White rot fungi and their enzymes for the treatment of industrial dye effluents, *Biotechnology Advances*. 22, 161-187.

Yasman, Y., Bulatov, V., Gridin, V.V., Agur, S., Galil, N., Armon, R. and Schechter, I., 2004, A new sono-electrochemical method for enhanced detoxification of hydrophilic chloroorganic pollutants in water, *Ultrasonics sonochemistry*. 11, 365-372.

Yildiz, B., 2006, *Untersuchungen zur Prozessoptimierung des kombiniert anaerob-aeroben Abbaus von C.I. Reactive Orange 107*, Master Thesis, Fachhochschule Köln, Institut für Anlagen- und Verfahrenstechnik Institute of Chemical Engineering and Plant Design, Cologne, 78p.

Young, L. and Jian, Y., 1997, Ligninase-catalysed decolourization of synthetic dyes, *Wat Res.* 31, 1187-1193.

Yuzhu, F. and Viraraghavan, T., 2001, Fungal Decolourization of dye wastewaters:a review, *Bioresource Technology*. 79, 251-262.

Zhang, H., Duan, L., Zhang, Y. and Wu, F., 2005, The use of ultrasound to enhance the decolourization of the C.I. Acid Orange 7 by zero-valent iron, *Dyes and Pigments*. 65, 39-43.

Zhao, X., Hardin, I.R. and Hwang, H.M., 2006, Biodegradation of a model azo disperse dye by the white rot fungus *Pleurotus ostreatus*, *International Biodeterioration and Biodegradation*. 57, 1-6.

Zille, A., 2005, Laccase Reactions for Textile Applications, PhD Thesis. Universidade do Minho. Italy, 151p.

APPENDIX

App 1. The LC-MS/MS system used during experimental studies

LC/MS-MS system used for the analysis contained three parts: an Agilent 1100 HPLC gradient system with diode-array detector (DAD), Canada, an ion chromatographic cation suppressor unit from Metrohm, Switzerland, and a Qtrap hybrid mass spectrometer from Applied Biosystems with electrospray ionization (ESI), and atmospheric-pressure chemical ionization (APCI).

The chemicals used in this chromatographic method were analytical-reagent grade ammonium acetate, HPLC-grade LiChrosolv water and gradient grade LiChrosolv acetonitrile, formic acid (Merck, Darmstadt, Germany). The ion pairing agent tetrabutylammonium acetate (TBAAc) was purchased (purity >99%) from Fluka (Buchs, Switzerland).

The reference substances such as aromatic amines, sulfone aromatic amines and sulfone azo dyes used for the calibration for LC/MS-MS system and data evaluation were provided from Dystar, Leverkusen. The composition of the reference solution was given in Table App.1.

To elucidate the structures of the wide variety of compounds of interest in a complex concentrate matrix, two different separation methods were developed and optimized for LC-DAD analysis by Prof. Rehorek's group (Rehorek and Plum, 2006). The first method was based on ion-pair chromatographic (IPC) gradient separation with tetrabutylammonium acetate (TBAAc Method). A short column packed with a 3- μ M particle C₁₈ phase was used and applied in combination with ion chromatographic cation suppression (IC) before mass spectrometry. The second method was selective for highly polar polysulfonated azo dyes and for nonsulfonated aromatic amines (NH₄Ac Method).

The negative-ionization mode is particularly useful for sulfonated compounds, and cation suppression helps prevent the matrix interfering with ionization. Cation suppression removes the high salt load from the sample and the tetrabutylammonium cations from gradient elution. In general, the LC-MS method with ion suppression between the LC-DAD and the ESI-MS is more stable in

routine operation than without it. It is particularly useful for small simple sulfonated aromatic amines.

Table App 1 The composition of the reference solution.

Name	C (µM)
Reactive Orange 16 (Hydrolyzed)	100
Reactive Black 5 (Hydrolyzed)	100
Reactive Orange 107 (Hydrolyzed)	100
Direct Blue 71	10
Acid Orange 7	100
5-Amino-4-hydroxy-3-[4-(2-hydroxy-ethanysulfonyl)-phenylazo]-naphthalin-2,7-disulfonsodiumsalt	10
4-Amino-5-hydroxy-3-[4-(2-hydroxy-ethanysulfonyl)-phenylazo]-naphthalin-2,7-disulfonsodiumsalt	50
p-Base	50
H-Acid	50
N-acetyl-p-Base	50
Orthanil acid	50
Metanil acid	100
Sulfanil acid	50
4,6-Dihydroxynaphthalin-2,7-disulfonic acid	50

The gas used in LC/MS-MS system consisted of nitrogen (purity 99.999%) produced from gas generator from PEAK Science (Scotland). The MS was operated in different modes described in the following:

- 1) Multiple reaction monitoring mode (MRM): resolution Q1: unit, resolution Q3: unit, dedector parameters (negative):CEM 2300 V, MRM transients
- 2) Enhanced MS (EMS)
- 3) Enhanced product ion (EPI): Q1 is operated as a standard quadrupole mass spectrometer; Q3 is operated as a LIT mass spectrometer under specified conditions (Plum and Rehorek, 2005).

The operating conditions for LC-MS/MS system used in the experimental studies were presented in Table App.2 (Yildiz, 2006).

Table App 2 The operating conditions for LC-MS/MS system used during experimental studies.

Agilent 1100 LC Pump:

1 mL/min

1. TBAAc-Method:

Eluent A: 5 mM aqueous Tetrabutylammoniumacetate solution

Eluent B: Acetonitrile

Time [min]	Eluent A[%]	Eluent B[%]
0	95	5
1	95	5
10	40	60
11	0	100
12	0	0
13	95	5
15	95	5

2. NH₄Ac-Method:

Eluent A: 10 mM aqueous Ammonium acetate (NH₄Ac) solution pH 5,5

Eluent B: Acetonitrile

Time [min]	Eluent A	Eluent B
0	100	0
1,5	100	0
12,5	45	55
15	0	100
16	0	100
17	100	0
20	100	0

Autosampler Agilent 1100:

Injection volume: 20 - 100 µL

Column:

ProntoSIL 120-3-C18 AQ 3 µm, 60x4 mm, (Bischoff, Germany), 40 °C

ProntoSIL 120-3-C18-ace-EPS 3 µm, 125 x 4 mm, (Bischoff, Germany), 40 °C

Agilent1100 Detector:

Diode-array detector (DAD); Range 200 - 800 nm

753 Suppressor (Methrom):

Regeneration solution 200 mM Sulfuric acid with 20% Acetone; Neutralization with HPLC-Water and 5% Acetonitrile (used for Method 1)

MS-Parameter:

Ion source: Turbo Ion spray

Temperature: 400 °C

Entrance potential: -10 V

Declustering potential: -50 V

Curtain gas: 40 psi

Nebulizer gas: 45 psi

Gas for the collision-induced dissociation (CAD): High mode

Turbo-Gas: 80 psi

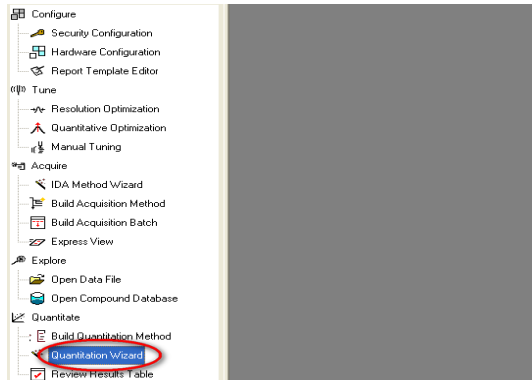
Collision energy: -90 V : -10 V (EPI-Mode), -50 V (MRM-Mode)

Scan area: 50 - 1000Th (EMS-Mode)

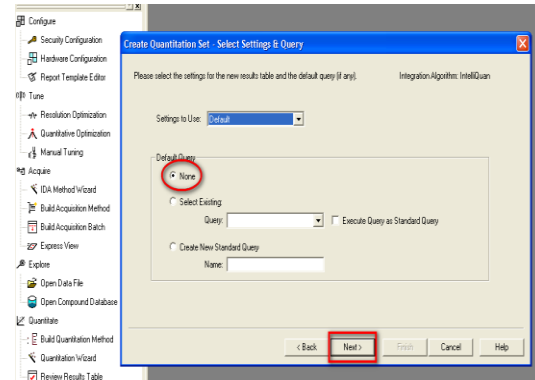
Scan rate: 4000 u/s

App 2. The evaluation of DAD data and calculation of relative concentration

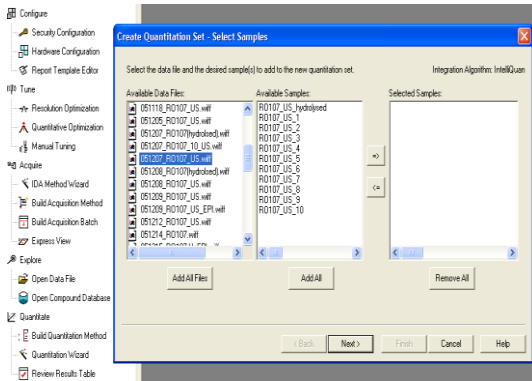
1. Open Analyst Software and select Quantitation Wizard.



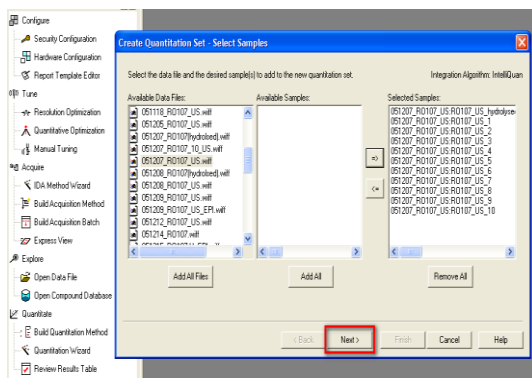
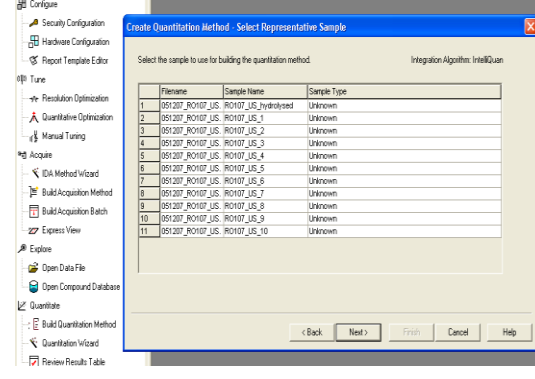
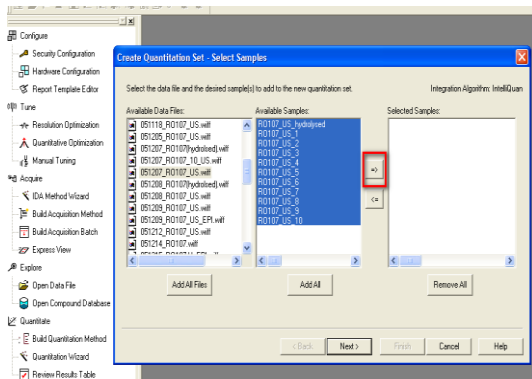
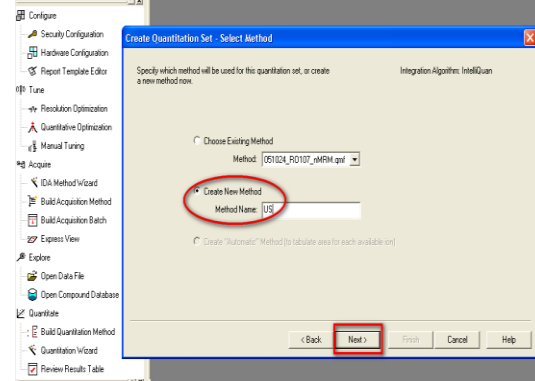
3. Select the settings for the results table and click "Next".



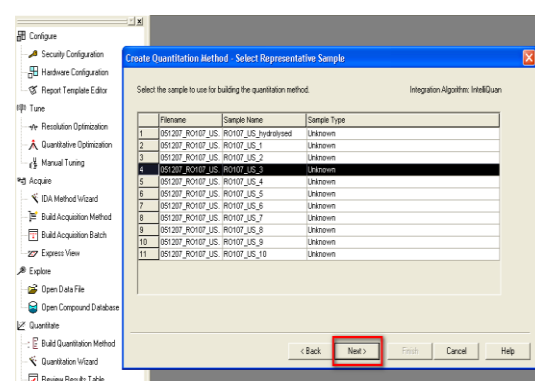
2. Choose which data you want to evaluate and click "Next".



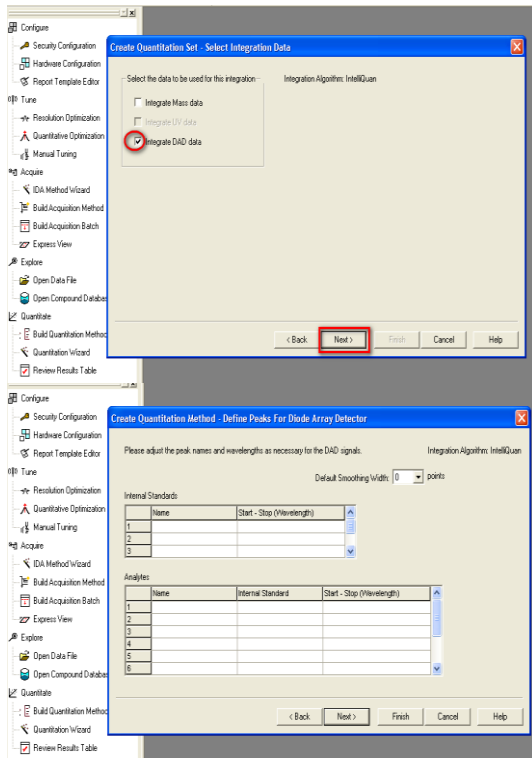
4. Create a method for data evaluation.



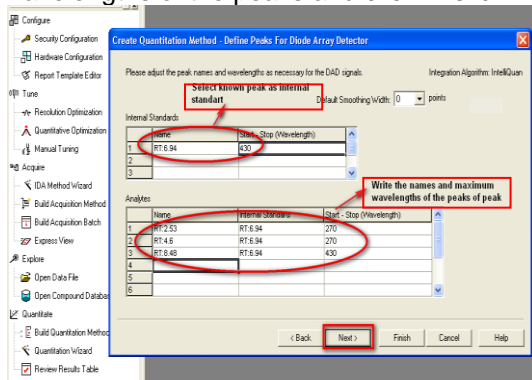
5. Select one of your samples as reference.



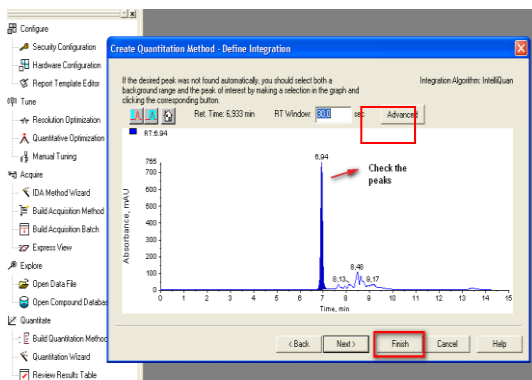
6. Select DAD data integration and click "Next".




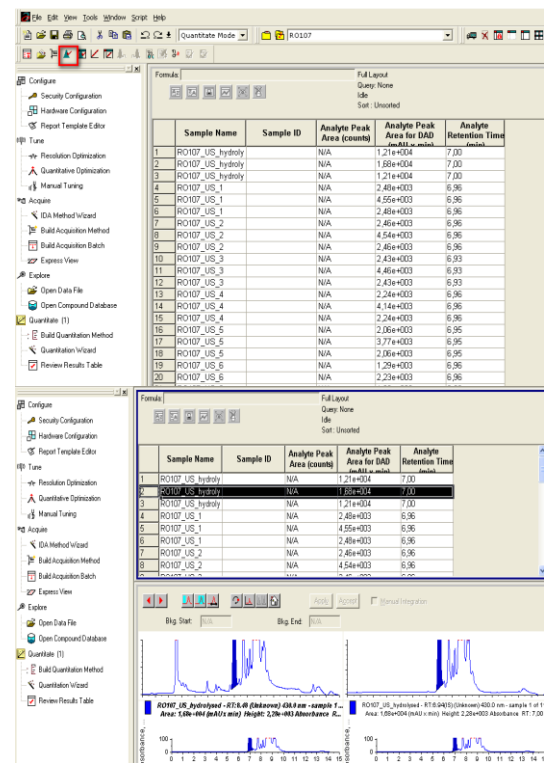
7. Select the known peak as internal standard and write the names and maximum wavelengths of the peaks and click "Next".



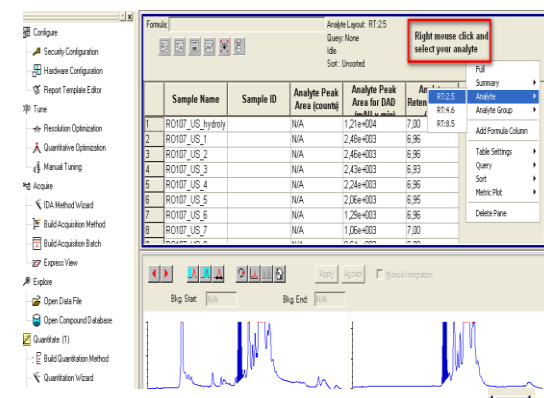
7. Check the peak area and click "Finish".

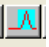


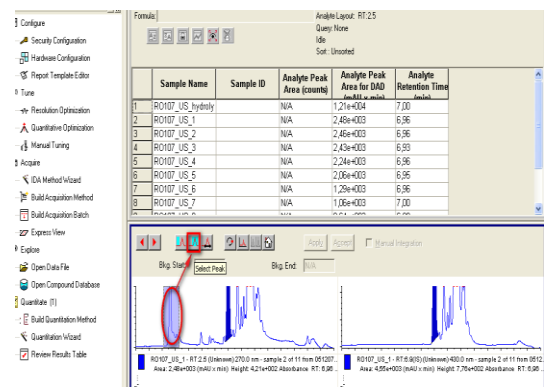
8. Click  symbol.



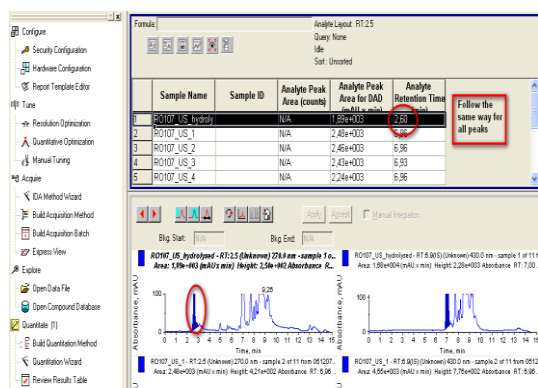
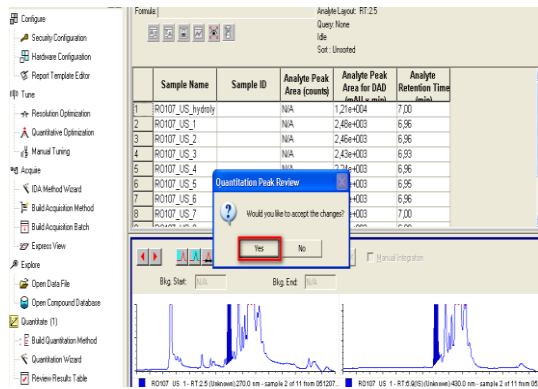
9. Right Mouse click and select your analyte.



10. Choose your analyte peak and click  symbol.



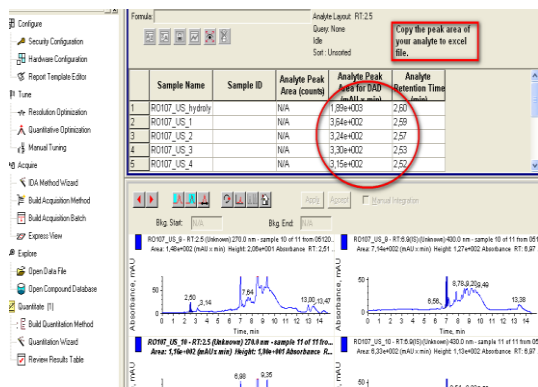
11. After calculating the peak area automatically click “Yes” and follow the same way for all peaks.



Sample Name	Time (h)	DAD Peak Area (mAUxmin)	Relative Concentration
RO107_US_hydrolysed	0	1,89E+03	= (C2/MAX(\$C\$2:\$C\$12))
RO107_US_1	0,3	3,64E+02	
RO107_US_2	0,5	3,24E+02	
RO107_US_3	0,0	3,30E+02	
RO107_US_4	0,1	3,15E+02	
RO107_US_5	0,1	2,82E+02	
RO107_US_6	0,4	2,19E+02	
RO107_US_7	0,5	2,10E+02	
RO107_US_8	0,6	1,90E+02	
RO107_US_9	0,8	1,48E+02	
RO107_US_10	0,7	1,16E+02	

Sample Name	Time (h)	DAD Peak Area (mAUxmin)	Relative Concentration
RO107_US_hydrolysed	0	1,89E+03	100,0%
RO107_US_1	0,3	3,64E+02	19,3%
RO107_US_2	0,5	3,24E+02	17,1%
RO107_US_3	0,0	3,30E+02	17,5%
RO107_US_4	0,1	3,15E+02	16,7%
RO107_US_5	0,1	2,82E+02	14,9%
RO107_US_6	0,4	2,19E+02	11,6%
RO107_US_7	0,5	2,10E+02	11,1%
RO107_US_8	0,6	1,90E+02	10,1%
RO107_US_9	0,8	1,48E+02	7,8%
RO107_US_10	0,7	1,16E+02	6,1%

12. Copy the peak area of your analyte to excel file and calculate the relative concentration.



App 3. Dye calibration curve for fungal degradation

The concentration of residual dye in the growth medium during fungal degradation was determined spectrophotometrically and the calibration curve obtained at 425 nm was given in Figure App.1.

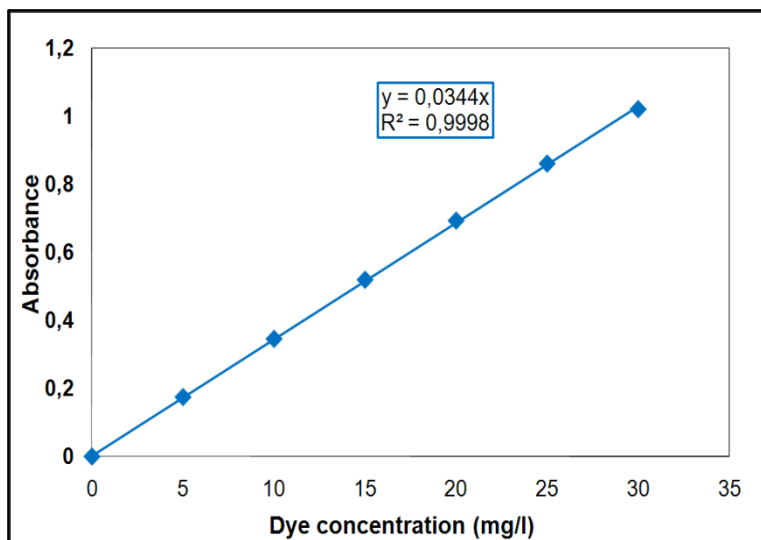


Figure App 1 The calibration curve of C.I. RO107 dye.

App 4. Determination of glucose concentration and glucose calibration curve

This method detects reducing ends of carbohydrates (reactive "end" a site that is not involved in a glycosidic linkage). An alkaline solution of 3-5 dinitro-salicylate is reduced to 3-amino 5-nitro salicylic acid by reducing sugar. The reaction produces a compound that absorbs light strongly at 575 nm. According to the authors of the test, sodium potassium tartrate is introduced to prevent the reagent from dissolving oxygen, phenol to increase the amount of colour produced and bisulfite to stabilize the colour obtained in the presence of the phenol. The alkali is required for the reducing action of the reducing sugar on dinitrosalicylic acid.

Reagents:

- Dinitrosalicylic acid (DNS) Reagent;

Compound	(w/v) %
3,5 Dinitrosalicylic acid	1.0
Sodium hydroxide	1.0
Phenol	0.2
Sodium sulfite	0.05

For the preparation of DNS reagent, all solid components were placed in a container and dissolved simultaneously by stirring with the required volume of sodium hydroxide solution sugar on dinitrosalicylic acid.

- Sodium potassium tartrate solution (40 g/100 ml).

Procedure;

Standard curve:

1. Various dilutions of standard reducing sugar solution (mg/ml) were prepared.
2. The colour test was developed with 3 ml aliquots of DNS reagent added to 3 ml aliquots of glucose solution.
3. The mixture was heated in boiling water bath for 15 minutes.

1 ml of the sodium potassium tartrate solution was immediately added after the development of the colour. The solution was adjusted to ambient temperature under running tap water and the colour was read in the spectrophotometer at 575

nm. Glucose calibration curve was given in Figure App.2. Same procedure was applied for the samples containing unknown amount of glucose.

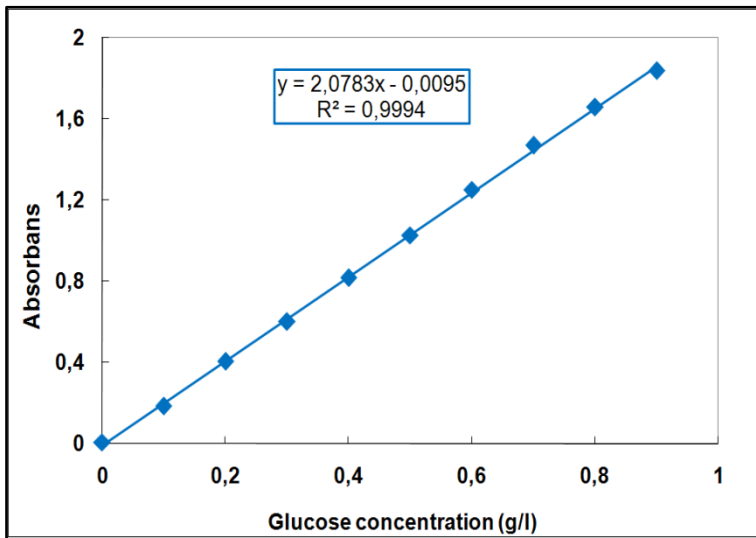


Figure App 2 The calibration curve of glucose.

App 5. The enhanced product ion spectrums and fragmentation patterns of components of hydrolyzed dye

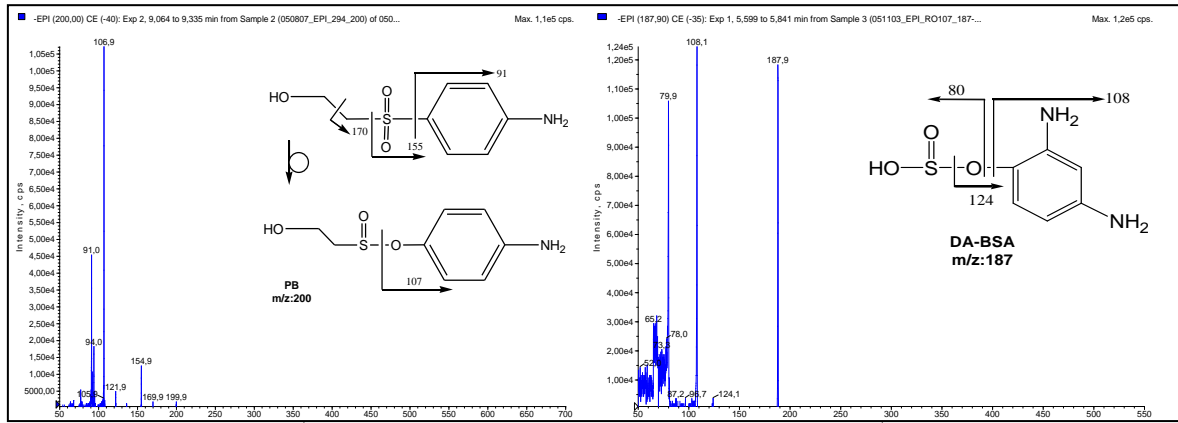


Figure App 3 Enhanced Product Ion (EPI) spectrum and fragmentation pattern of p-base and DA-BSA.

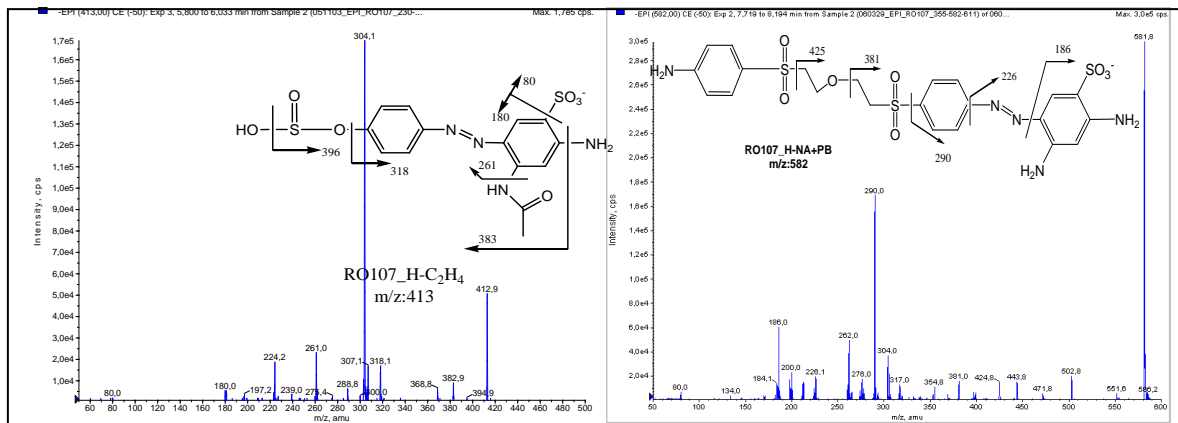


Figure App 4 Enhanced Product Ion (EPI) spectrum and fragmentation pattern of RO107_H-C₂H₄ and RO107_H-NA+PB.

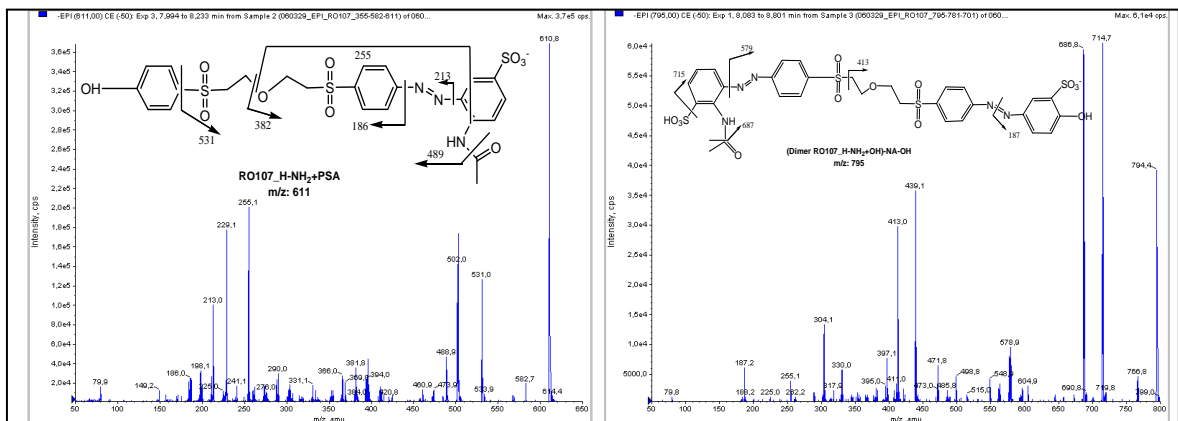


Figure App 5 Enhanced Product Ion (EPI) spectrum and fragmentation pattern of RO107_H-NH₂+PSA and (Dimer RO107_H-NH₂+OH)-NA-OH.

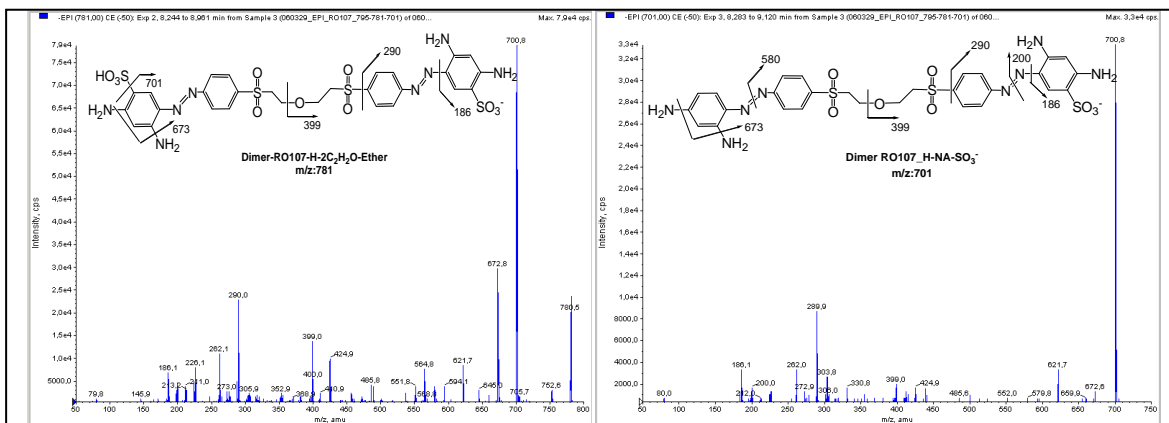


Figure App 6 Enhanced Product Ion (EPI) spectrum and fragmentation pattern of Dimer RO107_H-2C₂H₂O-Ether and (Dimer RO107_H-NA)-SO₃⁻.

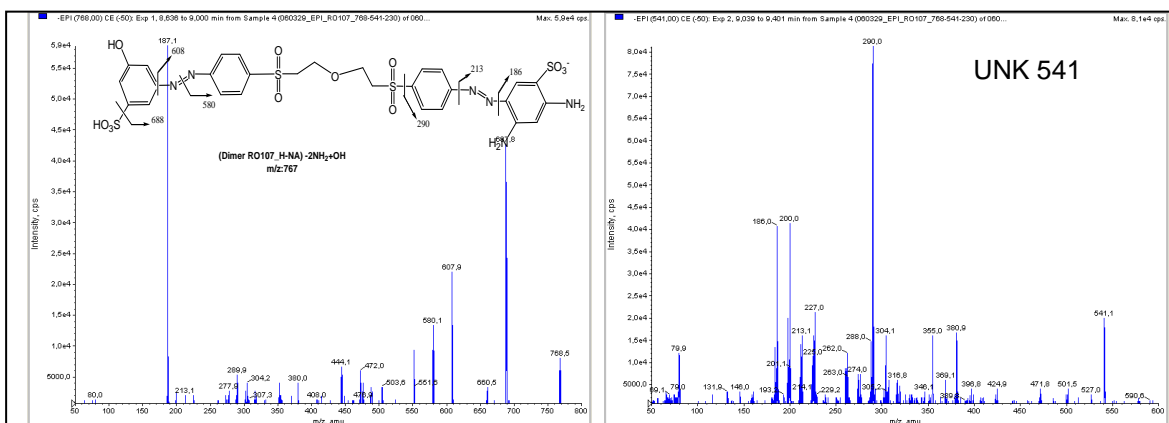


Figure App 7 Enhanced Product Ion (EPI) spectrum and fragmentation pattern of (Dimer RO107_H-NA)-2NH₂+OH and UNK 541.

CURRICULUM VITAE

Name-Surname : Özlem TUNÇ

Date of Place : Ankara

Date of Year : 1977

Marital Status : Single

Education and Academic State:

High School 1991-1994

Bachelor's Degree 1995-2000

Master of Science 2000-2002

Foreign Language : English

Work Experience:

2000-2008 Hacettepe University, Chemical Engineering Department,
Research Assistant.

2008- General Directorate of State Hydraulic Works, Department of
Technical Research and Quality Control, Engineer.